The Catalytic Membrane Reactor for the conversion of methane to methanol and formaldehyde under mild conditions

By

R. M. Modibedi (M.Sc.)

Submitted in fulfilment of the requirements for the degree of PhD in Chemistry in the Department of Chemistry, South African Institute of Advanced Materials Chemistry, University of the Western Cape

Supervisor: Professor Vladimir M. Linkov November 2005

DECLARATION BY CANDIDATE

"I declare that *Catalytic Membrane Reactor for the Conversion of Methane to Methanol and Formaldehyde under Mild Conditions* is my own work and that all the sources I have used or quoted have been indicated and acknowledged by means of complete references."

Remegia Mmalewane Modibedi

Signed:……..  Date…February 2006

KEYWORDS

Methane (natural gas), selective oxidation, inorganic ceramic membrane papers, silica, deposition method, catalysts, reactor, methanol, formaldehyde, temperature programmed reactions

ABSTRACT

The thesis describes the development of new catalytic system for the conversion of natural gas (methane) to liquid products such as methanol and formaldehyde. This technology can allow the exploitation of small and medium size gas fields without the need to build an expensive gas to liquid (GTL) plants or long pipelines. The technology is based on a concept of non-separating membrane reactor where an inorganic membrane paper servers as a catalyst support through which a reaction mixture is flowing under mild conditions and short residence times.

Inorganic membrane supported catalysts for the conversion of methane to methanol and formaldehyde under mild conditions were investigated. Inorganic ceramic membrane paper '1P-397-1' was the most preferable support material for the deposition of active metal centres. The support material was modified with silica prior the impregnation with oxidation catalysts. The BET surface area of the support material increased with the number of silica layers, with 3 layers of silica showing 27.86 m^2/g. The pore volume and narrow mesoporous region increased with the number of silica layers deposited on the support material.

Pt, PMo, SiMo and Fe were deposited on the support using wet deposition. The quality (weight %) of Pt on the support increased with the number of silica layers while those of Fe and SiMo were similar to when the unmodified support was used. The maximum concentrations obtained on the support modified with 3 layers of silica were 153 ppm Pt, 14 ppm Fe, and 182 ppm Mo (SiMo). PMo showed high concentration of Mo on unmodified support than on support modified with 3 layers of silica of 1579 ppm and 658 ppm respectively. SEM/EDX results showed

homogeneous distribution of Pt, PMo and Fe on the support. TPR showed that platinum was reduced at temperatures lower than 60°C. TPO showed that SiMo-based catalysts adsorbed less oxygen than PMo-based catalysts due to the low loading of Mo in SiMo catalysts suggesting that PMo catalysts activate oxygen better than SiMo. PMo adsorbed oxygen at temperatures lower than 120°C. PMo-based catalysts desorbed carbon dioxide (TPD) at temperatures lower than 300°C implying the presence of basic sites on these catalysts. Pt, SiMo and Fe based-catalysts did not desorb carbon dioxide. TPD of methane showed that PMo catalysts activate the C-H bond of methane at low temperatures.

Methane conversion into methanol and formaldehyde increased with increase in contact time for Pt-based catalysts. High methane conversion of 1.84% with low selectivity to methanol of 0.91% was observed at 120°C. The selectivity of carbon dioxide was 3.7% and that of formaldehyde 38.9%. A decrease in the oxygen content in the reaction mixture resulted in enhanced formation of formaldehyde and water (selectivity of both was 41%) between 60 and 90°C. Support modified with 3 layer silica for Pt, PMo and SiMo showed relative per pass CH_3OH yields of 16.2, 11.1 and 3.3 respectively at 30°C, GHSV= 666 h^{-1} and CH_4:O_2 = 15:1.

Supported PMo catalyst showed catalytic activity in oxidation of natural gas (lower alkanes) under mild conditions. Products detected were ethanol, methanol, and formaldehyde. Carbon dioxide was not detected in the products of reaction. Methane conversion in natural gas decreased with increase in reaction temperature. The highest methane conversion (60%) and selectivity to methanol and formaldehyde (6 and 39% respectively) were observed at 120°C, 1:3 natural gas to air ratio and GHSV= 952 h^{-1}.

TABLE OF CONTENTS

LIST OF FIGURES

LIST OF TABLES

ACKNOWLEDGEMENTS

My greatest gratitude is to The Lord GOD Almighty for in him we live and move and have our being.

I would like to thank my supervisor Professor Vladimir Linkov for all his assistance and motivation. Special thanks to the staff members, post-doctoral fellows, and fellow students at the SAIAMC and the UWC chemistry department. Gerry Masters, Ben Bladergroen and Mkhetwa Maluleke I am grateful for your friendship. I am very grateful to ESKOM and the NRF for the financial support during the research. Special thanks to Prof. Vladimir Belyakov of the Ukrainian Institute of General and Inorganic Chemistry, especially to the members of the staff, Sergey, Nicholai, Tanya, Katya, Luada, Alexey and Tanya for the support. I would like to extend my gratitude to Dr L. Belyakova of the Ukranian Institute of Surface Chemistry for her insight and knowledge.

The Chemistry lab technicians, Andile, Timothy, and Ben, Lucas your help is highly appreciated. I would like to thank the Physics Department for the SEM/EDX studies, Basil, Gerald and Nolan, Tshepo from Ithemba labs for XRD analysis and Dr Andreas Spath from UCT for ICP/MS analysis. I am grateful to the contribution of Mvungase Marushule, Gabriel Marepule, Bongani Beja and Mario Williams. I extend my gratitude to Barbara Rodgers, Amanda Swartz and Nicolette Hendricks-Leukes for their friendship, encouragement and their assistance in the lab.

Finally, I would like to thank my family whose support was invaluable. My mom, my aunt, my great grandmother, my grandmother, Judith, Thembinkosi, Tshepiso, Rose, Tshegofatso, Tumelo, Tshireletso, Kearabiloe, Lefentse and Kelebogile, I am grateful for your loving support, your patience and understanding during the hard times. I wish to thank Vincent for all the love and encouragement. To the UWC ministry, Cape Town Church of Christ thank you for your encouragement, support, and friendship.
I LOVE YOU ALL.

GLOSSARY OF TERMS

Calcination: the catalyst is heated in oxidizing atmosphere at a temperature usually as high as or a little higher than that encountered during reaction. This treatment has the purpose of decomposing the metal precursor with the formation of an oxide and removal of gaseous products (usually water, CO_2) and the cations or the anions which have been previously introduced.

Catalysis: alteration of the speed of a chemical reaction, through the presence of an additional substance, known as a catalyst, that remains chemically unchanged by the reaction.

Catalyst: a material that enhances the rate of the reaction by lowering the activation barriers, and while being intimately involved in the reaction sequence, it is regenerated at the end of it. A catalyst is only effective when a reaction is under kinetic control.

Cabosil (Cab-O-Sil): untreated fumed silica is a fine white synthetic amorphous colloidal silicon dioxide. It has an extremely small particle size of 0.2 to 0.3 microns

Chemisorption: it is a strong adsorption involving real bond breaking or weakening in the reactant and the making of bonds to the surface.

Gas hourly space velocity (GHSV): ml total gas flow (at NTP) per ml catalyst per h

Heteropolyacids (HPAs): are early transition metal oxygen anion clusters that exhibit a wide range of well-defined molecular structures, surface charge densities, chemical and electronic properties. They have acid and redox catalytic properties as well. Among various HPA structural classes, Keggin-type HPAs have been mostly investigated as catalytic materials. The acid and redox catalytic properties of HPAs have been conventionally modified by replacing the protons with metal cations and/or by changing the heteroatom or the framework polyatoms. Other unique features that make solid HPAs commercial catalysts are their characteristic adsorption property and pseudo-liquid-phase behaviour depending on adsorbates.

Heterogeneous catalysis: the catalyst and the reactant are in different phases.

Homogeneous catalysis: the catalyst and the reactants are in the same phase, e.g. O_3 and Cl_2 in the atmosphere (ozone destruction)

'Incipient wetness' technique: the volume of the solution containing the precursor does not exceed the pore volume of the support. By removing the air trapped in the inner pores allows a deeper penetration of the solution and a consequent more uniform distribution of the metal precursor should be attained. It is a simple, economic and able to give a reproducible metal loading which, is however, limited by the solubility of the metal precursor.

Incipient wetness technique: the first step is to saturate high surface area supports with solvent (generally water) containing dissolved metal salts. The solvent is evaporated and the salt decomposed by heating, and generally the catalyst is then reduced.

Inert membrane reactors (IMRs): a porous membrane reactor in which the membrane removes products or adds reactants. The catalyst is located apart from the membrane structure

Membrane reactor: is a multi-functional reactor in which the chemical reaction is combined with a membrane separation in one apparatus.

Membrane separation: a selective transport of certain species occurs.

Physisorption: involves the forces of molecular interaction which embrace permanent dipole, induced dipole and quadrupole attraction or it is often termed van der Waals adsorption (weak adsorption).

Periodic operation: the operation where a parameter like feed composition, flow direction or temperature is intentionally modulated in time.

Permselective membranes: membranes are charged and used as transport channel for several components.

Poison: electronegative element that blocks the active sites on the surface of the catalyst and thus reduces the reaction rate.

Promoter: a substance that enhances the activity of the catalyst by improving reactions at sites adjacent to it. They are usually alkali metals and electropositive elements.

R_0 (Homonuclear exchange): is exchange catalysed by the oxide surface, but does not involve exchange with oxygen of the oxide lattice.

R_3 is the process of oxygen exchange over oxides. This type of mechanism involved exchange with the whole of the lattice oxygen, not merely the surface layer indicating that the mobility of oxygen throughout the oxide lattice was a facile process.

Sintering: if a catalyst is produced which consist of separated metal particles, the total surface energy can be minimised by merging of these units to form fewer bigger ones. These result in lower surface area and higher average surface coordination. Hence causes a loss in efficiency of a catalyst that generally occurs during its lifetime in an industrial plant.

Space velocity: the mass/volume of feed per unit of catalyst per unit of time (WHSV = weight hourly space velocity = x kg-feed/$kg_{catalyst}$/hour).

Space time yield (STY): Amount of product per unit catalyst volume or mass, per unit time (g/$kg_{catalyst}$/hour).

Support material: a thermally strong, support phase, which, is ceramic and refractory in nature. They have high surface area forms and maintain their areas even in very harsh temperatures and environmental conditions. They are highly porous and have a range of pore sizes. It maintains the integrity of the metal phase where the selective reaction takes place and hence helps maintain their activity over a longer period

Supported catalysts: consist of an active phase dispersed on a carrier

Type IV isotherm: According to the S. Brunauer, L. S. Deming, W. S. Deming, and E. Teller (BDDT) classification of a purely mesoporous silica, a multiplayer of adsorbate is formed, with increasing relative pressures. Depending on the mean pore diameter, capillary condensation takes place resulting in an increase in adsorption volume. As the relative pressure approaches unity, an abrupt rise indicates the bulk condensation of adsorbate gas to liquid. Instead of retracing the adsorption curve, the mesoporous or macroporous behavior shows a wide hysteresis loop indicating the filling and emptying effects of the pores by capillary condensation

Zero point of charge (PZC)/ isoelectric point: a pH at which the surface of the oxide will not be charged.

ABBREVIATIONS

DMTM: direct partial oxidation of methane to methanol

SiMo: Silicomolybdyc acid hydrate [$H_4SiO_4.12MoO_3.xH_2O$]

PMo: Phosphomolybdic acid hydrate [$H_3Mo_{12}O_{40}P.xH_2O$]

DMF: N, N-dimethylformamide

SEM: Scanning Electron Microscope

EDX: Energy dispersive x ray spectroscopy

BET: Brunauer–Emmett–Teller

TPR: Temperature programmed reduction

TPO: Temperature programmed oxidation

TPD: Temperature programmed desorption

XRD: X-Ray Diffraction

ICP-MS: Induced Coupled Plasma-Mass Spectroscopy

GC: Gas Chromatography

GC/MS: Gas Chromatography/ Mass Spectroscopy

CHAPTER 1 LITERATURE REVIEW

1.1 Introduction

Environmental concerns and the limited availability of the world's crude oil reserves are the main driving forces for a future shift towards more sustainable feedstocks for the chemical industry. Methane is being considered as an alternative feedstock to those derived from the oil industry. Methane is the principal constituent of natural gas, landfill gas, or coal-bed methane. It is also a by-product of oil refining and the manufacture of chemicals. Currently, methane is being used for home and industrial heating as well as for the generation of electrical power. Methane is greatly under-utilized for chemicals and liquid fuels although the methane reserves exceed the liquid petroleum reserves[1]. Methane could be the fuel of the future for a short term.

The geographical distribution of natural gas is illustrated in Figure 1.1. Methane is found in large amounts in regions that are far removed from industry and it is often produced offshore. However, the main problem for effective methane usage is transportation. Pipelines may not be available for transporting this remotely accessed gas to potential markets and liquefaction for shipping by ocean-going vessels is expensive[2]. 11% of this gas is re-injected and another 4% is flared or vented, which is a waste of a hydrocarbon resource[3].

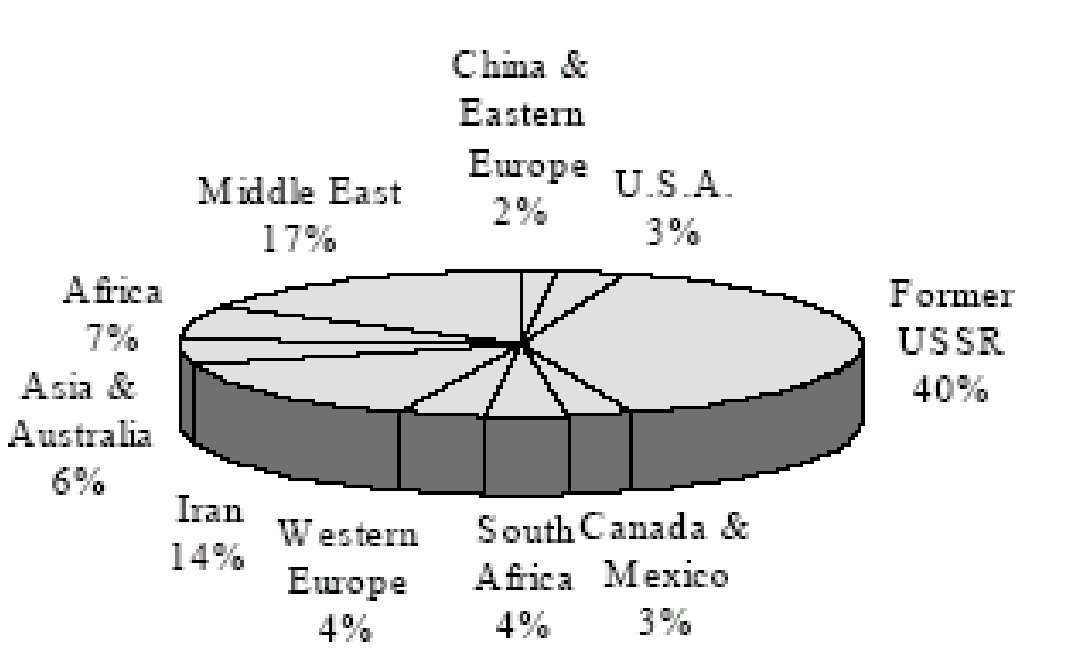

Figure 1.1: Geographical distribution of proven natural gas reserves[3]

One of the solutions to this problem considered is the conversion of methane to value-added liquid fuel products, such as higher hydrocarbons and oxygenates.

1.2 Methane conversion to methanol and formaldehyde

Methane conversion follows two routes[4] i.e. indirect and direct conversion as shown in equation (1).

$$CH_4 \overset{1}{\Rightarrow} CO / H_2 \overset{2}{\Rightarrow} CH_3OH \overset{3}{\Rightarrow} CH_2O \qquad (1)$$

$$CH_4 \overset{4}{\Rightarrow} CH_3OH$$

The presently used commercial indirect conversion of methane includes the production of methanol from methane via high temperature catalytic steam reforming

to form synthesis gas ($CO + H_2$) in step 1. This energy-intensive, endothermic reaction is followed by catalytic conversion of the synthesis gas to CH_3OH.[5, 6] The direct partial oxidation of CH_4 to CH_3OH (step 4) is being widely studied because it is a simple one-step, exothermic process. This conversion eliminates the need for synthesis gas (step 1). If this can be done efficiently, the goal of achieving a cost-effective route to methane oxidation might be within reach. Direct conversion technologies can be classified into four groups, that is:

- direct partial oxidation (to methanol, methyl halides and others),
- oxidative coupling (to ethylene),
- reductive couplings and
- other direct conversion processes.[7]

The direct partial oxidation of methane to methanol and formaldehyde is important as methanol can be used as an energy source for example fuel cells and starting material for various chemical syntheses, such as the production of chloroform, methyl chloride. Methanol is also used as a solvent in paint strippers, paints, carburettor cleaners, and automobile windshield washer solutions.[8] Methanol is a liquid at room temperature and could be transported to market utilizing the existing petroleum pipeline, tanker network, and distribution infrastructure.

Methane is a very stable molecule. The conversion of this molecule generally requires high activation energy. The products obtained as a result of the oxidation reaction-methanol and formaldehyde- may undergo further oxidation to carbon oxides.[5, 9] The attempt to reach a high degree of methane conversion efficiency into methanol or formaldehyde leads to a sharp decrease in their selectivity.

Methane can be partially oxidized by oxygen to methanol by several methods, which include:

- biological oxidation
- gas phase oxidation[10] and,
- catalytic oxidation

In biological oxidation, methane mono-oxygenase (MMO) in methanotrophic bacteria catalyzes the selective oxidation of methane to methanol by oxygen under ambient conditions. The iron centers of MMO and cytochrome P-450 mono-oxygenase (heme iron and μ-oxo-bridged binuclear iron center, respectively) play a vital role as catalytic active sites in mono-oxygenation of various substrates with NADH as a reductant.[11, 3] Moro-oka[12] quoted the most probable mechanism proposed by Groves et al for hydrocarbon oxidation using cytochrome P-450. Figure 1.2 gives the structure of the active centre and the proposed mecchanism. This biological oxidation is an attractive process of what could be achieved if the process were commercialised.

The gas phase reaction is characterised by the following features:

- The reaction temperature usually starts around 370°C. High pressure shifts the initiation temperature to the lower side.
- The highest selectivity towards methanol is obtained at around 400°C.
- Methane conversion and selectivity results depend strongly on the methane to oxygen ratio in the feed. High methane conversion is attained at high oxygen concentration but methanol selectivity is low.
- Methanol is a stable product while formaldehyde decomposes quickly to carbon monoxide.[13]

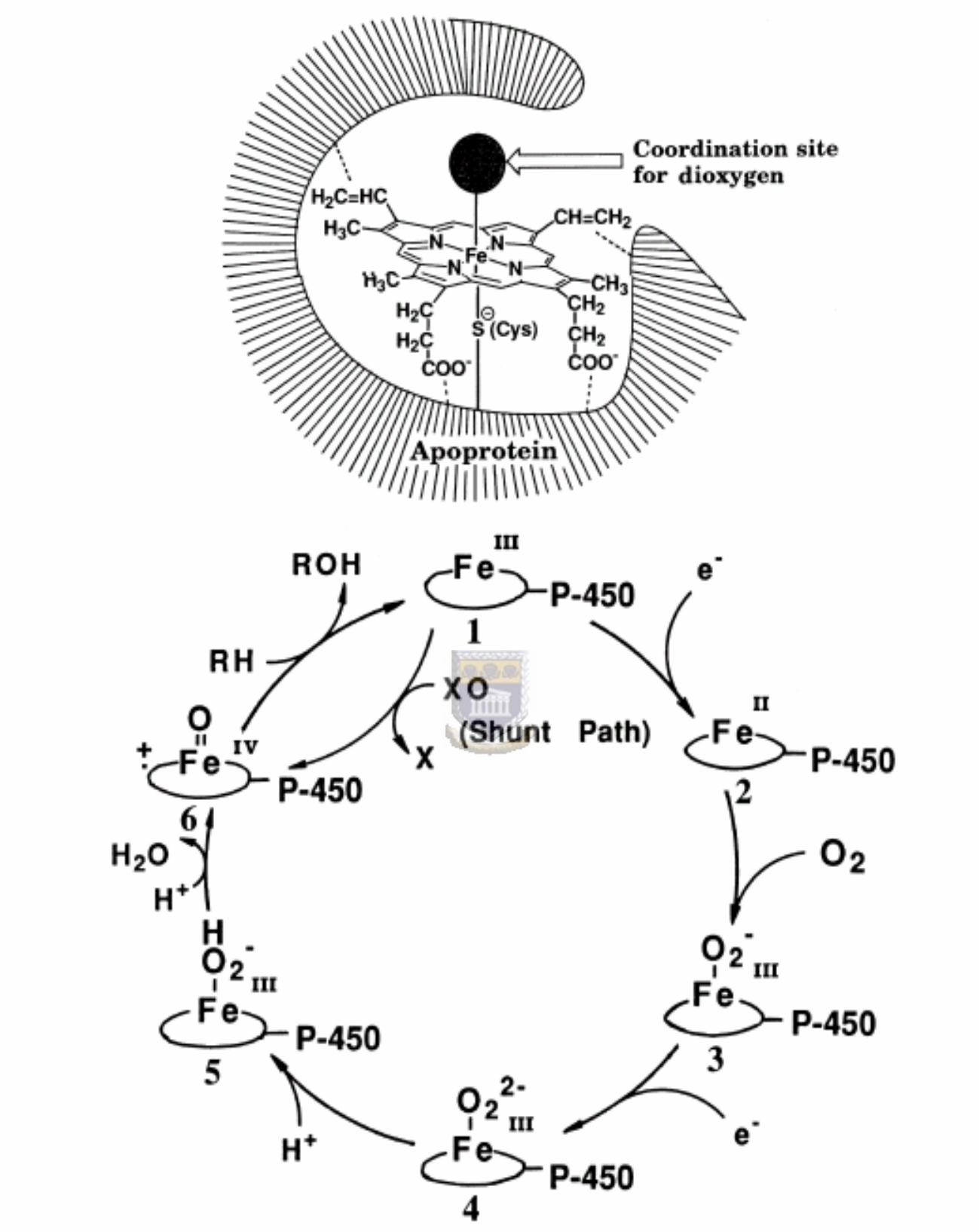

Figure 1.2: Structure of active site (top) and proposed reaction mechanism for cytochrome-P450[12]

Catalytic oxidation is a more effective method for the conversion of methane to methanol and formaldehyde. Catalysis has been broadly defined as a 'process whereby a reaction occurs faster than the uncatalysed reaction. The activation barriers of catalysed reactions are generally lower than for the uncatalysed process and the reaction is kinetically accelerated'.

1.3 Catalytic Oxidation

1.3.1 Mechanism for partial oxidation reactions

Molecular approach

The Mars-van Krevelen mechanism[14] proposed in 1953 usually occurs for partial oxidation reactions (see Figure 1.3). It involves both a redox function of the solid catalyst surface and oxygen insertion of the reagent molecule from lattice oxygen ions. The reaction conditions are demanding since the reaction involves abstraction of the substrate H atom, insertion of an O atom and electron transfer. This occurs on active sites with a size that varies from several atoms up to a complete crystalline face.

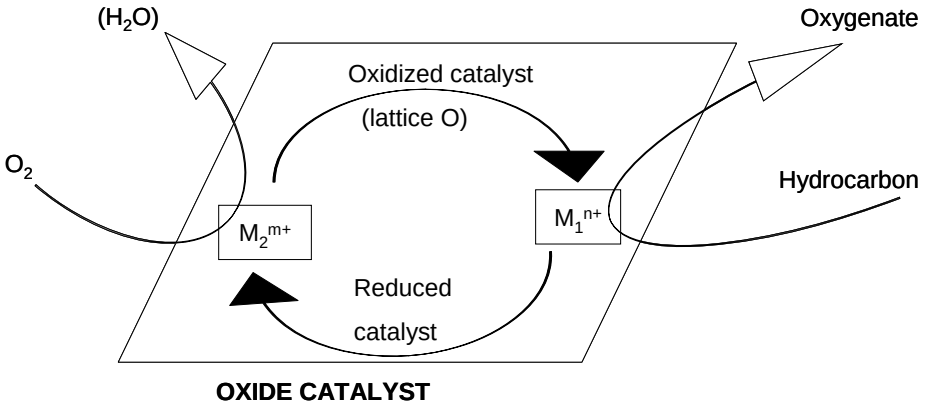

Figure 1.3: The Mars-van Krevelen reaction scheme for selective oxidation[15]

Since the early 1980s a molecular approach concept was developed that promotes the view of surface atoms which cause the complex reaction mechanism to take place at the catalyst surface. In this approach, several cations and oxygen ions are considered to constitute the active site[16]. Oxygen species on an oxide surface exhibit different properties. Monoatomic species with the electrophilic or nucleophilic character (O^-, O^{2-}) may exist or diatomic species (O_2^-, O_2^{2-}). The electrophilic character of the oxygen species is important since it favours the deprotonation of the nucleophilic hydrocarbon molecule or the weak allylic attack. Electrophilic oxygen species correspond to O^-, superoxo (M-O-O) or peroxo (O_2^{2-}) species while nucleophilic species are metal oxo species (M = O).

The kinetic analysis of the high pressure partial methane oxidation has shown that[17]:

1. The process has two phases that differ in their time scales.

The very short initial stage involves the chain-branched mechanism, which is very similar to the mechanism of H_2 oxidation. It is very sensitive to initial conditions, especially pressure. This stage (auto-accelerating phase) is completed by a subsequent quasi-stationary phase, which is characterised by the approximate equality of the rates of branching and radical recombination. The second phase is considered as a degenerate chain-branched mechanism. Chain branching is connected with intermediate products. The most important branching reactions in this phase are interaction of methyl peroxide and hydrogen peroxide radicals with methane, methanol, formaldehyde and H_2O_2.

2. Formation of the main products (CH_3OH and HCHO) proceeds simultaneously and independently. Only a relatively small part of the formaldehyde product forms from the oxidative and thermal decomposition of methanol. The difference in their

concentrations is only due to the difference in their stability to further oxidation. The largest amount of methanol forms at the end of the reaction just before total oxygen consumption. It explains the very high sensitivity of methanol yield to residence time and temperature during incomplete oxygen conversion.

3. The increase in O_2 concentration decreases the selectivity for methanol formation and reduces the whole rate of the process.

4. Two stationary regimes of the process exist differing in radical concentration and process velocities of over 4 orders of magnitude. There additionally exists a critical pressure for the transition between these two regimes.

A high-pressure region above the critical pressure of the initial chain-branched phase provides a very high velocity for radical generation, so that any catalyst, promoter, or other source of radicals can hardly compete with it. Usually their influence on the process is negligible. It also explains the failure of numerous attempts to improve the high-pressure process by means of a catalyst.

Dowden's 'virtual mechanism' for selective oxidation of methane as cited in[18] and illustrated in Figure 1.4 was designed based upon deciding the nature of the important catalyst functions for the oxidation of methane to methanol, formaldehyde and carbon oxides. It is a classical Langmuir- Hinshelwood mechanism, where all the reactions take place on the surface. The dissociation of methane and the activation of dioxygen require quite different sites. Dowden mechanism suggests that the catalytic cycle could be closed by the elimination of water from neighbouring –OH groups, to regenerate the active sites for oxygen dissociation. Another feature of the mechanism is that it bypasses the formation of methanol as an intermediate and methanol production will require a reductive interaction of adsorbed hydrogen with $–OCH_3$.

However the mechanism does not take account of the gas phase reactions that may occur.

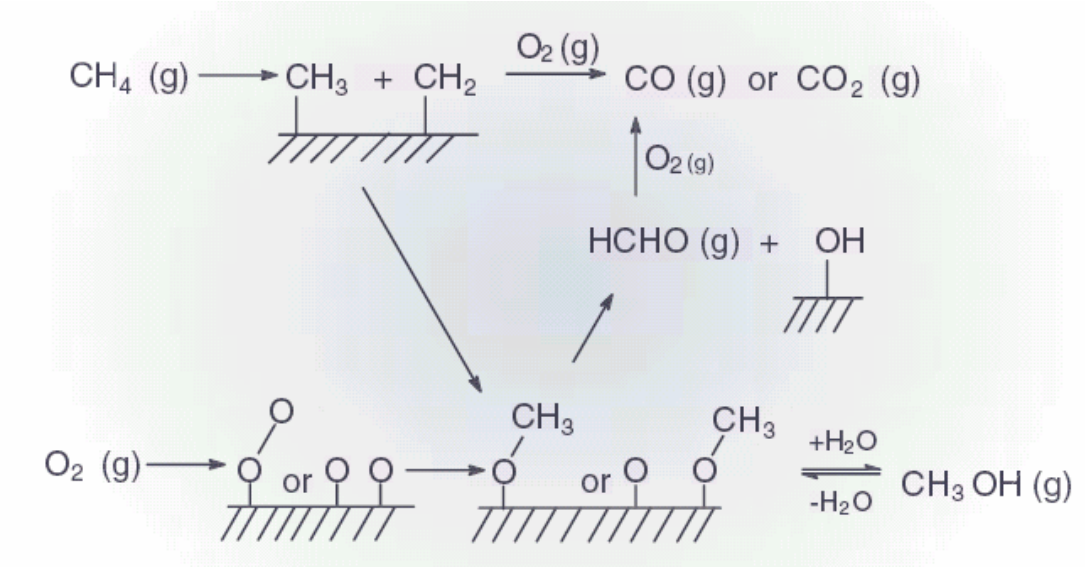

Figure 1.4: Virtual mechanism proposed by Dowden for the conversion of methane to methanol[19]

Dehydrogenation (activate methane) and oxygen insertion (formation of methanol) were the two important functions required for the catalyst. Dowden considered that the dehydrogenation functionality could be provided by V^{5+}, Fe^{3+}, Cu^{2+} and the oxygen insertion functionality could be provided by V^{5+}, Fe^{3+}, Zn^{2+}, Mo^{6+}, Ti^{4+}. Using this approach for mixed oxides, phosphates and tungstates, promising yields of methanol were found, e.g. $Fe_2O_3.MoO_3$ at 50 bar, 500°C, a 97:3 mixture of methane: oxygen gave a yield of 0.87 $kg_{methanol}/kg_{catalyst}/h$. Hutchings et al.[20, 21, 10] extended this approach by adding a further aspect of the virtual mechanism, namely the stability of the product under the conditions in which it is formed.

Taylor and Hutchings [20] utilised Winter's [22, 23] data for the activation of oxygen using the $^{16}O_2/^{18}O_2$ exchange reaction. The exchange reactions may take place by one or a combination of reaction mechanisms. Homonuclear exchange (R_0) is exchange catalysed by the oxide surface, but does not involve exchange with oxygen of the oxide lattice. Exchange of lattice oxygen with the gas phase can also take place via mechanisms denoted as R_1 and R_2 which are numbered in accordance with the number of lattice oxygen species participating in the exchange process. The oxides MoO_3, and WO_3 showed exchange of the whole of their lattice oxygen with the gas phase. The diffusion of oxygen throughout the lattice of these solids was faster than the surface exchange, which was therefore the rate determining process. The exchange mechanism for these oxides operates by a combination of R_1 and R_2 processes. R_3 is the process of oxygen exchange over these oxides. This type of mechanism involves exchange with the whole of the lattice oxygen and not merely the surface layer, indicating that the mobility of oxygen throughout the oxide lattice was a facile process. The lability of lattice oxygen is an important concept in selective oxidation reactions, particularly with respect to the Mars-van Krevelan mechanism, in which lattice oxygen is the active oxygen insertion species.

Methanol stability was determined over various oxides based on the temperature at which 30% of methanol feed was converted to carbon oxides. With a methanol/O_2/He ratio of 1/4/12 at 12000 h^{-1} over Sb_2O_3 oxides methanol showed exceptional stability as only 3 % methanol conversion was exhibited at 500°C. The higher temperature oxides-MoO_3, Nb_2O_5, Ta_2O_5 and WO_3- showed high methanol conversion to formaldehyde and dimethylether which are desirable by-products from methane partial oxidation process.[21] The most active catalyst for the activation of methane

based on the CH_4/D_2 exchange reaction at 500°C was Ga_2O_3. CH_3D was the primary product whilst traces of CH_2D_2 were detected at higher rates of exchange. ZnO also showed high activity. MoO_3, Nb_2O_5, Ta_2O_5 and WO_3 were reduced under reaction conditions and were either inactive or showed very low activity for the exchange reaction.[21]

1.4 Catalyst development for the oxidation of methane to methanol and formaldehyde

A key to direct conversion of CH_4 to CH_3OH is the development of catalysts that will activate the relatively inert C-H bond in CH_4. Although successive elimination of H atoms from CH_4 decreases the free energy, complete oxidation is thermodynamically more favoured than partial oxidation. Thus, the catalysts developed to date for partial oxidation only yield significant selectivity to CH_3OH at low conversions. At higher conversions, complete oxidation occurs.[24]Generally, catalysts operate under conditions where gas phase homogeneous reactions are more effective and the partial oxidation products are unstable. Based on the hydrogen balance current kinetic models predict a limiting selectivity of 67% methanol for the homogeneous process. It is against this background that new approaches for the development of more effective catalysts are required.[20] Both homogeneous and heterogeneous processes have been reported for CH_4 oxidation.[24] Separation of the products from the reactants in homogeneous catalysis as well as the uncertainty in the selectivities may present difficulties. The approach to catalyst design is based on three components and for selective oxidation the approach involves identifying catalysts that:

- do not catalyse the oxidation of the required product under the reaction conditions;
- activate the oxidant;
- activate the substrate (hydrocarbon).[21]

The desired catalyst needs to provide a product with high activity, selectivity and stability. The active phase must be in a sufficiently highly dispersed form which results in a large specific surface area and consequently in a maximum specific activity[25]. Metal-based catalysts have been a source of interest since the early 1970s. Rare earth oxides and alkaline earth oxides, and in general non-reducible metal oxides, activate methane and ethane only at temperatures higher than 500-600°C.[26] Most of the catalysts used for methane partial oxidation are metal oxides. It has been well recognized that the acidic and basic nature as well as the redox properties are the most important properties of metal oxide catalysis. Although redox properties are considered to be the most important in the catalytic oxidation of hydrocarbons, Moro-oka et al.[27] demonstrated that the acidic property of metal oxide catalysts plays some important roles in the catalytic oxidation of hydrocarbons, especially in determining the selectivity of the reaction product.

Aoki et al.[28] cited a study by Atroschenko in which various metal oxides were investigated as catalysts for the partial oxidation of methane. He reported that MoO_3 was one of the best catalysts at elevated temperatures and pressures. MoO_3 has been extensively studied for this reaction in unsupported and supported form and in conjunction with additional catalyst components. WO_3 has been less well studied than MoO_3 for methane partial oxidation. Although Ga_2O_3 and ZnO have the ability to activate methane, MoO_3 and WO_3 were chosen because methanol was relatively stable

and selective oxidation products, mainly formaldehyde, were predominant. MoO_3 and WO_3 also show moderate activity for heterolytic oxygen exchange which operates by an R_3 type mechanism involving complete exchange of the bulk lattice oxygen in the gas phase. MoO_3 demonstrates oxygen insertion ability by virtue of its n-type semiconductivity. V_2O_5 also has a heterolytic oxygen exchange mechanism similar to MoO_3 and WO_3. It is a well known oxidation catalyst which has been studied for methane partial oxidation in supported form and also exhibits dehydrogenation and oxygen insertion properties which are important factors for selective methane oxidation.[20]

In an investigation of the reaction mechanism of formaldehyde formation over silica catalyst in the temperature range 630-780°C[29, 30] it was proposed that formaldehyde was formed by a surface reaction rather than by gas-phase radical reactions. Residence time experiments indicated that both formaldehyde and C_2 hydrocarbons were primary products and apparent activation energies determined for total methane conversion, formaldehyde and ethane production, indicated that different pathways were operative. The proposed mechanism is shown in Figure 1.5.

Methane is suggested to dissociate on a siloxane bridge and be chemisorbed as two possible intermediates, one of which decomposes to generate the observed formaldehyde, whilst the other releases methyl radicals which couple in the gas phase to form ethane. The siloxane bridges may be more accessible in the silica gel than those generated upon fumed silica.[10]

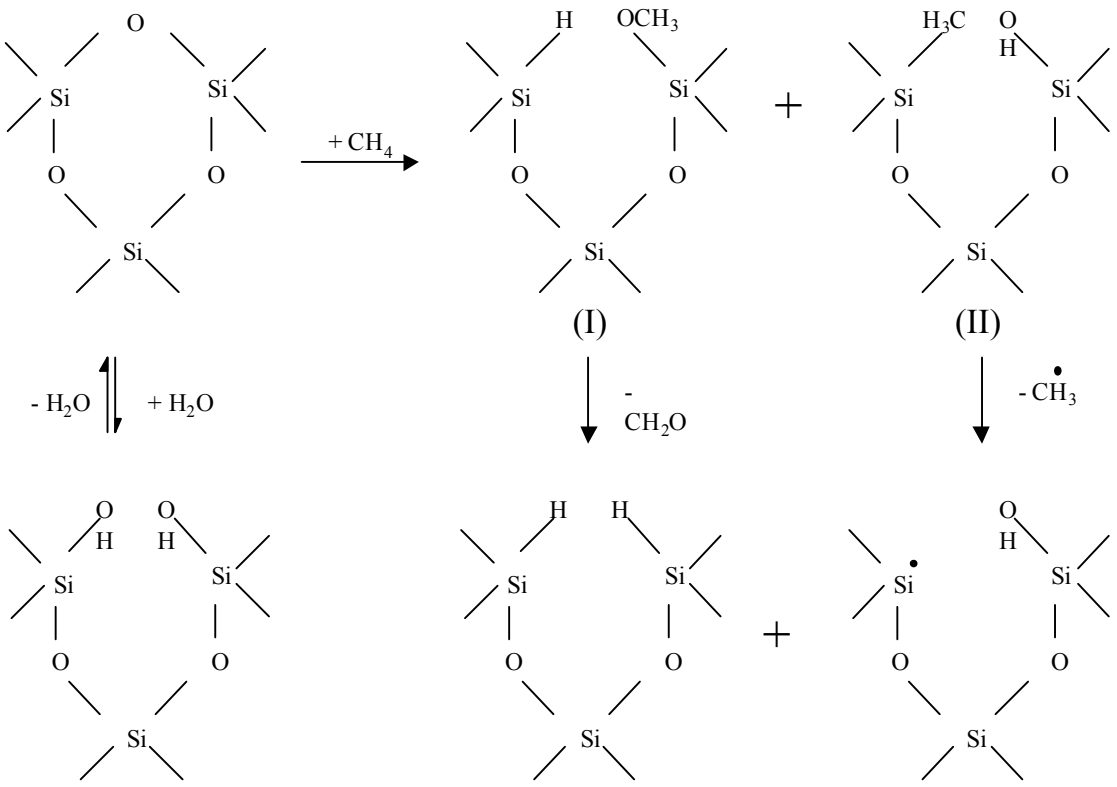

Figure 1.5: Schematic mechanism for methane oxidation over SiO_2 catalyst[10]

Spencer et al.[31] obtained 25% formaldehyde selectivity with 6.9% methane conversion using O_2 as oxidant over Na-free MoO_3/SiO_2 catalyst. Liu et al.[32] found that the catalytic activity of MoO_3/SiO_2 for the partial oxidation of methane by N_2O was significantly enhanced when a small amount of water vapour was added to a feed gas. Zhang et al.[33] investigated the catalytic performance of Mo/ZrO_2 catalysts in selective oxidation of methane to formaldehyde with molecular oxygen as oxidant. 47.8% formaldehyde selectivity and 4.0 % yield of formaldehyde were obtained on 12 wt.% Mo/ZrO_2 catalyst at 400°C, 5.0 MPa, $CH_4/O_2/N_2$ (10/1/3) at 12,000 ml/g catalyst h^{-1}. The physico-chemical properties of these catalysts, such as surface area, structure, particle size, reducibility, ion oxidation state and surface composition have been comparatively characterized by using BET, X-ray diffractometer (XRD), LR spectra

(LRS), H_2-temperature-programmed reduction (TPR) and X-ray photoelectron spectroscopy (XPS) techniques. The interaction between Mo and ZrO_2 induced the changes in physico-chemical properties, which in turn determined the catalytic performance. $Zr(MoO_4)_2$ in Mo/ZrO_2 catalysts were closely related to the formation of formaldehyde. The higher the density of MoO_3, the higher was the specific activity. The Mo=O species of $Zr(MoO_4)_2$ enabled selective oxidation of methane to formaldehyde, while the many more lattice oxygen species and bulk MoO_3 accelerated further oxidation of formaldehyde.[33]

Selective oxidation of methane in CH_4–O_2–NO_2 was examined by Takemoto et al.[34] using MoO_3 catalyst at atmospheric pressure in the temperature range of 500-650°C. The selective oxidation was enhanced with the addition of NO_2 to the reaction system of CH_4 and O_2, in comparison with the gas-phase reaction. The initiation reaction took place between CH_4 and NO_2. The presence of MoO_3 catalyst increased CH_2O selectivity and decreased CH_3OH selectivity, compared with those for the gas-phase reaction in CH_4–O_2–NO_2. Based on variations in reaction selectivities at several reaction conditions, it was explained/concluded that formaldehyde was a main product on the MoO_3 catalyst and methanol was formed through gas-phase reactions[34] Taylor et al.[20] found that methanol was most stable over the oxides MoO_3, WO_3, Nb_2O_5, Ta_2O_5 and SbO_3 whilst it was destroyed readily by CuO and Cr_2O_3. With the exception of Sb_2O_3 the conversion of methanol over these catalysts was relatively high, however, high selectivity to the partially oxidised products formaldehyde and dimethyl ether were observed. The reaction was carried out at 15 bar pressure and between 450-500°C.

Kawabe et al.[35] prepared SnO_2 films on sapphire substrate by the reactive radiofrequency (RF) magnetron sputtering method. Selective oxidation of methane was performed on these materials with O_2. The dense texture type SnO_2 film showed a higher reactivity for the oxidation of CH_4 than that of the columnar texture type one. The selective formation of HCHO was especially observed for the dense texture film and CH_3OH formation on the SnO_2 columnar texture type film at around 620K. The oxidation of CH_4 was therefore strongly affected by the surface morphology of SnO_2 film.[35]

V/SiO_2 and/or Ba/SiO_2 catalysts revealed clearly that CH_4 is activated by O_2 only at moderate temperatures (ca. 823K) if small amounts of NO are present in the feed stream. The addition of NO (1.0 vol.%) was to increase the radical population in the gas phase and to shift selectivity to oxygen-containing molecules. CH_3OH was easily oxidised in the presence of a high specific area V/SiO_2 redox catalyst than in the case of the non-redox Ba/SiO_2 catalyst, for which HCHO and CH_3OH yields remain at a level only slightly lower than for the homogeneous reaction. On the contrary, higher yields to HCHO (1.7%) and CH_3OH (1.6%) can be achieved at 923K over a low specific area catalyst.[36]

Cobalt oxide showed intermediate performance for methanol stability and has a very high activity for homonuclear oxygen exchange and proved unstable during heterolytic oxygen exchange studies.[20] The metals that are active for the oxidative addition of methane to a metal complex include Ir, Rh, Re and Pt. H_2PtCl_5/Na_2PtCl_4 in aqueous solution can oxidize methane at 120°C and 60atm to give a mixture of methanol and methyl chloride, which system can be catalytically operated in the presence of oxygen.[13]

Palladium catalysts are effective for the hydroxylation of higher alkanes and aromatics when using O_2-H_2 gas mixture. Pd activates hydrogen easily. Oxygen was reduced by this activated hydrogen which is then transformed to the active oxygen species for the selective oxidation of alkanes and aromatics. Methane oxidation by O_2-H_2 mixture was performed in the temperature range 573K to 773K and a pressure range of 4.2 to 50.7kPa over Pd based catalysts (Pd supported on various materials: SiO_2, Al_2O_3, H-ZSM5, Fe_2O_3/SiO_2 and CuO/SiO_2). Carbon oxides (CO and CO_2) were the only products obtained and no methanol, formaldehyde or C_2 hydrocarbons were produced. The hydrogen in the mixture increased the conversion of oxygen greatly, but decreased that of methane. This was ascribed to the competitive reaction between H_2 and CH_4 toward O_2. Hence such catalysts were not appropriate for the partial oxidation of CH_4 in the presence of H_2.[37]

The oxidation of methane to oxygenates over metallic palladium dissolved in oleum (H_2SO_4) was studied by Michalkiewicz and co-workers.[38] Methanol was obtained by the transformation of methane into methyl bisulfate and dimethyl sulfate. Subsequently, methanol was formed as a result of ester hydrolysis. The reaction conditions were temperature 160°C, pressure of methane 3.5MPa, time 2h, content of sulphur trioxide in fuming sulphuric acid 30% (SO_3 is a strong oxidizing agent). Palladium can be recovered and used many times without reduction in the process yield. The by-products formed in the process may be reclaimed and reused.[38]

Since methane mono-oxygenase is an enticing example for the oxidation of methane to methanol by oxygen under ambient conditions, Fe containing solid catalyst could be a promising catalyst for selective oxidation of methane to methanol if the Fe site is

situated in suitable structural conditions. Some iron containing catalysts are active for the partial oxidation of methane. Iron oxide (Fe_2O_3) showed mid-range activity for oxygen exchange and methanol stability. It is an important component of many methane partial oxidation catalysts for example $MoO_3/Fe_2O_3/SiO_2$ and Fe/SiO_2.[20] [Fe]SOD catalyst (> 10 wt.% Fe in sodalite zeolite) produces methanol with a high selectivity at > 400°C, and 54.4atm. However it was difficult to evaluate the role of the catalyst since the homogeneous radical reactions in the gas phase prevail at such high reaction pressure.[37]. It was confirmed that the empty reactor tube was more effective for methanol production than the [Fe]SOD catalyst under such reaction conditions. It was found that catalysts with Fe in aggregative state show better reaction performance, and [Fe]zeolite catalyst shows similar activity and selectivity with Fe_xO_y/SiO_2. Cu^{2+} exchanged Fe-ZSM-5 catalyst produced 0.6% methanol from the oxidation of methane by N_2O. Cu played a more significant role in the formation of methanol than Fe since no methanol was produced over Cu-free H-FeZSM-5. When a small amount of Fe was doped into ZnO and silica, formaldehyde formation was enhanced (< 1% yield) but no methanol was formed. Fe-Nb-B-O complex oxide or Li- or Zn-doped $Fe_2(MoO_4)_3$ catalysts produced 4% formaldehyde from the oxidation of methane by oxygen and no formation of methanol was reported[11]. Lunsford[3] cited a study by Otsuka et al. in which $FePO_4$ was a model catalyst for the production of methanol and formaldehyde when H_2 is added to the methane and oxygen reagents. H_2 reacts with O_2 to form a surface peroxide species, which is responsible for the activation of methane. They achieved methanol and formaldehyde selectivities of 23% and 45% respectively.[3]

Wang and Otsuka[37, 11, 16] also examined Fe containing compounds for CH_4 oxidation by O_2-H_2 mixture performed in the temperature range 573K to 773K and pressure range 4.2kPa to 50.7kPa. The presence of hydrogen increased methane conversion for $FePO_4$, Fe-APO-5 (Fe: Al: P; atomic ratio = 0.1:0.9:1.0), ferrisilicate (ZSM-5 analogue, Fe: Si; atomic ratio = 1:50), and Fe-ZSM-5 (Fe content = 2 wt.% and Si/Al = 50) catalysts while for Fe_2O_3 methane conversion decreased. The addition of H_2 induced methanol production using $FePO_4$ and Fe-APO-5. These two catalysts have iron atoms in tetrahedral coordination with oxygen atoms. FeO_4 tetrahedral units are isolated by PO_4 or AlO_4 tetrahedral units. V, Cr, Mn, Co, Ni, Cu, Zn, and Al phosphates showed no favourable effect with H_2 on the partial oxidation of CH_4. Otsuka and Hatano[39] examined the activity of silica-supported oxides of Ca, Mg, La, Ce, Pr, Sm, Y, Fe, Al, Ga, Bi, Zr, B, P, As, W, Sb, Sn, Nb and Ba. It was observed that catalysts having an intermediate acidity were most active for methane conversion, but selectivity to formaldehyde increased with the acidity of the oxides with formaldehyde yield < 0.5%.[40]

There have been several attempts to oxidize lower alkanes by using heteropoly catalysts. The catalytic function of heteropoly compounds in the solid state has attracted much attention because their redox and acidic properties can be controlled at atomic/molecular levels. The addition of transition metals to heteropoly compounds is important to control the redox properties and to enhance the catalytic performance. It has been reported[41] that the hydrogen form of $H_3PMo_{12}O_{40}$ catalyzed the oxidation of lower alkanes and that the substitution of V^{5+} for Mo^{6+} modified the catalytic activity and selectivity. The addition of iron under oxygen-poor conditions increases conversions. Iron promotes the re-oxidation of the catalyst.[41]

Chan and Wilson[42] carried out the oxidation of methane over porphyrin and phthalocyanine complexes encapsulated in zeolites with molecular oxygen under the reaction conditions of 3.4 atm and 650 K. CO_2 was the main reaction product with a very poor methanol selectivity (<10%). However Raja and Ratnasamy[43] converted methane to a mixture of methanol and formaldehyde at ambient conditions with TON (turnover number) above 100 and high selectivity (CO_2 less than 5%) using phthalocyanine complexes of Fe and Cu encapsulated in zeolites as catalysts and O_2/tert-butyl hydroperoxide as oxidants.

Mixed metal oxides for example silica-alumina with redox properties are important catalysts for selective oxidation of hydrocarbons. The bi-functional catalysis protects the organic reactant from complete oxidation by a cycle whereby it reacts rapidly with an intermediate oxide of limited reactivity but at negligible rate with O_2 and with other metal oxide groups that might convert it into CO_2 and water.[3] Mixed oxide catalysts showed very high selectivity for formaldehyde (> 85%) at low methane conversions at relatively low reaction temperatures, <850 K, where oxidative coupling to C_2 hydrocarbons is not normally observed.[44]

1.4.1 Supported catalysts

In order to obtain a catalyst with high activity, selectivity and stability, the active component is usually deposited on the surface of a support, a highly porous, thermostable material and is able to disperse the active species as well as to increase its thermal stability and hence increase the catalyst life.[45, 46, 47, 48]

Supported catalysts in general are rapidly gaining importance, despite the traditional preference of preparative chemists for homogeneous reactions. Many examples in the

literature and in industrial practice illustrate conclusively that the adsorption of a reagent on a carrier may significantly up-grade a chemical transformation into practicability, selectivity, and efficiency,[25, 49, 50] not to mention the advantages in the work-up and the options for the recovery of the reactant. Many of the commonly used inorganic support materials have polar properties or are polyelectrolytes. Any charged or polarizable substrate in solution will accumulate near to their surface due to dipole-dipole and/or electrostatic interactions. This may increase the effective concentration of the dissolved reaction partner near the interface by several orders of magnitude, which may result in a substantial acceleration of the reaction.[51]

In the oxidation of hydrocarbons, supported metal oxide catalysts exhibit different activity and selectivity to the desired oxygenated hydrocarbon products, depending on the support material. Compared to bulk oxides, higher activity and selectivity to the desired products over supported catalysts can in part be attributed to the formation of easily reducible supported metal oxide phases.[29] The dispersion of the active phase on supports is one of the most important parameters for catalytic reactions on supported oxides. It was shown that metal oxide-support interaction controls both the reducibility and dispersion of the active phase and in some cases leads to dramatic enhancement in catalytic activity and selectivity relative to unsupported oxides.[52] Increasing dispersion is generally obtained by decreasing the concentration of the active species on the support, without the real control of the nuclearity of the deposit. The supported oxide can exist as clusters, heaps, or isolated ions. The nuclearity of the deposit can be controlled by the use of polyoxometalates. These anionic oxide clusters have the advantage of a known nuclearity. Moreover, since generally they are soluble

in various solvents without structure change, they can be used directly, which makes deposition easier.[52]

SiO_2 and Al_2O_3 are both well known as acid-base catalysts and as supports for hydrogenation and oxidation reactions.[53] The catalytic activity of SiO_2 and Al_2O_3 in oxidation reactions is due to their weak acidity. Cairati and Trifiro[53] concluded that the oxidation of methanol to formaldehyde occurs through the elimination of protons from the surface methoxy group by adjacent oxygen ions upon SiO_2 and Al_2O_3 supports. Other supports, such as Al_2O_3, TiO_2, ZnO, MgO and SnO_2 have also been studied.[54, 55, 56] It has been reported that ZnO does not catalyse methane conversion to formaldehyde but no detailed investigation has been done for ZrO_2 as a support for metal oxide catalyst in methane oxidation.[29]

Silica-supported V_2O_5 is the most active catalyst for conversion of methane to formaldehyde by using molecular oxygen or N_2O and has been extensively researched for the last two decades. Considerable space-time yields of formaldehyde have been achieved over the silica-supported V_2O_5 catalysts. Though there have been conflicting views over active sites and reaction pathways for the selective oxidation of methane to oxygenates over the silica-supported catalysts[57, 58, 59, 60]. Wang et al.[60] studied the selective oxidation of methane in fixed bed down-flow quartz reactor. They found out that the accessible surface tetrahedral V^{5+} species were the active sites for methane conversion to oxygenates. On the basis of the accessible surface tetrahedral V^{5+} species, the turnover frequency for both methane conversion and oxygenates formation substantially decreased with increase in vanadium content with 1 wt.% V_2O_5-SiO_2 xerogel catalyst exhibiting the highest activity as well as the highest selectivity for methane conversion to oxygenates. This result appears to suggest that

the accessible surface tetrahedral V^{5+} species tend to form polymeric V^{5+} species at high vanadium content which is not active for methane conversion to oxygenates.

The partial oxidation of methane to methanol and formaldehyde by molecular oxygen was investigated over crystalline silica and silica supported $FePO_4$ at a pressure of 1 atm and in the temperature range 723–973 K. The quartz phase of $FePO_4$, as well as silica supported $FePO_4$ prepared by impregnation (5 wt.%), were tested in a continuous flow reactor. $FePO_4$ showed high selectivity to formaldehyde at low conversion which suggests that formaldehyde is the primary reaction product but selectivity decreased rapidly with an increase in conversion. The highest space-time yield of formaldehyde observed for the unsupported catalyst was 59g/kg_{cat}-h. Above 5% methane conversion, carbon oxides were the only products. Exhibiting a formaldehyde selectivity of 12% at about 10% conversion formaldehyde selectivity did not fall off rapidly with silica-supported $FePO_4$. Quantifiable yields of methanol were observed at very low conversion levels (below 3%).[61] Wang and co-workers[62] studied the partial oxidation of methane with both oxygen and N_2O over $FePO_4$ supported on MCM-41 (one of the mesoporous molecular sieves). Characterizations with XRD, Raman spectroscopy, XPS, and H_2-TPR suggested that the supported $FePO_4$ species with loading amounts lower than 40 wt% are located and dispersed in the mesopores of MCM-41. These $FePO_4$ species can be reduced more readily than the unsupported $FePO_4$ at lower temperatures. Methane is selectively converted to methanol, formaldehyde, and dimethyl ether over the supported and the unsupported $FePO_4$ with N_2O at milder temperatures (300–500°C), while formaldehyde is mainly produced along with carbon oxides with oxygen at relatively higher temperatures (400–600°C).[62]

Supported $FePO_4$ catalysts were prepared by impregnation of alumina (Alfa Aesar, 182 m^2/g), titania (Degussa, 61 m^2/g) and zirconia (Degussa, 47 m^2/g) with aqueous solutions of ferric nitrate and ortho-phosphoric acid. Prior to impregnation the supports were dried at 673K in air. It was observed that silica supported $FePO_4$ exhibits relatively high activity and selectivity for oxidation of methane to methanol and formaldehyde compared with other support materials.[29]

Yamada et al[63] measured methane oxidation catalysis on a series of silica support doped with one of 43 elements at three loadings to build a database to determine which element is suitable for this reaction. The catalytic performance was examined at around 773K with GHSV = 4760 h^{-1}. The ratio of CH_4/O_2 in the feed gas was varied from 90/10, 80/20 and 70/30 at atmospheric pressure. The elements found suitable for partial methane oxidation to methanol and formaldehyde were V, Fe, Sc, W, Mo and Os. Sc/SiO_2 is a good catalyst for partial methane oxidation and was active at low CH_4 concentration.[63]

1.5 Effect of variables on the methane oxidation reaction

1.5.1 Effect of pressure

While increased pressure can often accelerate reactions, it can favour undesirable secondary reactions, such as carbon deposition or the formation of undesirable by-products. Early studies found that high pressures encouraged the formation of methanol, or reduced the reaction time and the reaction temperature.[18] On the other hand the cost of gas compression is one of the most prominent factors in the total product cost.[64] Boomer et al[65] found that at pressures above 180 atm methanol yield

decreased. Therefore there are no advantages in using catalysts at high pressures. Sexton et al [66] studied the effect of pressure on the behaviour of 7Mo-2Na-cabosil in the range 101-1520 kPa using O_2 as an oxidant. At lower pressures the conversion was very small. A very small conversion was noted on increasing the pressure from 101 (0.3%) to 506 kPa (0.5%). On increasing the pressure from 506 to 1520 kPa a large increase in methane conversion from 0.5% to 13.5% was obtained which was accompanied by a decrease in formaldehyde selectivity. Recent work has tried to find optimum conditions for this conversion which study still continues.

1.5.2 Influence of temperature and residence time

Once a high enough temperature for complete oxygen conversion is reached, further temperature increases are undesirable because they may cause a decrease in methanol and formaldehyde selectivities.[64] Sexton et al[66] investigated the performance of different catalysts at various temperatures (500-600°C) with N_2O as oxidant. They found that the homogenous oxidation of methane by N_2O does not occur to a significant extent below 600°C. 5Mo-cabosil gave the poorest methane conversion at all temperatures. 7Mo-2Na-cabosil and 10Mo-2Cu-aerosil gave comparable conversions at each temperature examined. The best conversion, at 550°C was obtained using 2V-cabosil. With 7Mo-2Na-cabosil the selectivity to formaldehyde decreased with increasing temperature. The selectivity to methanol, however, increased with temperature. The combined selectivity to the partial oxidation products was approximately constant (4.5- 5%) at all temperatures examined. High residence time favours complete oxidation.[64]

1.5.3 Influence of the composition of the reacting mixture on the process

The partial oxidation is very sensitive to the methane/oxygen ratio. Methanol selectivity decreases with the reduction of this ratio. In the absence of methane-oxygen mixing volume or radical initiators, no gas phase activation of methane is expected.[67, 64] Hence the catalyst alone cannot activate methane since the void volume between the particles is too small to allow a significant activation of methane. Dilution of the reacting mixture by N_2 and, apparently other non-reactive compounds did not influence the process while the methane/oxygen ratio remained constant. The influence of small impurities of higher hydrocarbons on the process is well established. Their presence in natural gas lowers the necessary reaction temperature without producing changes in product yield. The best reaction conditions for low alkanes in terms of selectivity for the desired product (alkene or oxygenated compound) implies the use of hydrocarbon-rich conditions, thus with oxygen as the limiting reactant. Combustion reactions are thus minimized. The unconverted hydrocarbon can be recycled. The high exothermicity of the reactions of alkane oxidative transformation makes the use of nitrogen as the ballast unsuitable, owing to its poor thermal conductivity characteristics. Excess alkane is more suitable for strongly exothermic reactions.[68] Fornes et al.[1] observed that much higher formaldehyde yields were obtained when the CH_4:O_2 molar ratio in the gas feed was increased from 2:1 to 8:1 while keeping oxygen partial pressure constant at 0.1 (N_2 used as gas balance), temperature and GHSV. Thus, at 600°C reaction temperature and GHSV of about 250,000 l (N) /kg/h, the STY of HCHO obtained at a CH_4:O_2 ratio of 8:1 reached a value of 1370 g/kg/h, that is, about three times greater than the STY value obtained under the same reaction conditions but at a CH_4:O_2 ratio of 2:1

(STY = 441 g/kg/h). The increase in the CH_4:O_2 ratio slightly decreased the conversion of methane but did not significantly affect the formaldehyde selectivity.[1]

1.5.4 Influence of the oxidant

Pure molecular oxygen is the most commonly used oxidant.[41, 69] The reaction of lower alkanes with molecular oxygen is very interesting since dioxygen (O_2) is readily available and has a high reduction potential.[70] Molecular oxygen gave higher formaldehyde selectivity with decreased CO_x selectivity relative to N_2O.[10] The catalytic differences have been ascribed to the differing oxidizing power of N_2O and O_2. In accordance with the Mars-van Krevelen mechanism (in section 1.3.1) the re-oxidation of the catalyst will be less effective with N_2O, compared to O_2. The role of the dioxygen is also to regenerate or to maintain the oxidized state of the catalyst.[14] The oxygen atom incorporated into the substrate stems from the lattice and is in a (–2) oxidation state. The catalyst does not activate methane. Oxygen is the key to methane activation.[67] Oxygen is activated on the surface of the catalyst, thus enabling methane activation.[64] Methane conversion is limited by the oxygen feed concentration, which is kept low to avoid an explosive mixture. Most studies report that as the oxygen concentration increases, the methanol selectivity decreases.[32] Up to 30% savings may be achieved if air is used instead of pure oxygen.[64]

Ye Wang et al[16] reported that the selective oxidation of methane to methanol can be achieved by co-feeding hydrogen with oxygen and methane over $FePO_4$ catalyst. They showed through pulse reaction studies that an active oxygen species was formed in the presence of hydrogen as an activator of O_2. H_2O_2 and N_2O also proved to be effective

for the direct oxidation of methane to methanol over $FePO_4$ catalyst. O_2^{2-} is adsorbed on the surface Fe sites in the H_2-O_2 gas mixture and in N_2O.[16] Generally, conversion of air-based to oxygen-based processes in gas phase oxidation is preferred to reduce polluting emissions.[71]

1.6 Reactors used in oxidation reactions

The reactor design has been concerned with heat and mass transfer effects and pressure drop considerations.

1.6.1 Multiple adiabatic beds in series

This is the most commonly employed configuration for fixed beds and is simple in construction and operation and low in cost. The interstage cooling is done externally or internally using cold feed and/or diluent streams or by generation of steam internally or externally. Oxygen with steam can be used for cooling in a quench bed configuration. This will allow multiple injection of oxygen which will keep the oxygen concentration at a lower level and improve selectivity. Nevertheless, this suffers from dilution of the reacting mixture and the extra cost of steam. Synthesis of methanol is carried out in this type of reactor.[26, 72, 73]

1.6.2 Multi-tubular reactor

Multi-tubular reactors with shell and tube constructions are being used widely for highly exothermic reactions such as the oxidation of ethylene to ethylene oxide and o-xylene to phthalic anhydride. The coolant used may be molten metal, molten salts or water/steam. The main disadvantage of molten metals and salts as coolant is their high

viscosity. In multi-tubular reactors with fast exothermic reaction, various innovative attempts to improve selectivity and conversion for commercial oxidative reactions have been made.[26, 72]

1.6.3 Fluidized bed reactors

Fluidized bed reactors, though an inherently complex system of design and operation, appear quite attractive because of their superior heat management ability. The characteristics of the fluidized beds are dependent on the hydrodynamics determined by the gas velocity and the placement of internals. The major limitation is the fluidizability of the catalyst and its ability to withstand the abrasion associated with solid fluid movement.[73]

1.6.4 Multistage isothermal reactor

The partial oxidation reactions occur at very high rates and the residence time requirements are very small for the total conversion of oxygen. Consequently, very thin beds cooled by molten salts, etc., can be used and several beds can be stacked together with separate injection of oxygen. Such concepts have been proposed as pancake reactors for the oxidative conversion of methanol to formaldehyde.[68, 73]

1.6.5 Simulated counter-current moving bed chromatographic reactors (SCMCR)

SCMCR are chemical reactors in which reaction and separation occur simultaneously in integrated reactor/adsorbers. The adsorptive separation has very low energy requirements, so the SCMCR is environmentally benign from the standpoint of CO_2 emissions. The separation of product(s) from reactant(s) enables equilibrium limited

reactions to be carried to higher conversions than would be possible in conventional non-separative reactors. The SCMCR is also capable of improving yields of other intrinsically low conversion processes.[74]

1.6.6 Monolith reactor

Monoliths can be wire gauzes or ceramics with metal films deposited on them as illustrated in Figure 1.6. These are essentially fixed beds with a very large cross-section to volume ratio. The walls are wash coated with catalysts and gas flows through the catalyst layers rather than alongside. Short-length monoliths can be stacked together to provide the required length. An increase of residence time was found to have a negative effect on conversion and selectivity on syngas production. However, the fast reaction should provide an impetus to explore monolith reactors for all the oxidative reactions.[26]

1.6.7 Membrane reactors

Membrane reactors offer great promise of enhanced productivity for many well established reactions as well as emerging reactions like the oxidative processes. These types of reactor are discussed in more detail below (section 1.7).

Despite the fact that heterogeneous catalysis offer easier separation of catalysts from the product mixture as well as the possibility of continuous processing, heat transfer problems might be encountered. Membrane catalysis will limit heat transfer problems.

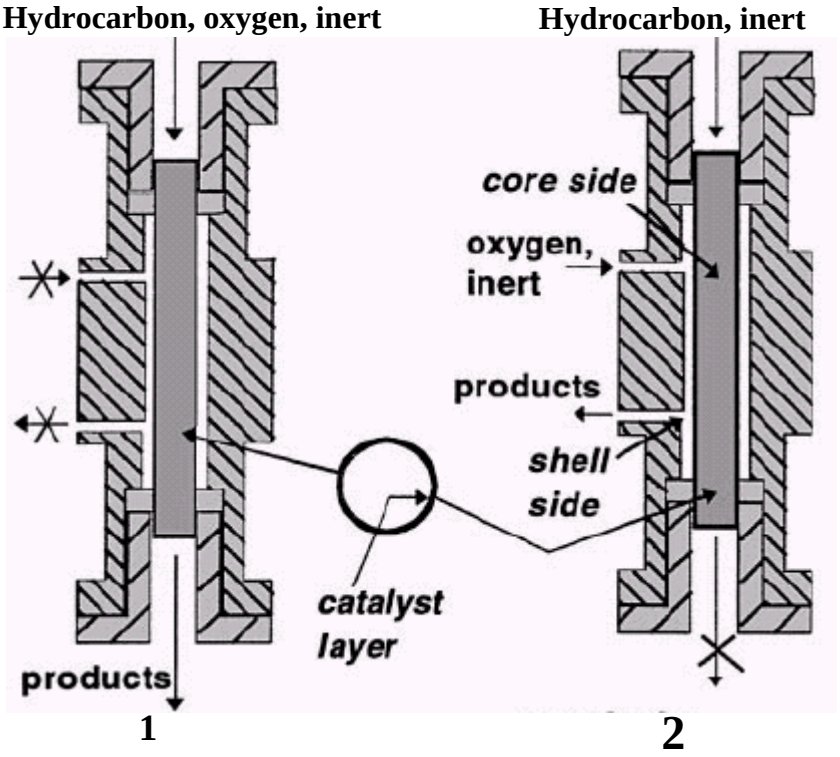

Figure 1.6: Reactor configurations for the selective oxidation of paraffins[26]

1: monolithic type reactor, 2: catalytic membrane reactor

1.7 Membrane Catalysis

In 1968 Michaels was one of the first researchers to suggest the combination of reaction and separation upon a membrane. The goal was to attain higher conversions by shifting the product distribution of equilibrium reactions through the selective permeation of at least one of the reaction products, by Le Chetalier's principle. Some years ago (1988), several researchers[75, 69, 76, 77, 78] suggested that applications of membrane reactors would probably be confined to high-value biotechnological products. A widespread interest in the use of ceramic membranes in chemical reactors under more severe operating conditions than those endured by polymeric membranes,

was stimulated by significant recent developments in the manufacture of both ceramic and metal membranes. Very thin and defect-free permselective inorganic layers with comparatively high thermal and chemical stability, and with relatively small and homogeneously dispersed pores, were attained and are nowadays constantly under development in many research groups (both academic and industrial) all over the world.

In 1990 Roth[75] outlined the future opportunities in industrial catalysis and indicated that homogeneous catalysis, zeolites and catalytic inorganic membrane reactors would be the most promising fields. Some reactions in catalytic inorganic membrane reactors could achieve higher conversions and improved selectivity to traditional processes such as in dehydrogenations and partial hydrogenations or oxidation and in the petrochemical industry, (that is ammonia synthesis, one step methanol production from methane, water-gas shift reaction, ethane dehydrogenation to ethylene, oxidative coupling of methane and steam reforming of natural gas). On the other hand, the application of non-separative catalytic inorganic membrane reactors is possible, in which membrane permselectivity is not regarded as a significant property. In this case the catalytic inorganic membrane reactor is a generally catalytically active diffusion barrier which does not convey any relevant enhancement to the conversion of equilibrium-limited reactions but influences the reaction selectivities by an unconventional and still widely unexplored use supported catalyst.[75, 69, 76, 77, 78]

There is considerable interest in the use of catalytic membrane reactors, where the oxygen supply is controlled either via selective ionic diffusion (dense membranes) or through the control of molecular diffusion (inorganic porous membranes). With porous inorganic membranes, the hydrocarbons and oxygen are fed separately to the

core and shell sides of the membrane reactors. One advantage lies in the possibility of supplying oxygen to the reaction zone in a distributed fashion over the entire reactor length, instead of feeding it together with the hydrocarbon at the reactor entrance. The laws of mass transport through the porous membrane govern the supply of the oxidant to the reactor medium. In this way, the concentration of dioxygen all along the reactor can be kept sufficiently low to favour kinetically the partial oxidation reactions instead of complete hydrocarbon combustion and by keeping the catalyst at a desired average oxidation level. Furthermore, the reactants are kept separate, thus avoiding any flammability hazard. High conversions can be achieved at lower temperature, leading to energy saving and reduced catalyst deactivation.[26, 79, 68, 80, 81]

Porous membrane reactor technology might soon compete with current industrial processes for the partial oxidation of light alkanes particularly non-permselective porous membranes acting as O_2 distributors.[82, 75]

Catalytic membrane reactors can be classified according to the physical process the membrane is involved in within the reactor.

(a) The extractor type is widely experimented for dehydrogenation reactions. Typically the membrane can be made of palladium or MFI zeolite. It selectively removes hydrogen from the catalyst fixed-bed with which it is in contact. This selective extraction brings about the well-known equilibrium shift, which will allow higher conversions than that is limited by thermodynamics in a conventional fixed bed reactor. Another advantage can be the selective extraction of a primary product when successive reactions may occur, with an improved selectivity towards this product.[83, 84]

(b) The distributor type is used when a second reactant is introduced through the membrane all along the length of the catalyst bed. In this way, the concentration of the distributed reactant is kept at a low level in the catalyst, while the total amount introduced may be high. This may limit secondary reactions, as was shown in the case of selective oxidations. This also allows the use of reactive mixtures that are forbidden in conventional reactors due to flammability problems.[83, 84]

(c) The contactor type applies when a membrane is in contact with two different reactant fluid phases and the catalyst. In conventional reactors, one of the reactants is usually favoured by the fact that the catalyst on its support is dispersed in its phase, allowing an easy contact between the two. The second phase reactant on the other hand has to suffer access limitations due to its lengthened diffusion path between the two-phase interface and the catalyst. The contactor type offers an improvement for the unfavoured reactant with two handling possibilities. The first alternative is the flow-through contactor in which a solution of the two reactants is forced through the membrane, constraining both reactants to come into contact with the porous network of the membrane and as close as possible to the catalyst particle. As a matter of fact, the catalyst particle is deposited in a double-ended pore of membrane, through which the pumped flux imposes the triple contact explained above. The second alternative can be called the interfacial contactor. In this case, the catalyst particles are also accommodated in the pores of the membrane, but this time each fluid phase is located on a different side of the membrane. The operational conditions allow a proper location of the interface, which is in the catalysed zone of the membrane.[83, 84]

(c)(i) In the gas–solid contactor type, mass transfer resistances are greatly reduced since reactants are forced to permeate across the membrane wall where the catalyst is dispersed. The permeation of a pre-mixed feed stream provides intimate contact between the molecules and the wall of the pores, thus minimising the diffusion resistance present in other systems, such as fixed bed reactors or monolith reactors.[83, 85]

Inorganic ceramic membranes have a number of advantages over organic membranes:

- Stability to high temperatures
- Solvent and chemical resistance
- Controlled, stable and narrow pore size distributions and thus good separation performance
- Mechanical stability
- Ease of cleaning and minimal fouling
- Compaction/swelling resistance
- High flux/volume ratios due to short length of the small pores in the membrane
- Ability to disperse catalytic materials by impregnation[24]

Farrusseng et al.[82] cited reports in the literature for the selective oxidation of alkanes in inorganic membrane reactors with porous membranes focusing on mesoporous membranes. Although the porous structure and thickness of the membrane are key parameters for the O_2 supply efficiency, few studies aimed at correlating the gas transport properties of membranes with reactor performance. The mass transfer

through a tubular membrane is a complex system involving a multi-component mixture in a tri-dimensional reactor.[82]

The membrane may be in the form of a cylindrical tube and the microporous separation layer is on either the inside or outside wall; in this case, the reactor may be operated as a plug-flow system. Alternatively, the membrane may be in the form of a flat plate, in which case the system is best thought of as a pair of continuous stirred-tank reactors, which will generally be the case if low flow rates are used through both sides of the reactor. In either of these two configurations, it is possible to feed the reactants together to one side of the membrane or to feed them separately from either side of the membrane; similarly, the products may emerge from one or other or both sides of the membrane or they may undergo some degree of separation by the membrane.[86]

The catalyst may be placed separately in contact with the membrane rather than in the membrane. In this case, the membrane may be in the form of a tube or as a flat plate. It would be normal for the reactants to be co-fed, as adequate mixing of the reactants throughout the catalyst bed is unlikely if one of the reactants is fed through the membrane; however, if it was advantageous to the reaction in question to have staged mixing of one of the reactants (e.g. in a selective oxidation reaction in which low partial pressures of oxygen favour higher selectivity), one of the reactants can be fed through the membrane.[86] Tubular membranes are more interesting than flat ones because of their easier integration into a reactor or separator module. However, defect-free tubular membranes are more difficult to obtain due to the development of

mechanical tensions during the drying/calcination steps that often lead to defects in the layer.[77]

Commercial ceramic membranes currently in use usually have an asymmetric structure consisting of a support layer (generally α-alumina) with large pores and low pressure drop, and a separation layer made of a different material (γ-alumina, zirconia, silica, etc.), which controls the permeation flux.[77] The $SiO_2/\alpha Al_2O_3$ membrane was synthesised by a multi-step infiltration method. The αAl_2O_3 tube was first internally filled with a commercial colloidal silica sol (Ludox AS 40- DuPont), then the tube was sealed at both ends with a paraffin sheet and placed in a dessicator under reduced pressure. This resulted in the infiltration of the silica sol into the pores of the support. After removing the residual sol, the membrane was dried in air and then calcined in air at 500°C for 12 h. The sequence of infiltration-drying-heat treatment was repeated until the N_2 permeance at room temperature was in the range of $2 – 4\times10^{-7}$ mol Pa^{-1} S^{-1} m^{-1}. The membranes were finally heat-treated in air at 650°C for 2 days in order to ensure the thermal stability of their porous structure.[82]

The mullite tubes ($3Al_2O_3–2SiO_2$) can be modified further by coating their inner surface with a silica layer synthesised by the sol–gel technique. Tetraethylorthosilane (TEOS) was used as the silica precursor. A sol was prepared by mixing TEOS, H_2O, CH_3OH and HCl in proportions (1.0:4.5:4.0:0.02) in volume. In order to coat the inner surface of the membrane, one end of the tube was closed and the solution was introduced into it.[87]

Various characterization methods are applicable to the characterization of catalytically active membranes. The pore sizes of the membrane layer are measured with mercury

porosimetry and capillary flow porometry. The cluster sizes of the deposited catalytic metals can be determined with XRD, CO-pulse-chemisorption and TEM. SEM, TEM and AFM methods are used to analyze pore and membrane structure. EPMA (electron probe microanalysis)/WDX (wavelength dispersive X- ray) is used to determine the metal distribution over the membrane length and into the membrane layer.[88]

Since methanol can be subsequently oxidized to CO, CO_2 and H_2O, it is desirable to remove CH_3OH continuously from the reactor zone to increase selectivity and hence a permselective membrane could be added to a reactor to accomplish this. Other researchers have quenched the product stream leaving the reactor. Liu et al.[32] combined a non-permselective membrane with a non-isothermal homogeneous reactor. The membrane separated high and low temperature regions in a non-isothermal reactor. It was found that selectivity increased significantly by maintaining a large thermal temperature gradient and distributing the gas flow evenly more than that obtained in the absence of the temperature gradient. The maximum yield obtained with this arrangement was 3.8%.[32]

1.8 Alternative approaches to partial oxidation of methane

An alternative route to partial oxidation of methane is the non-radical intermediate route for the activation of methane.[10] For example, the use of hydrogen peroxide as oxidant in liquid super-acidic conditions at low temperature has produced methanol with the selectivity higher than 95%. The use of ozone instead of H_2O_2 generated formaldehyde. Protonation of the resultant products was suggested to prevent their further oxidation and the reaction was stated to occur via an electrophilic insertion

mechanism. This approach possesses the advantage of high selectivity, but suffers from the disadvantage of being homogeneous and thus separation of the product presents difficulties. Another example of electrophilic activation of methane involves the reaction of methane with hydrogen peroxide and trifluoroacetic anhydride catalysed by Pd(II) species at 90°C. The reaction produces methyltrifluoroacetate, which could then be hydrolyzed to produce methanol.[68] The substitution of $Pd(O_2CCH_5)_2$ by either $Pb(O_2CCH_3)_4$, $Fe(O_2CCH_3)_2$ or $Co(O_2CCF_3)_2$ resulted in a yield of $CF_3CO_2CH_3$ that was either similar to or only marginally higher than that observed with peroxytrifluoroacetic anhydride alone.

A double-layered catalytic bed was shown to enhance the yield of formaldehyde[10] when 1 wt% Sr/La_2O_3 was used to provide a methyl radical flux to a MoO_3/SiO_2 catalyst. Ultra-violet radiation was used to enhance the selectivity of methane oxidation to formaldehyde using MoO_3/SiO_2 catalyst at 190-220°C. Experiments using optical filters demonstrated that wavelengths higher than 300 nm were able to induce reaction with ZnO-based catalysts in contrast to the MoO_3/SiO_2 which required less than 300 nm. In neither case was reaction observed to occur in the absence of irradiation. This type of approach although using fairly conventional catalysts offers the possibility of minimising undesirable gas-phase reactions because of the low temperatures involved. The economic feasibility of running the photocatalytic reaction on a large scale has to be established.

Gondal et al.[89] investigated the photo-catalytic conversion of methane into methanol under different experimental parameters such as catalyst concentration, laser power, laser exposure time, effects of a free radical generator (H_2O_2) and an electron capture

agent (Fe^{3+}), using visible laser light. The study was carried out at room temperature with a simple set-up using a laser light, water and a semiconductor photo-catalyst WO_3. Gas chromatography was used to analyse the reaction products (methanol, O_2 and CO_2). WO_3 was used as a photo-catalyst to replace the UV laser light with visible laser light. This greatly simplifies reactor design and permits flexibility in the selection of a laser source in the visible region. The oxygen to tungsten ratio in WO_3 at different temperatures was studied by XPS. It was observed that laser photo-catalysis conversion of methane is much faster (~15 min) than the conventional lamps where the process takes place over many hours (18 h).[89]

Larkin et al studied[90] the direct oxidative conversion of methane to organic oxygenates (methanol, formaldehyde, methyl formate, and formic acid) using a dielectric barrier discharge (DBD) reactor (a non-equilibrium plasma reactor). The DBD reactor is similar to a catalytic reactor because, just as with the catalytic reactor, the DBD reactor reduces the required temperature and pressure needed for reactions to occur within it by using high energy electrons to initiate reactions. This reactor can also control product selectivity by the electron energy distribution within the system. The effects of changing the electrical properties within the methane-oxygen DBD system were investigated. Increasing the gas gap from 4.0 to 12.0 mm caused the reduced electric field to decrease from 30 to 18 V/cm/Torr, which resulted in a shift in the product distribution from organic oxygenate liquids to ethane and acetylene. The effects of temperature on product selectivity were also studied through the use of a water jacket. Lowering the temperature of water within the water jacket from 75 to 28˚C resulted in a 54% increase in organic oxygenate selectivity and a 56% decrease

in CO_x selectivity. Organic oxygenates (principally methanol, formaldehyde, methyl formate, and formic acid) and water were collected in a dry ice/acetone (-55˚C) trap.[90]

1.9 Conclusions

Selective oxidation of methane to oxygenates will certainly remain a challenge for the future. Direct conversion of methane to methanol and formaldehyde in a single catalytic step with sufficiently high yield is a difficult challenge in catalysis. The majority of studies have focused on silica-supported vanadium and molybdenum oxide catalysts as silica appears to be the most effective support. Table 1.1 summarises the results of methane oxidation on supported catalysts from literature. High selectivity to the desired products is only achieved with low methane conversion. Although a large number of catalysts and several novel processes have been reported, none of them has satisfied the requirements for commercialization. Catalysis depends not only on the catalyst itself but also on reaction conditions such as feed gas composition, pressure, catalyst shape and reaction temperature. The reaction conditions must be optimised for each catalyst to demonstrate its best catalytic activity. Partial oxidation catalysts can be placed in a ceramic membrane to increase their selectivity to methanol. Catalytic membranes can be used to achieve high conversion per pass and allows reactions to be run under mild conditions.

Table 1.1: Selected data for methane oxidation to methanol and formaldehyde on supported catalysts

Catalyst	Reaction Temperature °C	Oxidant	CH_4 Conv. %	Product	Selectivity %	STY g (kg cat)$^{-1}$h^{-1}	References
MoO_3/ZnO	220/hv	O_2	0.08	HCHO	81	0.6	10
MoO_3/SiO_2	220/hv	O_2	0.08	HCHO	97	7.0	10
$BeO/B_2O_3/SiO_2$	600	O_2	2.8	HCHO	32	24	10
V_2O_5/SiO_2	650	O_2	0.521- 0.078	HCHO	35 - 48	793 - 819	10
V_2O_5/SiO_2	650	O_2	13.5**	HCHO	35	760	10
V_2O_5/SiO_2	600	O_2	1.49	HCHO	46.3	92	56
$FePO_4/SiO_2$	600	O_2	1.6	CH_3OH + HCHO	2 + 88	15 + 593	29
Fe sodalite	435	O_2	5.8	CH_3OH	25	186	10
$V_2O_5/MoO_3/SiO_2$	630	Air	8.47	HCHO	16.6	675	6
$Sr/La_2O_3/MoO_3/SiO_2$	630	O_2	8.2	HCHO	3.3	129	10
$SO_4^{2-}/SrO/La_2O_3//V_2O_5/SiO_2$	650	Air	15.1	CH_3OH + HCHO	n.a.	48 + 940	6
Molybdophosphoric acid/SiO_2	570	N_2O	5.1	HCHO	12.0	0.6*	18
Molybdophosphoric acid/SiO_2	450	N_2O	0.8	HCHO	42.0	0.34*	18

n.a. data not given in paper
•*Yield %
•**calculated using GHSV of 43 100 h^{-1}

Moreover, recycling can be reduced and less downstream separation of product is required. According to S.Azgui et al.[91], when selectivity towards a given product is an important factor, an improvement of the catalyst performance can be obtained by avoiding contact between reactants. Co-fed oxygen can react with C-H in the homogeneous phase and/ or be responsible for unselective processes.

1.10 Objectives of research work and structure of the thesis

The process of direct oxidation of methane to methanol is problematic due to low reactivity of C-H bonds in the methane molecule and much higher reactivity of the primary oxygenated product such as methanol. As a result, further oxidation towards carbon oxides takes place when attempts to increase the reaction conversion are made.

Homogeneous synthesis of methanol proceeds in the most effective way under high pressure (up to 200 atm) and at temperatures from 300 to 500^{o}C at low oxygen content in the reaction mixture. Under these conditions the oxidation of methanol to formaldehyde and carbon oxides takes place to a much lesser extent. As discussed in above, the key to any further improvement in this process may lie in the design of the reactor and the catalyst.

The purpose of this research project is to develop a low temperature and low pressure, inorganic ceramic membrane-based oxidation technology to convert methane to oxygenates and eliminating over oxidised products. The inorganic ceramic membrane will be applied as a non-separative catalytic membrane in the reactor in order to achieve small residence time of feed (methane and oxygen) on the catalyst bed. This approach was used to determine to what extent this technology can improve methanol and formaldehyde yields. The other objectives of this research are as follows:

- Identification of a suitable inorganic ceramic membrane as a support material for the catalysts;
- Study of the modification of the inorganic membrane material by silica;
- Selection of metal complex compounds which are catalytically active in reduction-oxidation processes;
- Study of methods to adsorb the catalysts on the ceramic membrane support material;
- Characterization of the prepared catalysts;

- Testing of produced supported membrane catalysts in the catalytic conversion of methane in the presence of molecular oxygen, at low temperatures (30-150°C);
- Optimisation of the reaction conditions (reaction temperature and pressure, ratio of methane to oxygen, flow rate of the feed etc) towards high conversion of methane and high selectivity to methanol and formaldehyde. This will help in predicting the activity/selectivity of the catalysts.

Structure of the thesis

The experimental details of the development of the desired catalyst including the modification of inorganic ceramic membranes by silica followed by the deposition of metal or metal complex compounds on the surface of modified membranes, the characterization techniques and designing and construction of a reactor for the oxidation of methane to methanol and formaldehyde under mild conditions are presented in Chapter 2. Chapter 3 describes the study of the suitability of inorganic ceramic membrane papers of different types for application as supports for catalysts. The effect of silica on various properties of these catalysts and characterization of these catalysts will be discussed in Chapter 4. Activity studies were done in association with determination of the reducibility and oxidation ability of the catalysts by temperature programmed techniques and discussed in Chapter 5. Chapter 6 studies the activity of PMo based catalysts in natural gas conversion. Chapter 7 describes the overall conclusions and recommendations.

CHAPTER 2: Experimental procedures for the modification of ceramic membranes, characterisation and activity testing of prepared catalysts

A variety of modified ceramic membranes containing metal complex compounds were prepared, capable of catalysing the oxidation of methane under mild conditions.

2.1 Catalyst preparation

2.1.1 Reagents used

Table 2.1: Reagents used in the preparation of catalysts

Reagents	Source	Purity
Fumed silica, surface area 380 m^2/g	Aldrich	99.8%
N, N-dimethylformamide	Aldrich	99.8%
Hexachloro Platinic Acid	Next Chimica	99.95%
Hemin, bovine (Hemin Chloride)	Aldrich	
Silicomolybdic acid hydrate	Aldrich	
Phosphomolybdic acid hydrate	Aldrich	A.C.S. reagent
Nitric acid	KIMIX	55%
Hydrochloric acid	KIMIX	32%

2.1.2 Preparation methods

A. SiO_2 preparation

20 g fumed silica was weighed in a glove box, heated in a furnace at 600°C for 2 h to remove adsorbed impurities and water and then cooled in a desiccators with molecular sieves heated at 200°C for 3 h. After cooling, 1000 ml distilled water was added to the fumed silica and stirred using the magnetic stirrer for 1h.

B. Modification of the support material with SiO_2

The inorganic ceramic supports were cut to the desired length according to the size of the reactor, heated in an oven in air at 120°C for 1 h to remove adsorbed water. The support materials were then cooled and weighed, after which they were dipped into the hydrated fumed SiO_2 in a vertical position.

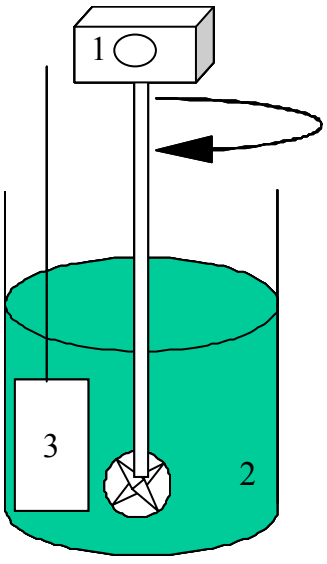

Figure 2.1: The reaction set up 1: overhead paddle stirrer, 2: fumed SiO_2 solution, 3: support material

The silica solution was stirred for 1 h using the overhead paddle stirrer while the support material was placed into the solution as illustrated in Figure 2.1. The modified supports were pressed by hand between two Petri dishes for 5 mins to remove excess solution. Thereafter they were air dried for overnight. Multiple layers of silica were coated on the support materials. After air-drying, the modified samples were heated in the oven at 120°C for 2 h to remove water.

C. Impregnation of the unmodified and silica-modified support materials with metal solutions

1. Deposition of $H_2PtCl_6.6H_2O$ on the support material

The unmodified and silica-modified support materials were impregnated with 0.01 M $H_2PtCl_6.6H_2O$ for 4 h and turned while in the solution every 30 mins after which they were rinsed with distilled H_2O and then hand pressed between two Petri dishes for 5 mins to remove excess solution. The samples were air dried overnight and then heated in air at 120°C for 1 h.

2. Deposition of Silicomolybdic acid [$H_4SiO_4.12MoO_3.xH_2O$] on the support material

0.01 g $H_4SiO_4.12MoO_3.xH_2O$ (SiMo) in 10 ml H_2O was prepared. The unmodified/ silica-modified support samples were immersed into the solution for 4 h and turned while in the solution every 30 mins after which they were hand pressed between two Petri dishes for 5 min to remove excess solution. The samples were air dried at room temperature overnight, then heated in air furnace at 500°C for 1 h and weighed after cooling.

3. Deposition of Hemin on the support material

1 % (g/vol) of hemin in DMF (dimethylformamide) was prepared. DMF was kept over molecular sieve 3A before being used. The unmodified/ silica-modified samples were soaked in hemin solution for 4 h and turned after every 10 mins while in solution. The samples were then hand pressed between two Petri dishes for 5 minutes to remove excess solution. The samples were air dried for 48 h and then heated in air at 120°C for 1 h.

4. Deposition of Phosphomolybdic acid [$H_3Mo_{12}O_{40}P.xH_2O$] on the support material

13.5 g of Phosphomolybdic acid (PMo) was added to 50 ml of 0.1 M nitric acid. Silica-modified and unmodified membrane supports were placed in the solution and then heated up to the boiling of PMo solution as illustrated in Figure 2.2. The boiling proceeded for 1 h and samples were turned while in solution every 10 mins. The samples were cooled and washed out with 0.1 M nitric acid solution. They were air dried for 24 h and then heated for 1 h at 120°C in air.

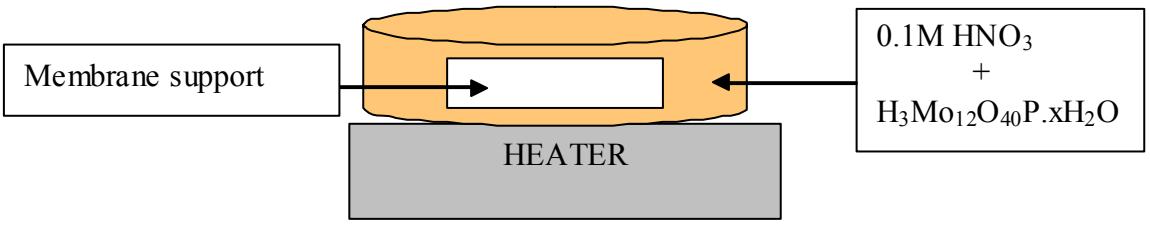

Figure 2.2: The reaction set up for deposition of support materials with PMo solution

2.2 Characterization techniques

The support material and the prepared catalysts were characterized using several techniques and the preparative details relevant to each are outlined as below:

2.2.1 Nitrogen adsorption porosimetry [BET]

Changes in catalyst surface area, pore volume and pore size distribution were determined using a Micromeritics ASAP 2010. The catalysts (0.3-0.5 g) were degassed in flowing helium of 99.999% supplied by AFROX at 110°C for 16 h and at 260°C for 1 h before characterising. The characterisation was based on the physical adsorption of nitrogen at liquid nitrogen temperature (77K). Pore diameter and specific pore volume were calculated according to the Barret–Joyner–Halenda (BJH) theory.[92] The specific surface area was obtained using the Brunauer–Emmett–Teller (BET) equation.[93, 94]

Brunauer–Emmett–Teller (BET)[93]

BET equation is the most widely used equation for the description of multilayer physical adsorption. BET theory is based on the assumptions that the first layer of adsorbate is taken up with a fixed heat of adsorption (H_1) whereas the second and subsequent layers are all characyerized by heats of adsorption equal to the latent heat of evaporation (H_L). By considering a dynamic equilibrium between each layer and the gas phase, the BET equation is arrived at:

$$\frac{p}{n^a(p_0 - p)} = \frac{1}{n^a{}_m C} + \left(\frac{C-1}{n^a{}_m C}\right)\frac{p}{p_0}$$

where p is the sample pressure,

p_0 is the saturation vapour pressure,

n^a is the amount of gas adsorbed at the relative pressure p/p_0,

n^a_m is the monolayer capacity, and

C the so-called BET constant and is given by:

$C = \exp (H_1 – H_L/ RT)$

The BET equation can be applied for determining the surface areas and pore volumes from adsorption isotherms, if the adsorption isotherms are of type IV according to IUPAC classification. The pore size distributions can be calculated from desorption isotherms. The IUPAC classification of pores according to their widths is micropores (diameter less than 20Å), mesopores (diameter between 20 and 500Å) and macropores (diameter exceeding 500Å).[94]

2.2.2 Scanning electron microscopy (SEM)

The ADDA Hitachi X650 scanning electron microscopy was used to take micrographs of the catalyst samples in order to determine the distribution of the catalysts over the membrane support. The samples were mounted on aluminium stubs and coated with carbon for conduction. The operating parameters are detailed below:

Accelerating voltage	10 keV, 25 keV
Beam current	2000.0 picoAmps
Tilt angle	0°
Resolution	>-9
Working distance	25.0 mm
Solid Angle Beam Current	12.2

2.2.3 Energy dispersive X-ray spectroscopy (EDX)

EDX allows qualitative and quantitative elemental analysis of the sample, and it provides the relative abundance of the elements as a weight percentage.

Accelerating voltage	25 kV
Tilt angle	0°
Take off	34.7
Res	145
Tc	40
Lsec	100

2.2.4 Elemental analysis using Inductive coupling plasma (ICP)

Elemental analysis of the catalysts was performed on an Elan 6000 Perkin Elmer/Sciex ICP/MS instrument. The following procedure was followed for the digestion of the catalyst supported on the ceramic paper[95, 96] prior to analysis.

Materials

- Aqua regia. Add 130 ml concentrated HCl to 120 ml water and mix. Add 150 ml of this solution to 50 ml concentrated HNO_3 and mix.
- Kjeldahl flask or similar digestion flask

Experimental procedure

1.0 g of the supported catalyst was weighed and placed inside a digestion flask. 15 ml aqua regia was added and swirled to wet the sample. The samples were left to stand overnight. The flask was then placed in the heating block and heated at 50°C for 30 min then raising the temperature to 120°C with continued heating for 2 h. The flask was cooled, 10 ml 0.25 M HNO_3 added and then the solution filtered through a

Whatman no.541 filter paper. The flask and filter paper were washed with small aliquots of 0.25 M HNO_3. The filtrate and washings were transferred to a 50 ml volumetric flask and made up to the mark with 0.25 M HNO_3. All standards were made up with 0.25 M HNO_3. The results were analysed and calculated.

2.2.5 Thermal analysis

Thermal analysis studies were followed to check the presence of organics on the inorganic ceramic membranes using a Rheometric Scientific STA 1500 and a RSI Orchestrator. The inorganic ceramic membranes were heated from room temperature to 800°C at a rate of 5 to 10 °C/min under nitrogen with 99.99% purity from AFROX.

2.2.6 X ray diffraction (XRD)

The crystallinity of the supported and unsupported catalysts was determined by XRD. The studies were performed on Bruker AXS D8 Advance with a Cu Kα tube and NaI(Th) detector. The voltage and current were 40 kV and 40 mA respectively. 2θ ranged from 10° to 90°. The inter-atomic distances (d-spacings) were calculated using Bragg equation:

$n\lambda = 2d\sin\theta$, where $n=1$, $\lambda = 1.5418$ Å

Crystal planes (Miller indices) were obtained from JCPDS database.[97, 98]

2.2.7 Temperature programmed reactions

The interaction of reactants with the catalyst surface is a key parameter in heterogeneous reaction systems. For example, the temperature at which species are desorbed from a surface is indicative of the strength of the surface bond: the higher the temperature, the stronger the bond. Therefore the adsorption of a probe molecule at low temperature, and subsequent monitoring of it's desorption/reaction

characteristics with temperature, is a simple way to characterize surface properties of catalysts and adsorbents. This is the basis of temperature programmed analysis methods in which, for a linear increase in temperature, the concentration of the reacting/desorbing particles is recorded as a function of temperature. The analysis is most often confined to a qualitative level by discussion of peak maxima, number and position of peaks, and total reactant consumption. However, if a more detailed picture is required, several theoretical models have been developed especially for TPD and TPR analysis.[99]

Temperature-programmed methods can provide useful information on solid surfaces, their interactions with adsorbed gas molecules, and thermal stability of surface desorption states.[100] The degree of reduction, and subsequent oxygen uptake and desorption of carbon dioxide and methane by the catalyst were measured. The experiments were performed on Micromeritics AutoChem 2910. A thermal conductive detector (TCD) was used. A dry-ice/acetone trap was used to trap H_2O and prevent it reaching the TCD.

A. Temperature programmed reduction (TPR)

In temperature-programmed reduction, a reducible catalyst is treated with a flow of reducing gas mixture while the temperature is ramped linearly. The rate of reduction is monitored continuously by measuring the H_2 content at the outlet of the reactor using a TCD detector when compared to that of reference gas. The total amount of hydrogen adsorbed is used to calculate the degree of reduction. The reducibility determines how reduced the catalyst will be under the reaction conditions. The experimental conditions are as follows:

Mass of sample	0.2 – 0.5 g

Temperature range	25 – 110 / 25 – 700°C
Temperature gradient	5 °C/min
Flow rate	50 ml/min
Reactant gas	100 % H_2 from AFROX

B. Temperature programmed oxidation (TPO)

Temperature programmed oxidation can be applied to determine the redox behaviour of catalysts. TPO determines the amount of the reduced species. The procedure is the same as in A TPR. The experimental conditions are as follows:

Mass of sample	0.2 – 0.5 g
Temperature range	25 – 110 / 25 – 700°C
Temperature gradient	5 °C/min
Flow rate	50 ml/min
Oxidant gas	10.4% O_2 in He from AFROX

C. Temperature programmed desorption (TPD) of CO_2

Temperature-Programmed Desorption (TPD) analyses determine the number, type, and strength of active sites available on the surface of the catalyst from measurement of the amount of gas desorbed at various temperatures. After the sample has been outgassed, reduced, or otherwise prepared, a steady stream of analysis gas flows through the sample and reacts with the active sites. Programmed desorption begins by raising the temperature linearly with time while a steady of inert carrier gas flows through the sample. At a certain temperature, the heat overcomes the activation energy; therefore, the bond between the adsorbate and adsorbent will break and the adsorbed species desorb. If different active metals are present, they usually desorb the reacted species at different temperatures. These desorbed molecules enter the stream

of inert carrier gas and are swept to the detector, which measures the gas concentrations.

Carbon dioxide desorption was used to determine the distribution of basic sites on the catalyst. The catalyst was pre-treated in helium at 120°C for 1 h, cooled down to 25°C and equilibrated with an adsorbing gas (carbon dioxide) for 90 min at room temperature. Pure carrier gas (helium) was used to desorb the previously adsorbed CO_2. The temperature was raised to 350°C and the desorbing carbon dioxide was measured. The experimental conditions were as follows:

Mass of sample	0.2 – 0.5 g
Temperature range	5 – 120/ 5 – 350°C
Temperature gradient	5 °C/min
Flow rate	50 ml/min
Adsorbing gas	99.0% CO_2 from AFROX

D. Temperature programmed desorption (TPD) of CH_4

The above procedure for TPD of CO_2 was followed using pure methane gas instead of carbon dioxide. The TPD of methane was studied in order to illustrate the behaviour of catalysts towards methane. 99.5% methane from AFROX was used.

2.3 Catalyst testing

2.3.1 Reactor design

Reaction studies were performed using a flat sheet membrane reactor shown below in Figure 2.3. The reactor consisted of two identical units (item 3, 5 and 4, 5) made of stainless steel. Each unit was based on a stainless steel plate in which a depression

with dimensions 6.0 cm x 3.0 cm x 0.2 cm was machined. This depression had a flow inlet and exit (connectors 3 and 4), respectively used for feeding the initial gas mixture and removing reaction products and non-reacted gases. On the opposite side of each unit a heating jacket (item 5) was equipped with connectors (items 5a and 5b) in order to supply the liquid heat carrier, which maintained the working thermal regimen of the reactor. Two similar units were joined together by 8 bolts not shown on the scheme. The rubber seal (item 2), which was placed along the perimeter of the flat catalytic element, made the joint between the two reactor units completely gas tight. Item 1 is a flat sheet ceramic membrane with a working surface of 18 cm^2 (6.0 x 3.0 cm^2).

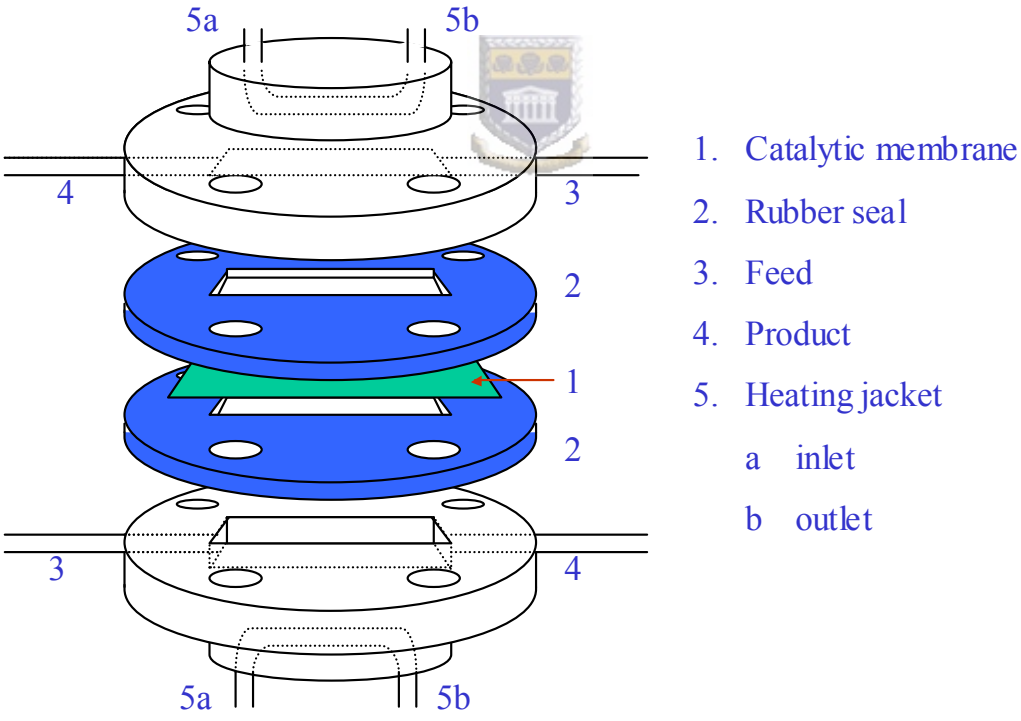

Figure 2.3: Schematic representation of the cross-section of the catalytic membrane reactor

A mixture of methane and pure oxygen was introduced into the reactor volume (3), passed through the catalyst supported on ceramic membrane (1) and then exited through the outlet (3). Reactor temperature was measured at the centre of the catalyst bed using (Type J) thermocouple placed in (4) - one of the exit for removing products.

According to the design of the reactor, different methods can be used for the introduction of gaseous reagents into the reactor and for the output of the reaction products from the reactor. Figure 2.4 illustrates the method followed in this study.

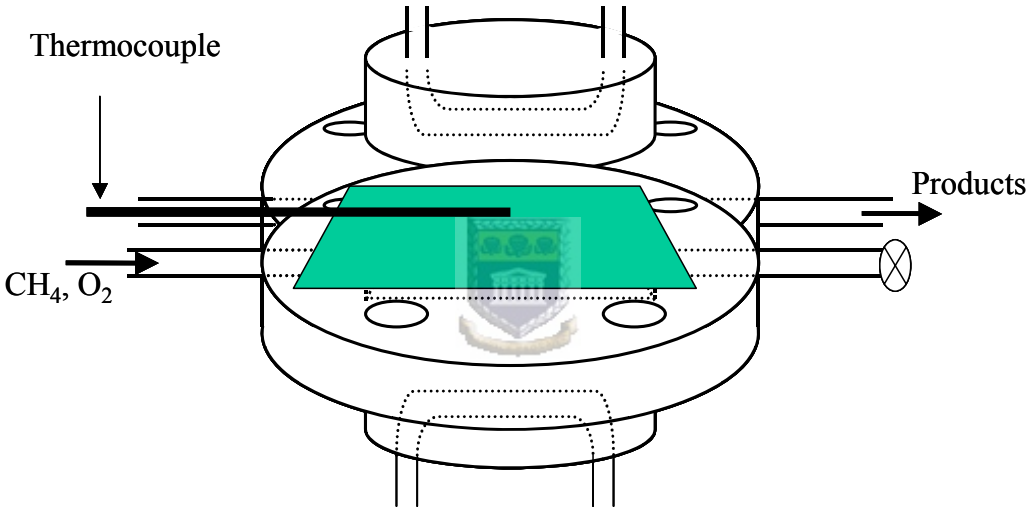

Figure 2.4: Schematic illustration of the introduction of feed (not to scale; exaggerated to clarify thermocouple and feed inlet and products outlet)

2.3.2 Flow system and analytical methods

Figure 2.5 represents the experimental flow system used to estimate the catalytic activity of different catalysts supported on ceramic membranes.

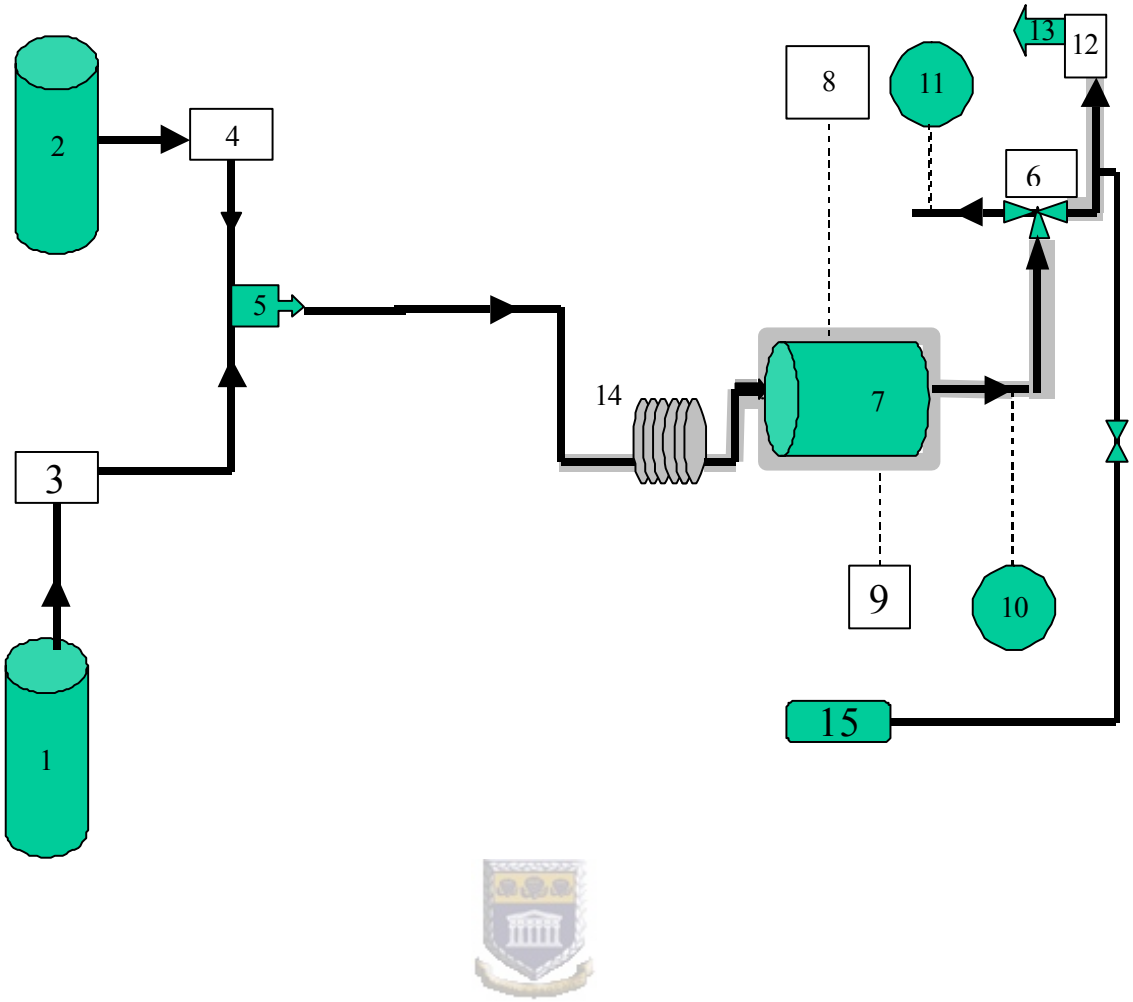

Figure 2.5: Flow system used for the partial oxidation of hydrocarbons

(1) Oxygen cylinder, (2) methane cylinder, (3) and (4) Brooks 5850s mass flow controllers, (5) mixing chamber, (6) 3 port valve, (7) membrane reactor, (8) temperature indicator for catalyst bed, (9) furnace with temperature controller + indicator for outside the reactor, (10) pressure gauge, (11) cold trap, (12) gas chromatography connected to the computer, (13) vent, (14) coiled tubing and (15) internal standard.

Pure oxygen was used as oxidant. Flash-back arrestors were installed just after the oxygen regulator to prevent an explosion. Stainless steel tubing was used for the

connections. Mass flow controllers metered the flow rate of feed gases (methane and oxygen), which were pre-mixed and pre-heated (indicated by the shaded area) in 50 cm coiled tubing before being introduced into the reactor. The pressure transducers were used to measure the pressure of the internal and external output. Needle valves controlled the pressure. Lines downstream from the reactor were also stainless steel tubing. The lines were heated with heating tape to prevent condensation and were equipped with a pressure gauge and regulating valve. An on-line SRI® 8610C gas chromatograph equipped with an FID, methanizer, and TCD was used in analysing the product stream. Product separation was achieved using a Haysep T column. Gas chromatography coupled to mass spectroscopy (GCQ Finnigan MAT GC-MS) was used for identifying the condensable products using a ZB Wax column, which confirmed in-line GC results. The condensable products were collected using a cold trap (dry ice and acetone) and then analysed by GC-MS. The experiments were run at atmospheric pressure. Inorganic membranes coated with catalyst were inserted into the reactor. The products were regularly analysed at regular time intervals.

Safety: Flammability limits

Vapour/air mixtures are flammable only over a limited range of vapour concentrations. This range is defined by the lower and upper flammability limits. Mixtures outside this range are described as, respectively, too "lean" or too "rich" for ignition. One of the most efficient ways to avoid an explosion is to make sure that one always works outside the limits of flammability. These limits are generally only known for standard conditions of pressure and temperature (1 bar and 20°C). In this case the flammability limits for methane in oxygen are 5.8 to 59.2% by volume.[32]

The reactions studied in this research work were carried out with the aid of the catalytic device (membrane reactor and the flow system) as constructed above. The experimental conditions followed in this study are shown in Table 2.2. Methane, methanol, formaldehyde, carbon dioxide and carbon monoxide were calibrated before running methane oxidation reaction in order to calculate methane conversion and selectivity towards products.

Table 2.2: Experimental conditions

Variable	Reaction conditions
CH_4 : O_2 ratios	20:1 - 1:1
Flow rates	5 ml/min - 40 ml/min
Reaction temperatures	30°C – 120°C
Pressure	atmospheric pressure

Prior to testing, the prepared catalysts were heated in a flow of helium gas at 150°C for 30 min to remove any absorbed water. The temperature was decreased to the desired reaction temperature and then testing commenced.

Natural gas

Natural gas was first passed through a gas cleaning unit to remove various compounds such as sulphur containing compounds that could affect the performance of the catalytic process. The same reactor as in Chapter 2.3.1 but with a smaller working area with dimensions 4.8 cm x 2.1 cm was employed. The reactor and heat exchanger temperature was maintained by pumping liquid heat carrier (transformer oil) through the heating jackets of the reactor and the heat exchanger instead of using a furnace.

The heat carrier was heated using thermostat type MWL-U4 produced in Germany. A Selmichrome-1 Gas chromatography was used for analysis of the reaction mixture and the reaction products. The quantitative determination of components of the reaction mixture (natural gas and air) and the main reaction products (CO_2, CH_2O, H_2O and CH_3OH) was carried out using a stainless steel chromatographic column with molecular sieve 5A and Hayesep T respectively. Confidence in the analysis was ensured by repeating the analytical procedure three times and the average value was used.

Sensitivity coefficients K_n for each component were determined according to the formula:

$K_n = S / C_n$,

where S – peak surface area and C_n – analyte content in the sample, μmol.

Molar concentrations of initial components in the reaction mixture such as methane ($C_м$) were calculated in μmol ml^{-1} from the volume flow rates of methane and oxygen into the reactor according to the formulas:

$C_м = 44.6\ V_m / (V_m+V_o)$

where V_m, V_o are methane and oxygen volume flow rates respectively, in ml min^{-1}.

Concentrations of reaction products and unreacted compounds were determined in μmol ml^{-1} by chromatographic analysis of the outlet gas mixture using sensitivity coefficients according to the following formula:

$C_n = S / K_n \cdot v$

where v – volume of gas sample in ml.

% Conversion = $100\ \Sigma C_n / C_м$,

where ΣC_n – sum of concentrations of carbon containing reaction products;

% Selectivity = $100\ C / \Sigma C_n$,

where C – concentration of a specific reaction product

Relative per pass CH_3OH yield = CH_4 conversion x CH_3OH selectivity

Relative per pass CH_2O yield = CH_4 conversion x CH_2O selectivity

CHAPTER 3 Selection of a suitable inorganic membrane as support material for catalysts

3.1 Introduction

Supported-metal catalysts are widely used in the chemical industry and for environmental protection. It is well known that the support has a great influence on the catalytic performance of catalysts, for example, by changing the charge and size of metal particles, by varying the particle shape and crystallographic structure, and by forming the specific active sites at the metal–support boundary.[101, 102, 103, 104] Accordingly, the search for an appropriate support is a crucial step in the course of preparing the supported-metal catalyst.[105] The general method is to test various supports and find the best one. The selection of a support is based on it having certain desirable characteristics. Principally they are[45]:

(i) Inertness,

(ii) Desirable mechanical properties including attrition resistance, hardness and compressive strength reduction only if a metal catalyst is desired,

(iii) Stability under reaction and regeneration conditions,

(iv) A high surface area is usually, but not always, desirable,

(v) Porosity including average pore size and pore size distribution,

(vi) Low cost.

Inorganic ceramic membrane papers used in this project as support materials for synthesizing catalysts were obtained from the Lydall Company in USA.[106] LYTHERM BINDERLESS PAPER is a 100% inorganic material processed from

high purity bulk alumina fibres formed into a flexible sheet. The paper is recommended for continuous use at temperatures up to 1650°C in applications where off gassing of the organic binder cannot be tolerated. Because it is processed from high purity alumina fibres, LYTHERM PAPER has a higher use temperature, is less chemically reactive, and has very low thermal shrinkage. It is a clean paper made from fibres that are free of shot and other unfiberized particles, yielding a very low thermal conductivity. It can be cut and handled without tearing and has a clean dust-free surface and the binder-less formulation prevents carbon pick up and surface discoloration. The papers possess excellent chemical stability and resist attack from most corrosive agents. Exceptions are hydrofluoric and phosphoric acids and concentrated alkali. Lytherm paper resists both oxidation and reduction.

3.2 Experimental procedure

Various Lytherm papers were studied to determine their suitability as supports for the oxidation catalysts. These materials contain γ-alumina and silica. The technical data of Lytherm paper (trade name 3000 LFH, 3000 LJH and 3000 LAH paper) from the company are shown in Table 3.1. Lytherm papers hydrolytic and mechanical stabilities were determined. (SEM/EDX) was used to take micrographs and the elemental analysis of the papers and thermal analysis studies were followed to check for the presence of organics. The surface area, pore size distribution and thermal stability of suitable paper were determined. All experimental details involving characterisation techniques are given in Chapter 2.3.

Table 3.1: Technical data of Lytherm papers provided by Lydall Company[106]

Melting point (°C)	1982
Maximum use temperature (°C)	1650
Density (kg/m^3)	96 - 128
Typical chemical analysis (weight %)	
Al_2O_3	87.50
SiO_2	9.20
Others	4.30

3.3 Results and discussion

The inorganic ceramic membrane papers when dipped in water will either absorb the water or float on top of the water. The hydrophobicity shows the presence of organics in the sample. The (3000 LAH and 3000 LJH) materials did not absorb water- they floated on water and it was difficult to modify them with silica. Hence these materials were regarded as unsuitable as supports for the oxidation catalysts. According to thermal analysis results for 3000 LJH presented in Table 3.2 and 3000 LAH presented in Table A1 of appendix on page 167, the initial mass loss for papers in the temperature region 50 – 100°C, could be attributed to the removal of physically adsorbed water which amounted to not more than 0.5%. 3000 LAH showed a significant mass loss above 100°C, which came to an end at 475°C. The total mass loss amounted to 8.9% and for 3000-LJH, to only 0.4%

Table 3.2: Thermal analysis of ceramic paper Lydall Technical Paper 3000-LJH

T °C	Initial mass g	Final mass g	Mass loss g	Colour and structure of sample	Mass loss mg/g	Mass loss %	Difference in mass loss Mg/g
50	0.58565	0.58345	0.00220	White, weak	3.75	0.375	0.25
100	0.60690	0.60615	0.00075	White, weak	1.23	0.123	0.25
150	0.60520	0.60405	0.00120	Yellow, weak	1.98	0.198	0.25
200	0.60455	0.60335	0.00120	Yellow, weak	1.98	0.198	0.25
250	0.62525	0.62345	0.00180	Yellow weak	2.87	0.287	0.25
300	0.63005	0.62790	0.00215	Light grey, weak	3.41	0.341	0.25
350	0.61885	0.61675	0.00221	Light grey, weak	3.39	0.339	0.25
400	0.60265	0.60020	0.00245	White, loose	4.06	0.406	0.25
450	0.60385	0.60155	0.00230	White, loose	3.80	0.380	0
500	0.61525	0.61260	0.00265	White, loose	4.31	0.431	0
550	0.60315	0.60070	0.00245	White, loose	4.06	0.406	0
600	0.58370	0.58100	0.00270	White, loose	4.62	0.462	0
650	0.60625	0.60340	0.00285	White, loose	4.70	0.470	0
700	0.61680	0.61430	0.00250	White, loose	4.05	0.405	0
750	0.60955	0.60710	0.00245	White, loose	4.04	0.404	0
800	0.60070	0.59855	0.00215	White, loose	3.58	0.358	0

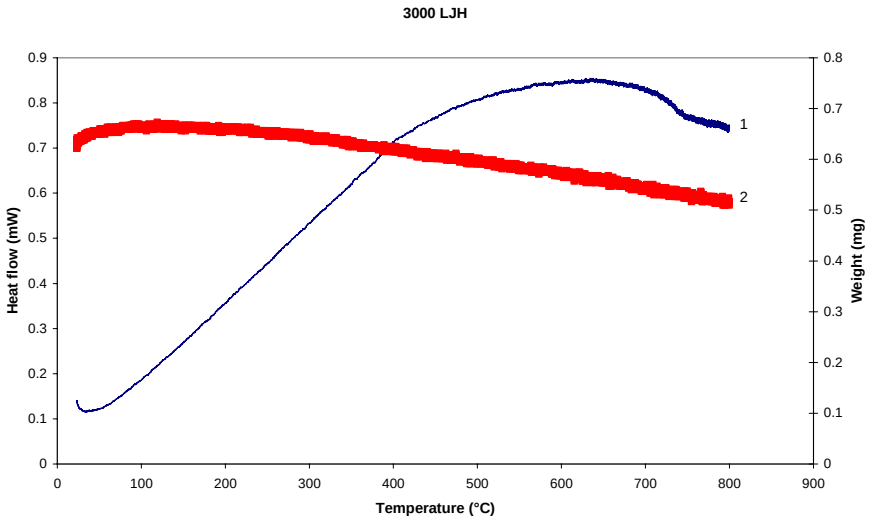

Figure 3.1: Graph of weight loss and heat as a function of temperature for paper 3000 LJH 1: heat flow, 2: weight

3000-LJH changed colour to a small extent, going through white, light yellow, grey, and finally became white. It showed a low content of organics but had a loose structure. Heat treatment of 3000 LAH from 400 – 800°C made the sample very loose and was accompanied by intensive colour changes, from white through yellow to dark brown and back to white. The colour changes together with the fact that significant mass loss occurred during heat treatment implies the presence of organic binders in large quantities in the paper. The temperatures at which papers changed their colour and lost significant amounts of weight were close to the decomposition temperatures of standard organic binders such as Latex and polyvinyl alcohol used during the manufacturing of the paper. Hence a weak paper structure was produced.

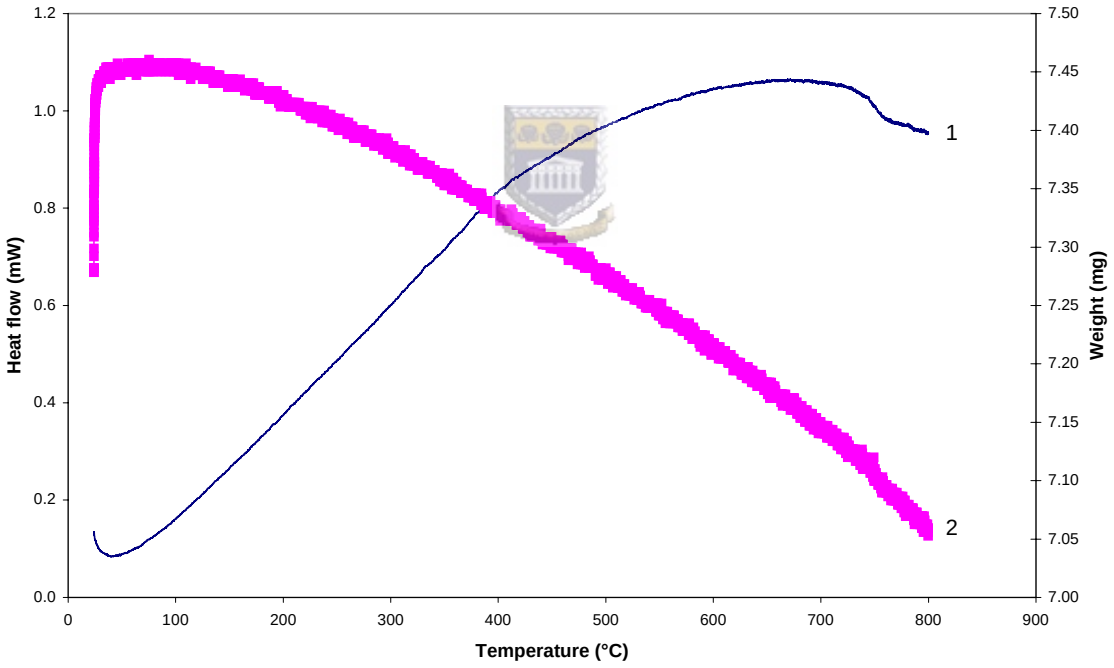

Figure 3.2: Graph of weight loss and heat as a function of temperature for 880 LFH paper 1: heat flow, 2: weight

3000 LAH paper was further treated at Lydall Company to remove organics to produce 880 LFH paper. The technical data for 880 LFH is shown in Table 3.3. Thermal analysis results in Figure 3.2 showed that 880 LFH was more thermally stable than 3000 LAH and 3000 LJH. A weight loss of 0.4 mg was observed between 100 to 800°C. The SEM photos of 3000 LJH and 880 LFH fibres were similar to each other (3000 LAH not shown because photos are the same) as observed in Figure 3.3.

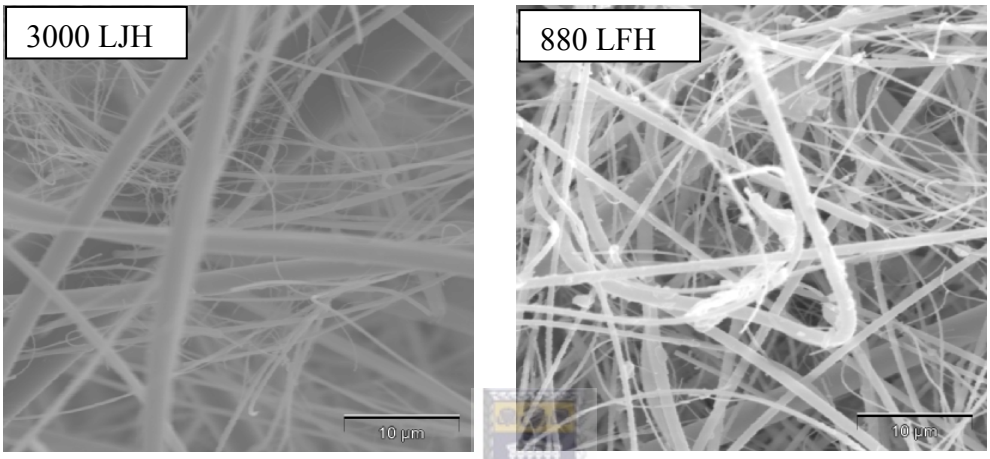

Figure 3.3: SEM image of 3000 LJH and 880 LFH papers at 10 µm

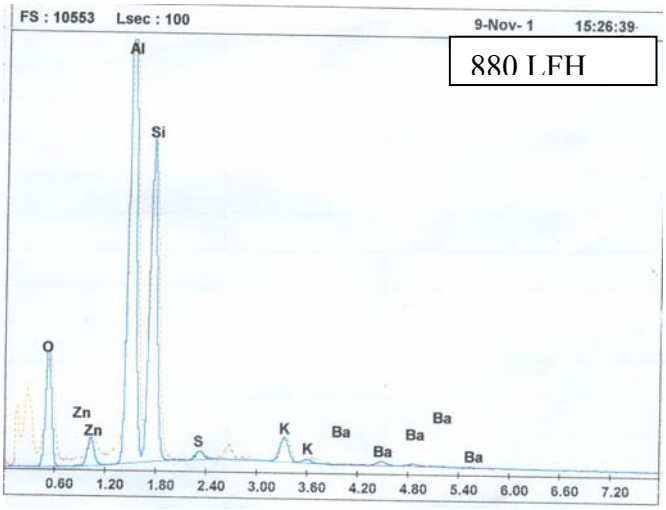

Figure 3.4: Elemental analysis graphs for 880 LFH paper from EDX studies

EDX results in Figure 3.4 showed the presence of impurities (K, Ba, S, and Zn) that were distributed across the surfaces of the 880 LFH paper. 880 LFH gave a low amount of the organic binder which was distributed very finely throughout the paper. Hence these papers were not suitable as catalyst supports. The 880 LFH paper was treated to prepare papers containing varying amounts of silica denoted as "IP-397-1" and "IP-397-2". These experiments were done at Lydall Company. The properties of these papers as provided by Lydall are listed in Table 3.3. Papers "IP-397-1" and "IP-397-2" were further treated at Lydall Company to improve the quality of the papers.

Table 3.3: Properties of papers 880 LFH, "IP-397-1" and "IP-397-2" provided by Lydall Company[106]

Property/Variation	880 LFH	"1P-397 -1"	"1P-397 -2"
Basis Weight (lbs/3000 ft^2)	205	259	164
Caliper @ 4 PSF (mils)	92	79	64
Density (lb/ft^3)	8.91	13.1	10.25
Caliper @ 8 PSI (mils)	n/a	65.3	46.9
MD Tensile (gm/in)	541	3479	3167
CD Tensile (gm/in)	n/a	2402	2425
Resistance @ 32 l/min/m^2 (mm H_2O)	28.9	254	284
Composition (wt %)			
Al_2O_3	56.1	35.4	23.6
SiO_2	41.9	47.8	51.2
Other Metal Oxides	2.1	16.8	25.2

SEM and EDX of papers "IP-397-1" and "IP-397-2" were performed in order to determine the relative elemental analysis and the presence of impurities.

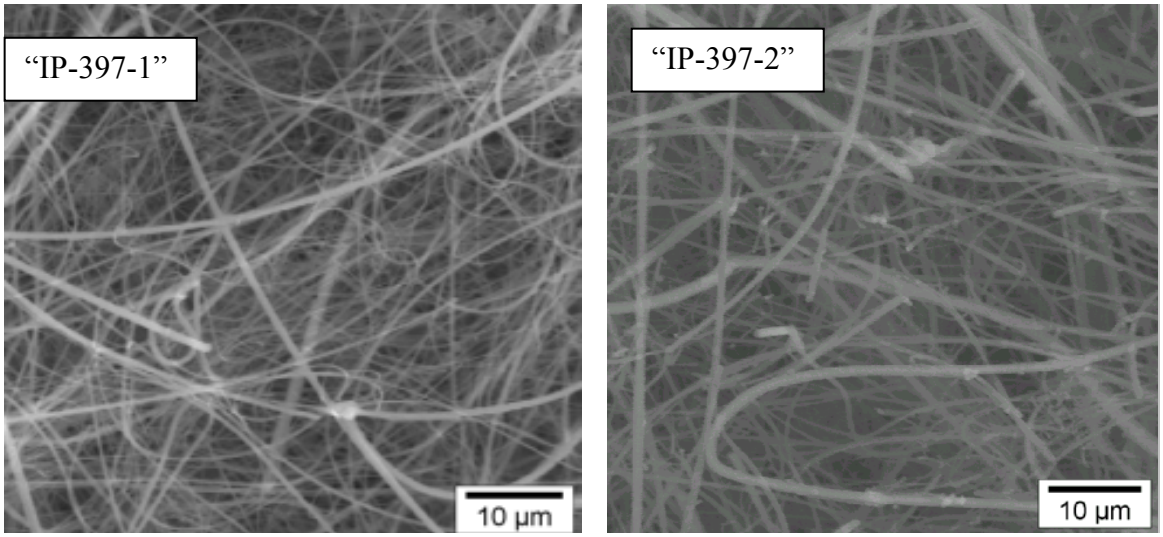

Figure 3.5: SEM image of paper "IP-397-1" and "IP-397-2"

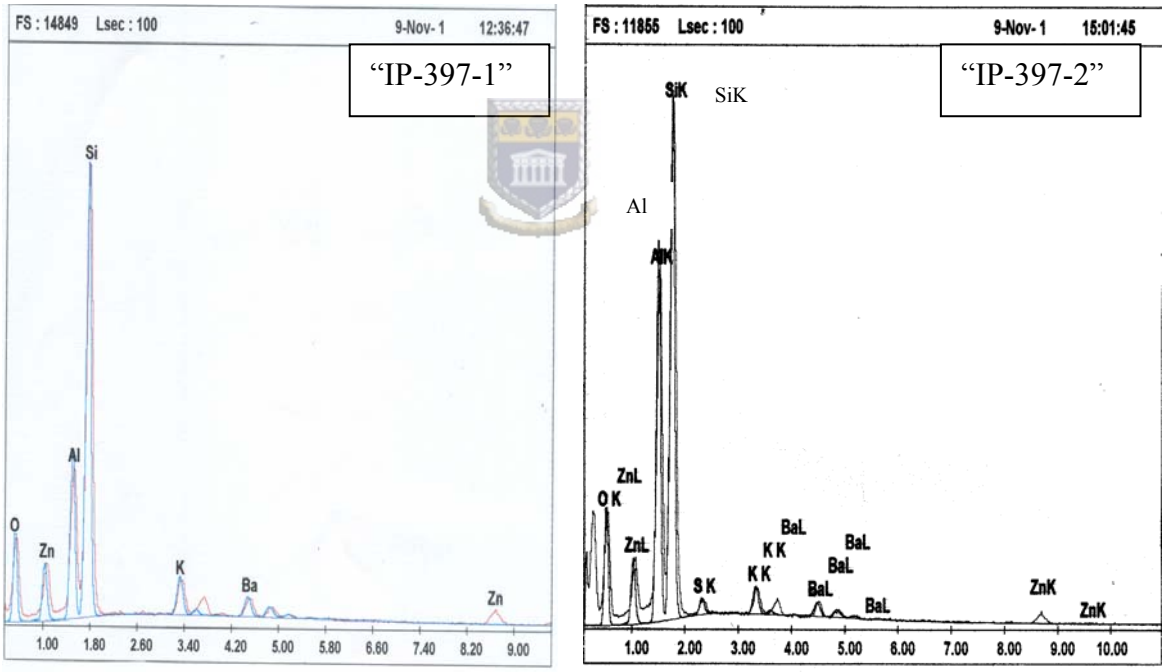

Figure 3.6: Elemental analysis results obtained from EDX of papers "IP-397-1" and "IP-397-2"

Paper “1P-397-1 has no sulphur on the surface while paper “1P-397-2 contained sulphur that might interfere in the oxidation reaction.[6] Paper “1P-397-1” was hence chosen as a suitable support for the catalysts. Thermal analysis, surface area and pore size distribution of paper “1P-397-1” were studied and the results are illustrated in Figures 3.7 and 3.8 below.

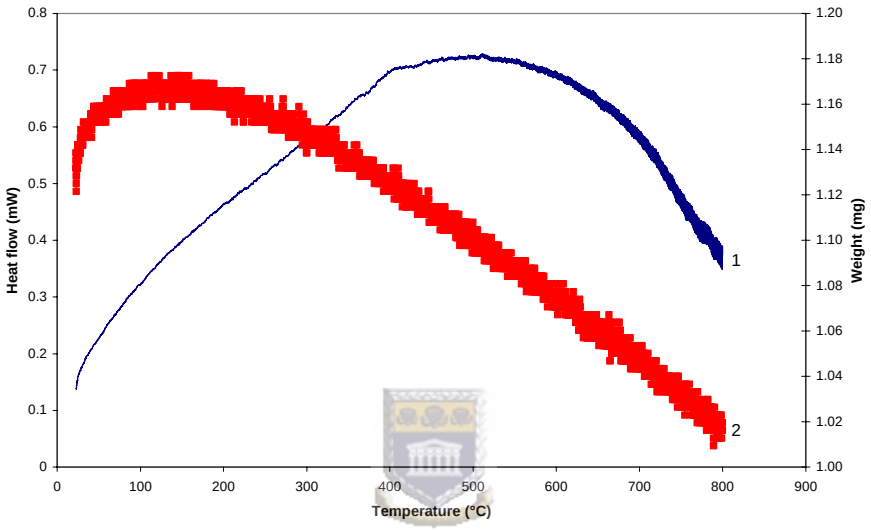

Figure 3.7: Graph of weight loss and heat flow as a function of temperature for paper “1P-397-1” 1: heat flow, 2: weight

“1P-397-1” was stable between 30 to 200°C and it started losing weight between 200 and 800°C (0.1 mg). “1P-397-1” did not change colour during the heating process.

The measured surface area (BET) of 1P-397-1 was 2.02 m^2/g and the pore size distribution is illustrated in Figure 3.8. Small micropore volume was observed in region 0-200 Å, whereas in the region 200-500 Å broad mesopore and macropore volume were observed.

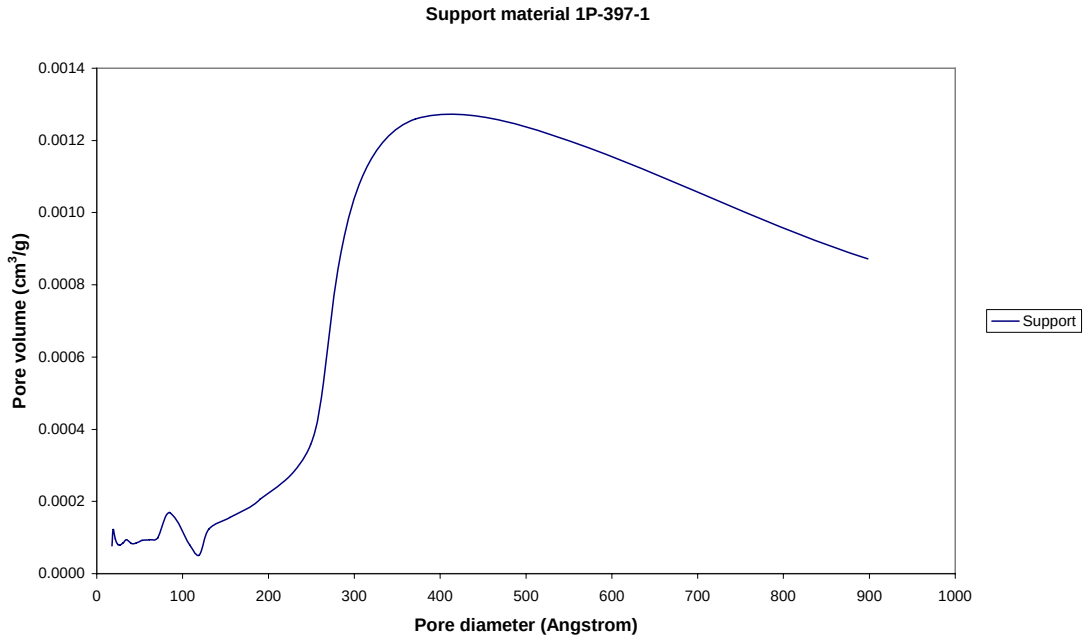

Figure 3.8: Pore size distribution of the support material, "1P-397-1" based on the pore volume ($f_v(r_p)$)

3.4 Conclusion

Inorganic ceramic membrane paper "1P-397-1" was the most preferable support material for the deposition of active metal centres. It is made up of 35.4 wt% Al_2O_3 and 47.8 wt% SiO_2. "1P-397-1" was thermally stable at temperatures that will be used in the oxidation of methane that is between 30 and 150°C. The SEM micrograph of the papers in Figure 3.5 above shows large pores between the fibres of the ceramic membrane material, making it difficult to deposit catalytic active groups on the surface of the ceramic membrane support. Therefore silica was chosen to modify the surface of the support material prior to deposition of a catalytic material in order to cover these pores. The second reason for modifying the support material with silica is

to minimise the impurities (K, Ba, and Zn) present in the support material that might interfere during the oxidation reaction and formation of any undesired products.

CHAPTER 4: Catalyst preparation and characterization

4.1 Introduction

Some of the commonly used methods for the making of heterogeneous catalysts are impregnation, slurry precipitation, co-precipitation, fusion, the Raney method, physical mixing, washcoating, and pelleting. The common preparation methods of dispersed metal/metal oxide catalysts require a combination of different unit operations, which can be described as:

(i) introduction of the metal precursor on the support,

(ii) drying and calcination, and

(iii) reduction (only if a metal catalyst is desired).[6]

In this research work the inorganic membrane was made catalytically active by the deposition of the active phase on the membrane support material. The impregnation (ion-exchange) method was chosen for the deposition of the active species. This procedure requires that the membrane support be brought into contact with a solution of the metal precursor, usually a salt, and then aged for a short time.[25] Inorganic ceramic membrane papers were modified with silica prior to the deposition of a catalytic material. The silica support can interact strongly with catalytic species and modify their catalytic behaviour.[52] Silica is an amorphous material of the general formula SiO_2. In bulk silica, the Si and O atoms are connected in tetrahedra of SiO_4^{4-} units linked through siloxane bonds (≡Si-O-Si≡) to form the silica network.[107] In ambient environments containing water vapour, the surface reacts with water and

becomes covered with silanol (≡Si-OH) groups, which possess excellent hydrogen bonding characteristics.[107] Amorphous silica is highly porous. Porosity introduces a large surface area inside the silica particles. Therefore, the introduction of silica on the membrane support will maintain and increase the surface area of the membrane support.[108] and enhance its thermal stability. Surface area, pore volume, pore size and particle size can be controlled independently by changing the method and specific parameters of silica preparation and therefore represent the four variables governing the chemical and physical behaviour of silica.[109]

The dispersion of the active phase on support materials is one of the most important parameters for catalytic reactions on supported oxides. The grafting of metals onto the surface of an inorganic support can lead to extremely active and selective catalysts.[69] The supported oxide can exist as clusters, heaps, or isolated ions.[52]

The active species chosen in this study were Pt, Hemin (Fe compound), SiMo and PMo. Platinum was chosen since it is used in the oxidation of CO by molecular oxygen to CO_2.[110, 111 112, 113] The selection of hemin for the preparation of catalytically active support materials for methane oxidation was based on the high activity of porphyrin compounds in different oxidation processes.[75, 114] Hemin heterogenisation can be carried out by adsorption, co-ordinated immobilisation with amino groups upon the carrier's surface or by the chemical reaction of functional side groups of hemin. Hemin is a metal complex compound of a tetra-azamacrocyclic ligand and the Fe^{3+}ion.[115] Hemin is present as a biocatalyst in oxidation reactions which take place in live organisms at low temperature and atmospheric pressure. Figure 4.1 represents the structure of hemin

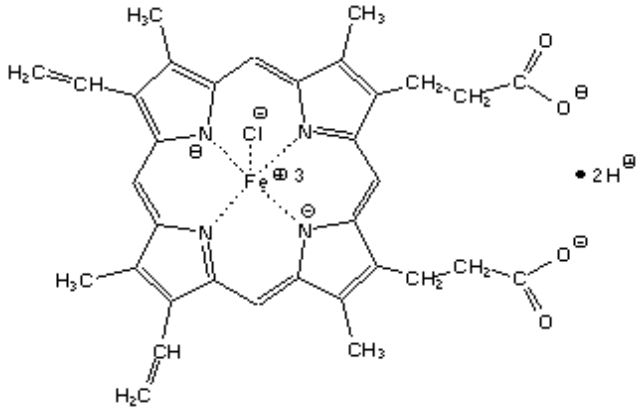

Figure 4.1: The structure of hemin[115]

Supported molybdenum oxides were selected because they play a role in industrially important reactions such as selective oxidation and metathesis of olefins.[46] Molybdenum-based chemicals have the versatility of a chemistry which can occur between the transitions of +4, +5 and +6 oxidation states. Materials made from molybdates are oxidation catalysts, have photo-activity, and can offer semi-conducting properties. Many of the properties of molybdenum can provide development opportunities and new commercial applications through the exploration of its chemistry.[116]

Heteropolyoxometalates with anions of the Keggin structure, represented in Figure 4.2, are interesting examples of isostructural catalysts, that is, those in which the elemental composition may be changed to produce an alteration of the catalytic properties while the structural features are retained. These heteropolyoxometallates are ionic solids with discrete anions and cations. The latter may be simple one atom inorganic ions or multi-atom organic species.

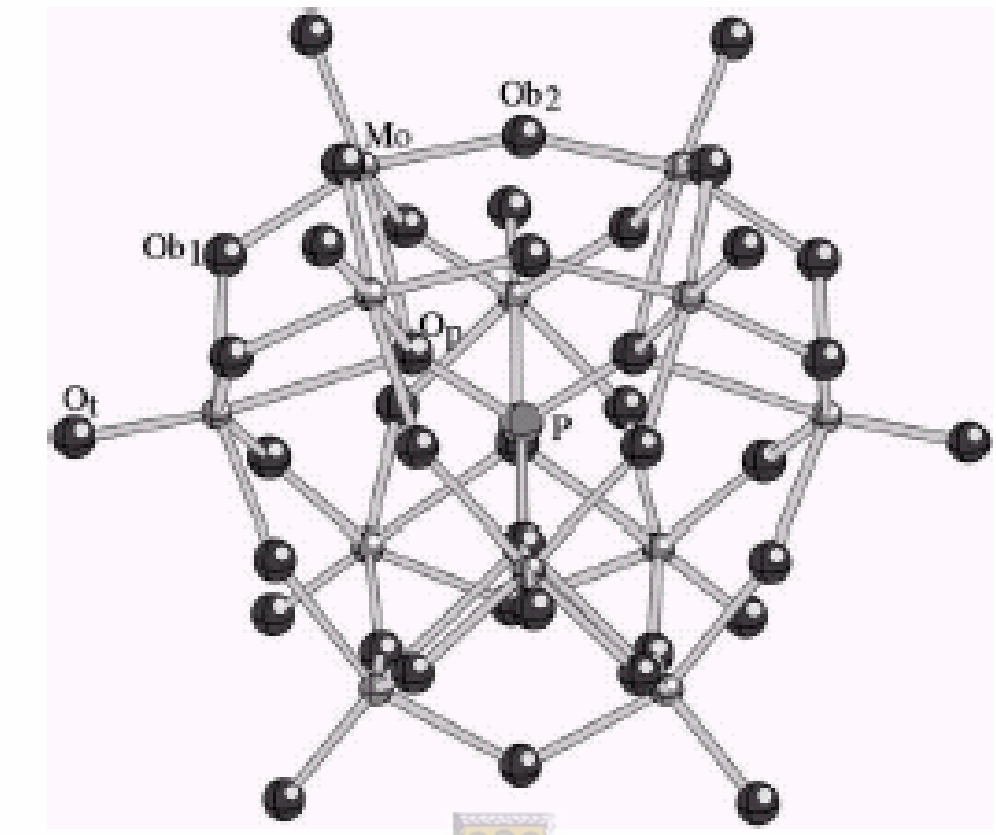

Figure 4.2: Ball-and-stick representation of the Keggin structure.[117] The different types of oxygen atoms are indicated (O_t is a terminal oxygen, Ob_1 and Ob_2 are bridging oxygens in one trimer and between two trimers, respectively, O_P stands for the oxygen in phosphorus tetrahedral environment).

The anions are large cage-like structures with a central atom such as phosphorus, which is surrounded by four oxygen atoms arranged tetrahedrally. Twelve octahedral with oxygen atoms at their vertices and a peripheral metal atom such as tungsten or molybdenum at their centres envelope the central tetrahedron and share oxygen atoms with each other and the central atom. The structures of the heteropoly anions are semi-quantitatively similar for either molybdenum or tungsten as peripheral metal atoms, although the bond lengths are slightly different with, for example, the peripheral

metal-terminal oxygen atom bond lengths being 1.66 and 1.70 Å for Mo and W, respectively.[118] Heteropolyoxometalates compounds with a general formula for the Keggin structure, $XM_{12}O_{40}^{x-8}$, where X is the central atom (Si^{4+}, P^{5+}), x its oxidation state, and M the metal ion (Mo^{6+}, W^{6+}), possess characteristic acidic and redox properties which can be controlled by substitution of the metal atoms of the anion (central and addenda atoms) and the countercations and is related to their catalytic activity. Due to their low surface area most recent studies have focused on heteropoly acids (HPA) loaded on different supports, which allow their use in heterogeneous reactions.[118] The catalytic function of heteropoly compounds in the solid state has attracted much attention because their redox and acidic properties can be controlled at atomic/molecular levels. The addition of transition metals to heteropoly compounds is important to control the redox properties and to enhance catalytic performance. There have been several attempts to oxidize lower alkanes by using heteropoly catalysts. It has been reported[41, 52] that the hydrogen form of $H_3PMo_{12}O_{40}$ catalyzed the oxidation of lower alkanes and that the substitution of V^{5+} for Mo^{6+} modified the catalytic activity and selectivity. The crystal structure of $H_4SiMo_{12}O_{40}$ shows that the $SiMo_{12}O_{40}^{4-}$ anion is of the Keggin type, consisting of $12MoO_6$ octahedra surrounding a SiO_4 tetrahedron. Moreover, cohesion between the Keggin units is achieved by means of hydrated protons and water molecules.[52]

4.2 Experimental procedure

All experimental details involving catalyst preparation and characterization are given in Chapter 2.

4.3 Results and discussion

4.3.1 Modification of the support material with silica

Multiple layers of silica were used to modify the surface of an inorganic ceramic support in order to immobilize catalytically active groups on them. The presence of silanol groups may allow the interaction of the adsorbed catalytic species with the surface of the support, usually through hydrogen bonding or dipole-dipole interaction.[94] The mass of the support material increased by about 2% after modification with 1 layer of silica and 5% increase in mass was obtained with 3 layers of silica as illustrated in Table 4.1.

Table 4.1: Mass increase and surface area of support after modification with silica

Sample no.	Sample description	Mass of support (g)	SiO_2 on support (%)	Colour	Surface area-BET-(m^2/g)
1	Support	1.1272	-	White	2.02
2	Support/1 layer silica	1.0770	2.36	White	13.91
3	Support/2 layer silica	1.1429	3.12	White	21.86
4	Support/3 layer silica	1.1670	5.14	White	27.86

The introduction of silica on the membrane support material increased the surface area of the membrane support as shown in the above table, where the unmodified support material has a surface area of 2.02 m^2/g. The surface area increased with the number of silica layers coated on the support material. 3 layers of silica showed a surface area of 27.86 m^2/g. The highest difference in the surface area between consecutive layers is 11.89 m^2/g that is, between zero layer and one layer. The increase in surface area was expected since amorphous silica is highly porous and porosity introduces large surface area inside the silica particles.[108] The large surface

area was desired in order to attach active species with high loading.[119] The morphology of the deposited silica on the support material was studied by using SEM. SEM micrographs are shown in Figure 4.3.

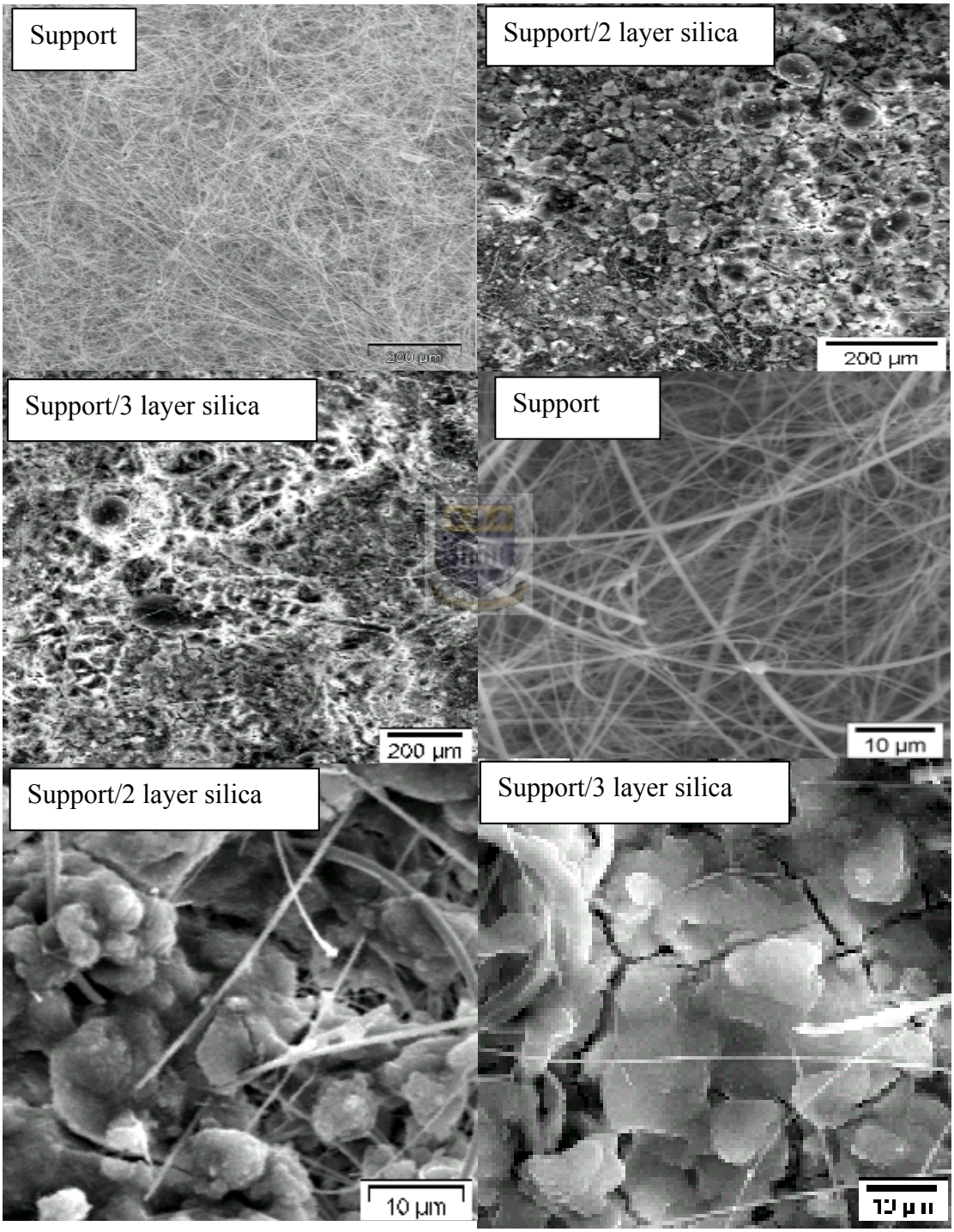

Figure 4.3: Micrographs of support and silica modified support

Silica covers the fibres of the support material leaving cracks on the surface. The cracks increase the surface area of the support for further deposition. At 10 μm the silica cracks can be easily observed. Analysis by EDX was done at several points on the surface and the difference of each element weight% at these points was ± 1%. EDX results in Figure 4.4 showed a decrease in the weight% of K, Ba and Zn after modifying the support with silica. K and Ba were less than 1% on the support modified with 3 layers of silica. K, Ba and Zn metals form part the support and they might have an effect on catalyst activity.

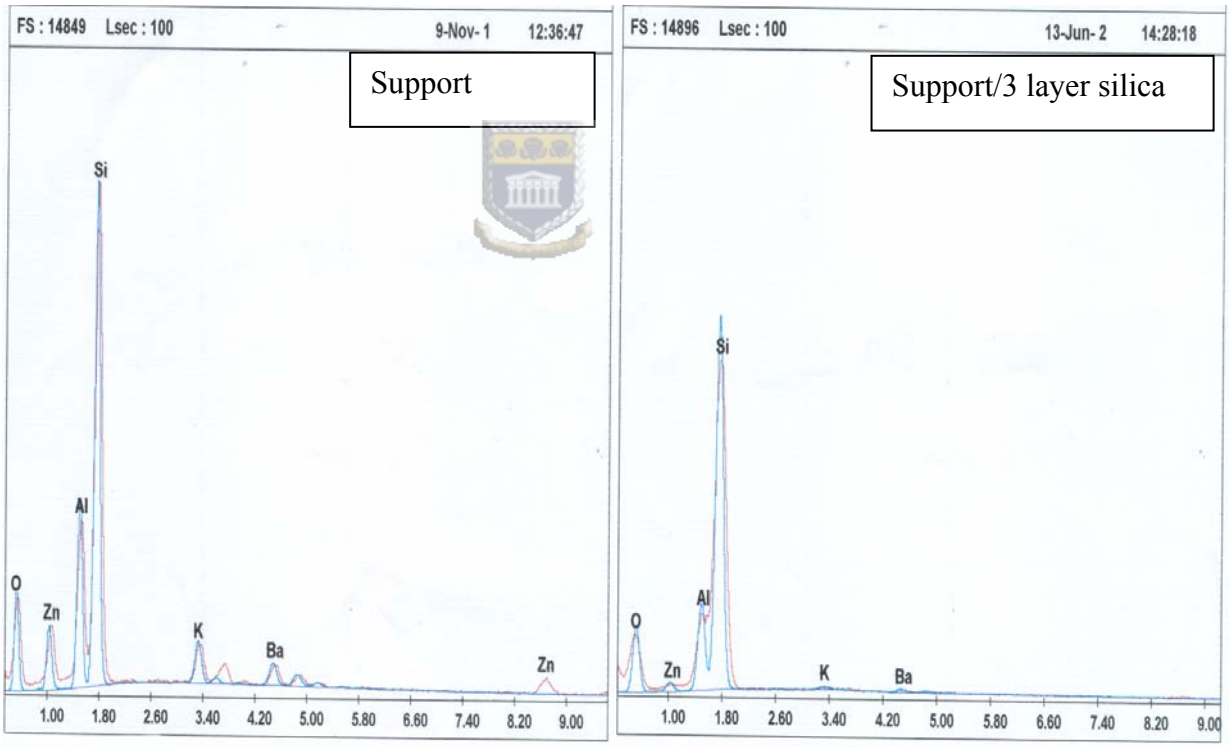

Figure 4.4: Elemental analysis graphs for the unmodified support and silica modified support obtained from EDX studies

According to the BDDT[94] classification, a type IV isotherm of the silica used in the modification of the support material exists which is typical of mesoporous silica. Therefore the adsorption-desorption curves are used to determine the pore size distribution of the support modified with silica and the catalysts prepared. Figure 4.5 illustrates the pore size distribution of support material modified with fumed silica, based on the pore volume. The support material showed a broad pore size distribution in the mesopore (200-500Å) and macropore (500-900Å) regions. Introduction of silica on the support material narrowed the pore size distribution.

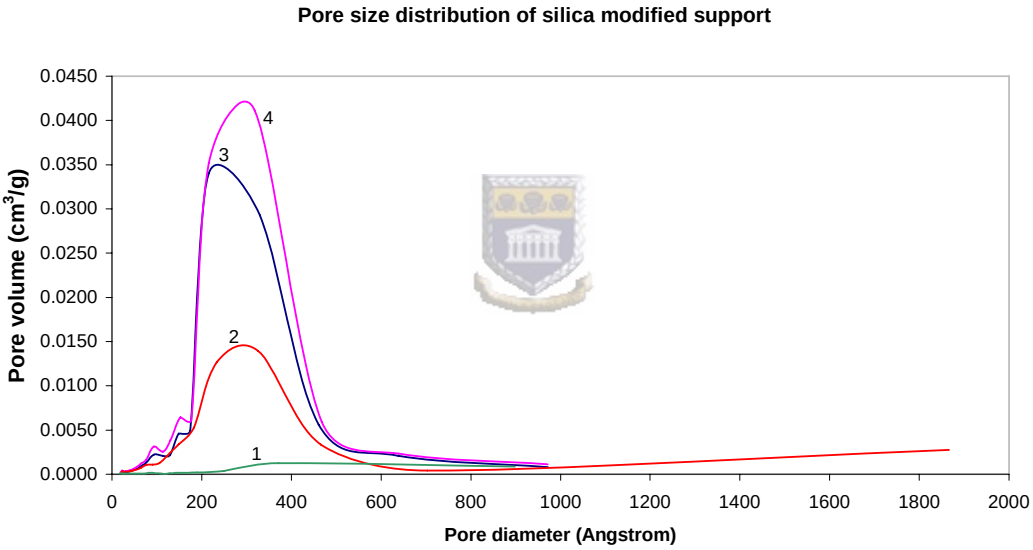

Figure 4.5: Pore size distributions of the silica modified support material, based on the pore volume (fv(rp)) compared to the unmodified support 1: Support, 2: Support/1 layers silica, 3: Support/2 layers silica, 4: Support/3 layers silica

The pore volume increased with the number of silica layers deposited on the support material. There are two regions of porosity that is, region 1 at 0-200Å, and region 2 at 200-500Å. In region 1 a small volume of micropores started to appear upon

modification with silica. Mesopores were observed in region 2. The mesopore volume increased with increased silica.

Table 4.2: Summary of the pore size distribution results for silica modified support

Sample description	0-200 (Å)	200-500 (Å)
Support	Small micropore volume	Broad mesopore and macropore area
Support/1 layer silica	No micropores	Small mesopore volume
Support/2 layer silica	Micropore start appearing	Mesopore volume increased
Support/3 layer silica	Small micropore volume	Large mesopore volume

3 layers of silica showed large mesopore volume and narrow pore size. The narrow pore is important to keep the molecule fixed at that position during the reaction. Modification of the support material with 3 layers of silica is important and interesting for further deposition with the active metal species due to the low impurities obtained on the surface of the support material as well as the narrow pore size distribution of the silica on the surface. On the unmodified support material, the Al-OH and Al-O-Si functional groups and surface Si-OH are present. Modification of the support with fumed silica increases the silanol groups and Si-O-Si bonds may have formed on the surface.

4.3.2. Impregnation of the unmodified and silica modified support materials with metal salts

The catalysts under study showed different responses to the effect of silica layers on active species deposition. The gain in mass of the prepared catalysts was determined and is shown in Table 4.3 as well as the colour change after active metal deposition. The various metal catalysts employed will be discussed separately below.

Table 4.3: Mass increase (%) of catalysts deposited on unmodified and silica modified support

Catalyst no.	Sample description	Mass of support (g)	*Catalyst on un/modified support (%)	Catalyst colour
1	Support	1.1272	-	White
2	Support/1 layer silica	1.0770	2.36	White
3	Support/2 layer silica	1.1429	3.12	White
4	Support/3 layer silica	1.1670	5.14	White
5	Support/hemin	1.1272	4.04	Brown
6	Support/1 layer silica/hemin	1.0770	2.63	Brown
7	Support/2 layer silica/hemin	1.1429	3.20	Brown
8	Support/3 layer silica/hemin	1.1670	4.10	Brown
9	Support/Pt	1.0576	11.7	Orange
10	Support/1 layer silica/Pt	1.1120	5.5	Orange
11	Support/2 layer silica/Pt	1.0845	12.7	Orange
12	Support/3 layer silica/Pt	1.0276	14.4	Orange
13	Support/PMo	1.1553	53.0	Lime/Yellow
14	Support/1 layer silica/PMo	1.0486	43.1	Lime
15	Support/3 layer silica/PMo	0.9738	60.0	Lime
16	Support/SiMo	1.1288	1.86	Yellow
17	Support/1 layer silica/SiMo	1.0180	1.55	Light yellow
18	Support/2 layer silica/SiMo	1.0056	1.60	Light yellow
19	Support/3 layer silica/SiMo	1.1128	1.95	Light yellow

* % catalyst = (grams of catalyst/ total mass) x 100

A. Deposition of $H_2PtCl_6.6H_2O$ (HCP) on the support material

Platinum deposition was higher on the support modified with 3 layers of silica than on the unmodified support as shown in Table 4.4 below. 1 layer silica on support gave the lowest mass percentage of Pt, even lower than the unmodified support. It was

expected that Pt deposition on 1 layer silica would be higher than that on unmodified support since silica increases the surface area for active metal deposition. This might be due to experimental error during the drying process.

Table 4.4: Gravimetric analysis of chemical composition and surface area of Pt-based catalysts

Catalyst no.	Sample description	(HCP) on support (%)	[Pt] on support (mg/cm^2)	Colour	Surface area - BET- (m^2/g)
1	Support	-	-	White	2.02
9	Support/Pt	11.7	0.244	Orange	3.19
10	Support/1 layer silica/Pt	5.5	0.163	Orange	6.23
11	Support/2 layer silica/Pt	12.7	0.244	Orange	10.72
12	Support/3 layer silica/Pt	14.4	0.326	Orange	17.10

In catalyst 9 the Al-OH functional groups of the porous support might have interacted with the metal atoms. The ≡Al-O-Si≡ bonds, which are weaker than the ≡Si-O-Si≡ bond, may have formed in catalyst 10 and hence less Pt loading may have resulted. High surface area and more Pt deposition on catalysts 11 and 12 were observed due to the introduction of ≡Si-O-Si≡ bonds after silica modification. The adsorption of H_2PtCl_6 on silanol groups occurs with protonation of silica modified support according to the schematic equation 1. In acidic media the adsorption surface site (≡Si-OH) is positively charged and therefore is covered by anions.[25]

$$\equiv Si–OH + HPtCl_6^- H^+ \leftrightarrow \equiv Si–OH_2^+ HPtCl_6^- \quad (1)$$

The BET surface area of platinum-based catalysts shown in Table 4.4 increased with the number of silica layers after impregnation with H_2PtCl_6. Impregnation of platinum on silica modified support resulted in a reduction in the surface area.

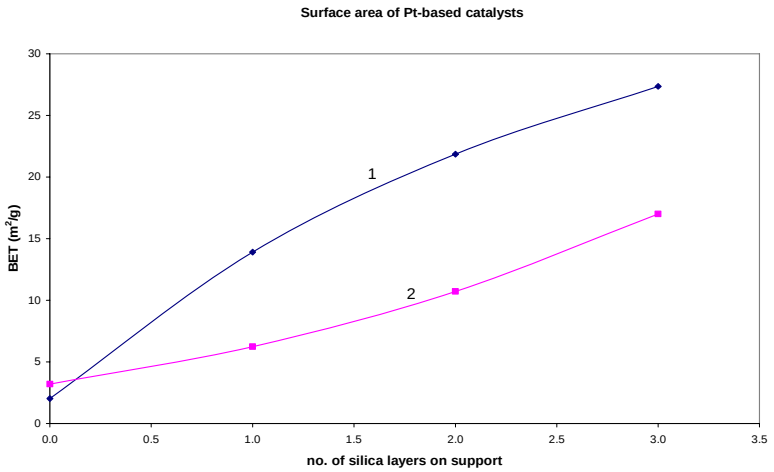

Figure 4.6: Surface area (BET) of Pt-based catalysts 1: Silica on support, 2: Pt on silica modified support

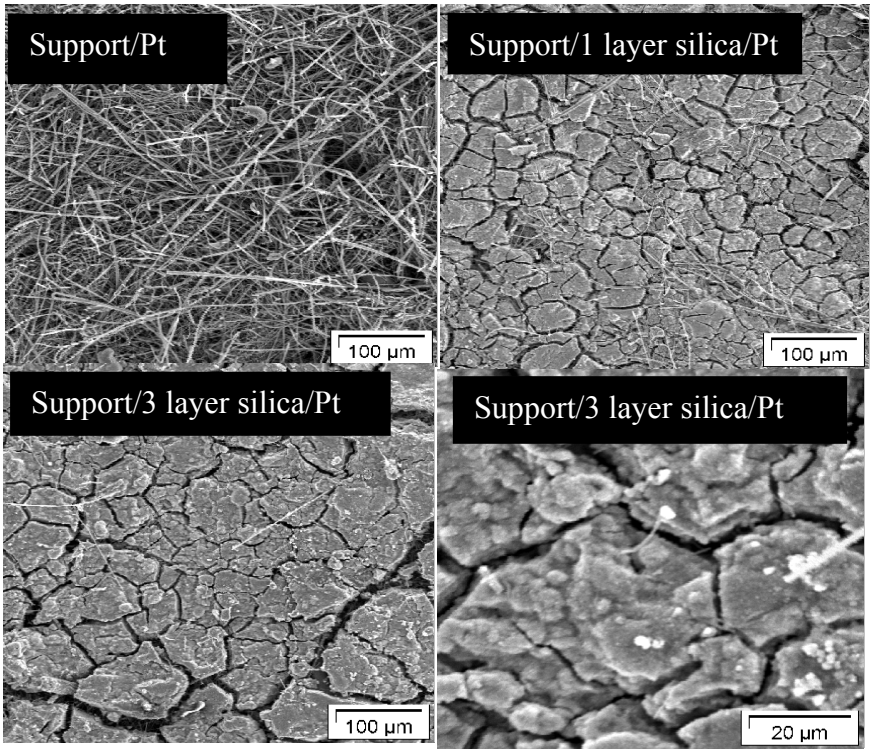

Figure 4.7: Micrographs of Pt-based catalysts at 10 kV

The 3 layer of silica on support material with BET 27.89 m^2/g as per Table 4.4 decreased to 17.10 m^2/g after platinum deposition. This decrease in the surface area of the silica modified support confirmed that platinum was adsorbed on the surface as illustrated in Figure 4.6. HCP therefore used ≈ 10 m^2/g of the available surface area.

Figure 4.7 shows SEM micrographs after depositing HCP on the unmodified and silica modified support. It was difficult to observe Pt particles on the surface. Pt particles might have migrated via these pores to inner layer of the fibre support and no agglomeration of Pt particles was observed.

Elemental composition of prepared catalysts was determined by EDX on several points on the surface and the results are presented in Figure 4.8.

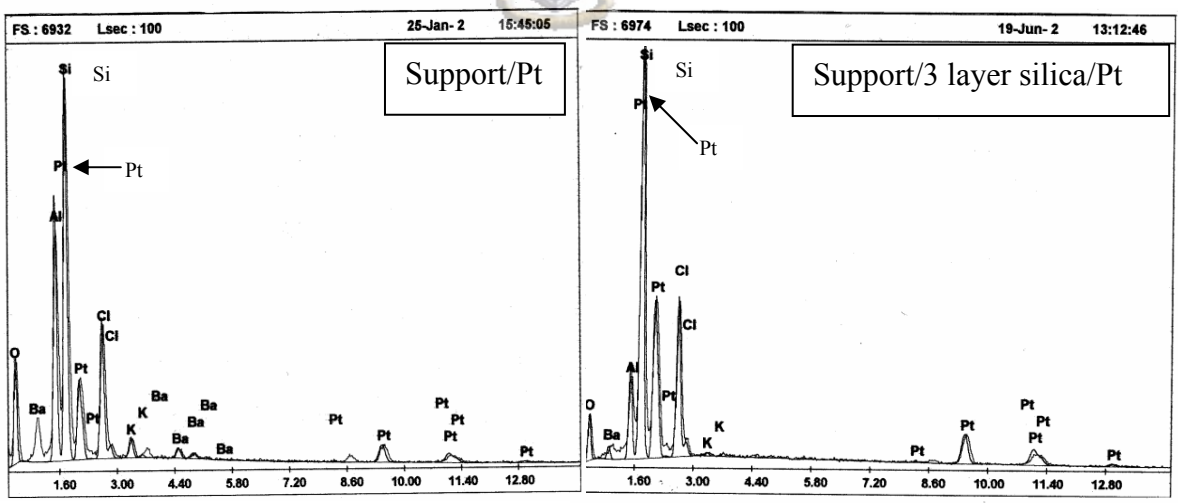

Figure 4.8: Elemental analysis graphs for Pt-based catalysts obtained from EDX studies

The sample with 3 layer silica on the support showed low percentage of impurities (elements K and Ba) present in the support material. Thus modification with silica minimised the amount of these elements impurities on the surface that might have an influence on the oxidation of methane with oxygen. The increase in the weight percent of Pt in Figure 4.8 between the unmodified support and the support modified with 3 layer silica suggested that the amount of Pt deposited increased with the number of silica layers on the support material. This is possibly due to the silanol groups present on the surface of the support modified with silica. These results confirmed the importance of modifying the support with silica prior to the deposition of the catalytic active group.

Table 4.5 shows the concentration of Pt on the unmodified and silica modified support obtained by ICP-MS.

Table 4.5: Elemental analysis (ICP-MS) for Pt-based catalysts

Sample description	Pt concentration (ppb)
Support/Pt	108628
Support/1 layer silica/Pt	111810
Support/3 layer silica/Pt	155620

The concentration of Pt on the unmodified, 1layer and 3 layer silica modified support were 108.63, 111.81, and 155.62 ppm respectively. The support modified with 3 layer of silica showed a higher Pt concentration than the other catalysts. 0.01 M H_2PtCl_6 solution before deposition process contained 2000 ppm Pt and only 155 ppm maximum was found on the support surface suggesting that a small amount of Pt was

deposited on unmodified and silica modified support. The ICP results, not only corresponded with the previous results (BET, SEM, EDX) that Pt deposition increases with the number of silica layers on the support it also reiterated the role of silica on silica modified support materials. Thus silica increased the surface area for the interaction of surface hydroxyl with the active metal centre. The pore size distribution of Pt-based catalysts is illustrated in Figure 4.9 and summarised in Table 4.6.

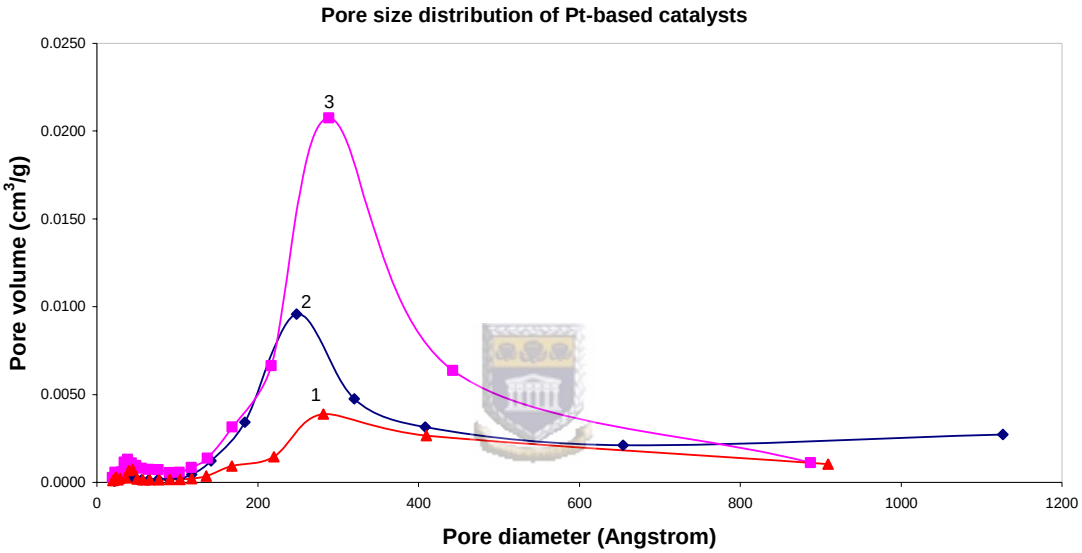

Figure 4.9: Pore size distributions of Pt-based catalysts, based on the pore volume (fv(rp)) 1: Support/1 layer silica/Pt, 2: Support/2 layer silica/Pt 3: Support/3 layer silica/Pt

Impregnation of platinum onto the unmodified and modified support showed a huge reduction in the volume of the mesopores attributive to the blocking of the support and silica pores respectively with platinum. For the 3 layer silica on support the 0.04 cm^3/g pore volume (see Figure 4.5) was reduced to 0.02 cm^3/g after the deposition of platinum. There are three regions of porosity compared to the two of Figure 4.5, that

is, region 1 at 0-200Å, region 2 at 200-500Å and region 3 from 500-800Å. A very broad pore distribution of platinum on unmodified support extending to the macropore region (500-800Å) was observed with a small volume. Increasing the number of silica layers on the support narrowed the pore size to a mesopore region (200-500Å) as summarised in Table 4.6 below. The pore volume increased from 0.0011 to 0.02 cm^3/g on Pt deposited on unmodified support and Pt on silica modified support respectively.

Table 4.6: Summary of the pore size distribution results for Pt-based catalysts

Sample description	0-200 (Å)	200-500 (Å)
Support/Pt*	Small micropore volume	Broad mesopore area, small volume
Support/1 layer silica/Pt	Small micropore volume	Broad mesopore area and increase in volume
Support/2 layer silica/Pt	Increase in micropore volume	Broad area and increase in mesopore volume
Support/3 layer silica/Pt	Small micropore volume	Large mesopore volume

*The pore size distribution of Pt on unmodified support is presented in Figure A1 of appendix in page 168.

The XRD scans of the support material and silica modified support showed an amorphous structure as was expected since amorphous silica was used. Figure 4.10 presents the XRD scans of Pt based catalysts. Platinum deposited on fumed silica showed the crystalline platinum peaks at $2\theta = 40$, 47 and 68° as summarized in Table 4.7. These inter-atomic distances (d-spacings) are acceptable and within range of the d-values for pure polycrystalline Pt.[97, 120]

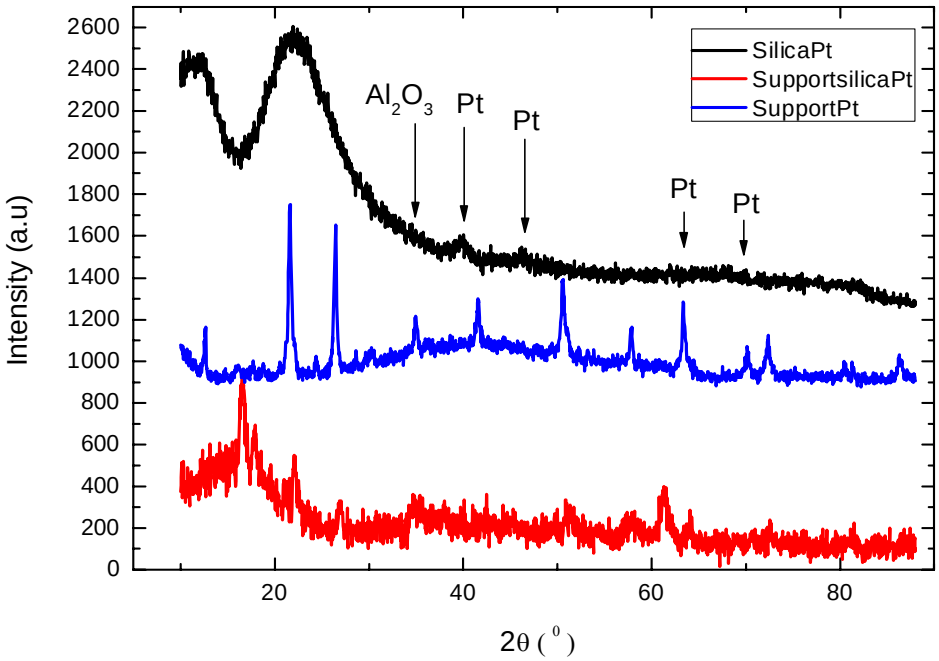

Figure 4.10: XRD scans of Pt-based catalysts step: 0.020, step time: 15 seconds

The reference values for the pure metal have the 3 most intense d-spacings with values: 2.265, 1.962, 1.1826Å.[97] The discrepancies in the inter-atomic distances might be due to imperfections in the crystals on oxide support material and the possible interference from the mesoporous silica.

Table 4.7: Inter-atomic distances for crystal planes of the Pt unit cell

Sample description	2 theta, (°)	d (Å)* (Bragg equation)	Crystal plane (Miller indices)
Silica/Pt	40	2.254	111
	47	1.933	200
	68	1.379	220
Support/Pt	41	2.201	111
	68	1.379	220
Support/silica/Pt	-	-	-

*nλ= 2dsinθ, n=1, λ= 1.5418Å

Support/Pt and Support/silica/Pt showed SiO_2 peaks at 2θ = 22, 31 and 36.7° which corresponded to the diffractogram of cristobalite. 2 platinum peaks were observed for Support/Pt at 2θ = 41 and 68° with d-spacings 2.201 and 1.397Å respectively. However, Support/silica/Pt showed no platinum diffraction but the diffraction at 2θ = 64° is due to PtSi compound.

B. Deposition of Hemin on the support material

The increase in mass was observed after impregnating the silica modified and unmodified support with hemin dissolved in DMF as illustrated in Table 4.8.

Table 4.8: Mass increase and surface area of hemin-based catalysts

Catalyst no.	Sample description	Hemin on un/modified support (%)	Catalyst colour	Surface area -BET- (m^2/g)
5	Support/hemin	4.04	Brown	3.96
6	Support/1 layer silica/hemin	2.63	Brown	7.11
7	Support/2 layer silica/hemin	3.20	Brown	8.69
8	Support/3 layer silica/hemin	4.10	Brown	11.43

The mass increase in the unmodified support was the same as in the 3 layer silica modified support. Both the 1 layer and 2 layer silica modified support showed lower mass increase and was also less than the hemin adsorbed on unmodified support. The effect of modifying the support with silica prior to deposition of active species was not monitored, since it was envisaged that the amount of hemin deposited will increase with the number of silica layers on the support. It is now understood that silica was washed off from the support during impregnation with hemin -the deposit

of silica being left at the bottom of the beaker in the hemin/DMF solution after the deposition process. Large amounts of deposition were found in the case of sample 6 and 7. Hence the amounts of hemin deposited were low. The low mass increase in catalysts 6, 7 and 8 was accompanied by an increase in surface area. This increase in surface area suggests that hemin was to some extent adsorbed on the support material and since hemin is a complex porphyrin compound (hemin structure provided in Figure 4.1) it might have contributed to the high BET surface area results of these catalysts.

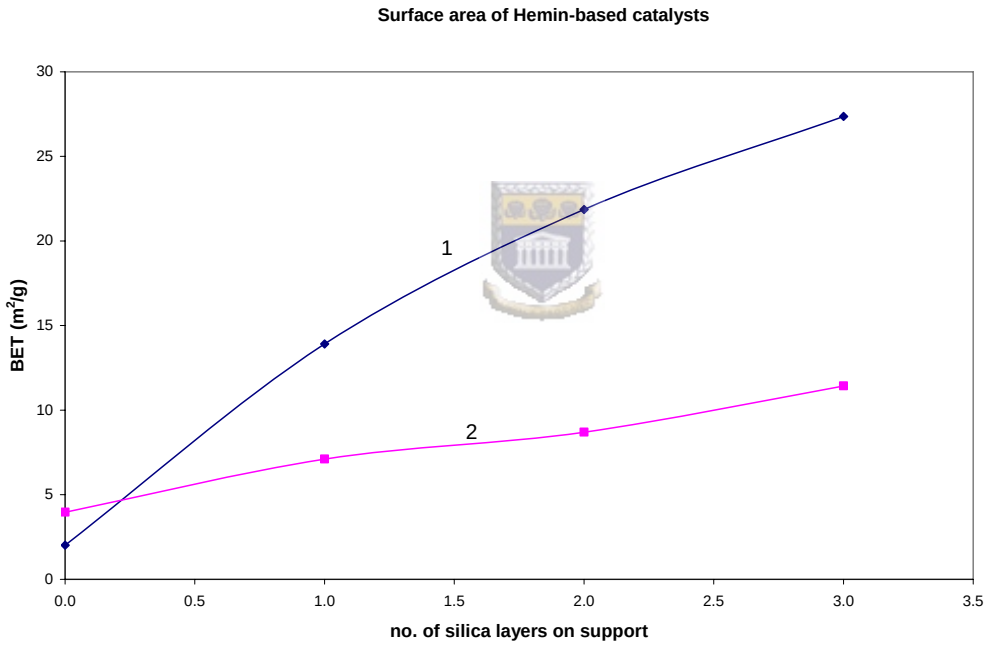

Figure 4.11: Surface area (BET) of hemin-based catalysts 1: Silica on support, 2: Hemin on silica modified support

High surface area on catalyst 6, 7 and 8 was also due to the introduction of ≡Si-O-Si≡ bonds after modifying the support with silica. The reduction in surface area of silica modified support after hemin deposition on the surface provides a proof that hemin

was adsorbed on the surface by filling silica pores. When immersing silica (PZC = 2) in hemin solution (pH is above silica's PZC), its surface was negatively polarized and hence will adsorb cations according to the general schematic equation 2.[25]

$$\equiv Si\text{-}OH + OH^- \leftrightarrow \equiv Si\text{-}O^- + H_2O \quad (2)$$

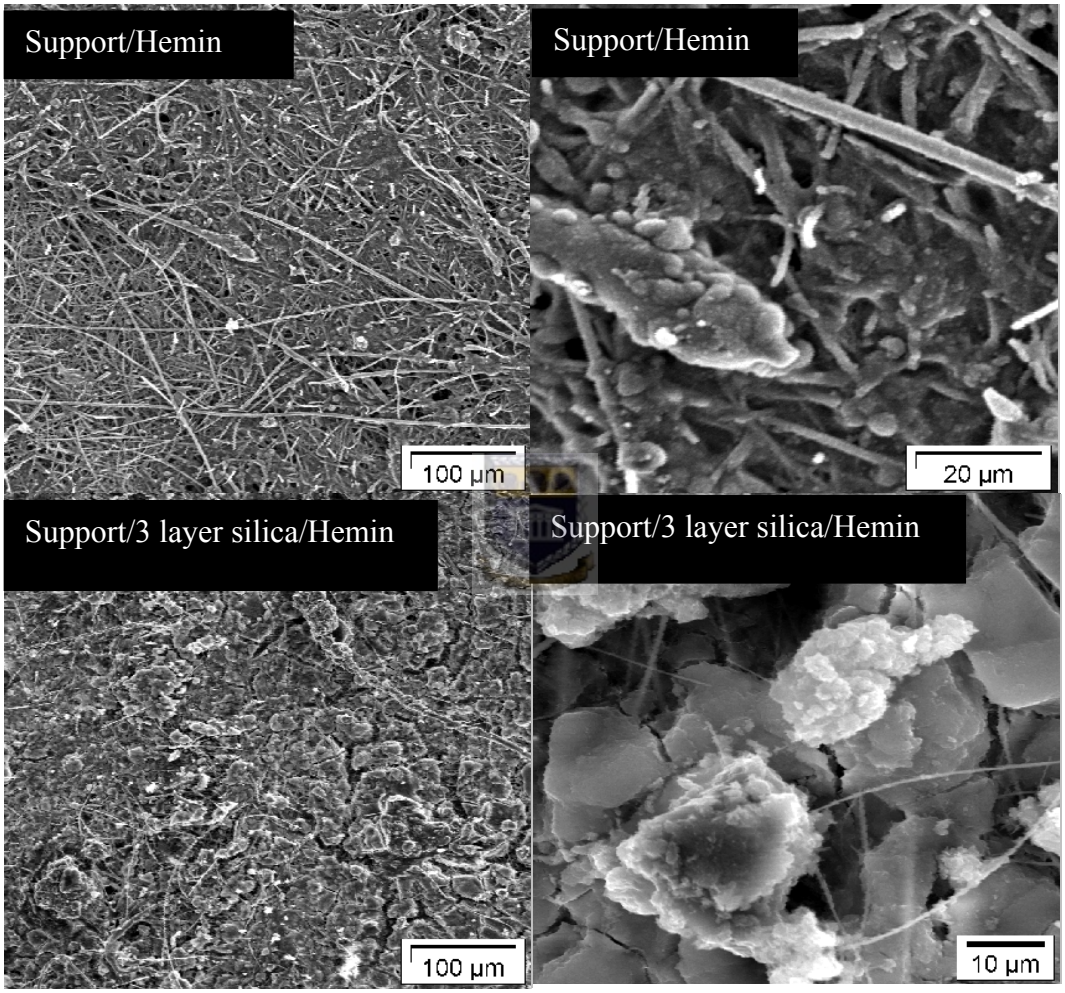

Figure 4.12: Micrographs of Hemin-based catalysts at 10 kV

Hemin was homogeneously distributed on the surface of the support as illustrated in Figure 4.12. Hemin covered the pores on the surface of the support material but only few fibres were observed on the surface of the unmodified catalyst. Thus modification with silica was needed to minimize the impurities- K, Ba and Zn- on the support

material. The SEM observation agrees with the EDX results presented in Figure 4.13. The weight% of the impurities (K, Ba, and Zn) was higher in the support/hemin than in the hemin/3 layer silica/support. The Al weight% which is part of support since the inorganic membrane is made up of alumina and silica as discussed in Chapter 3.2 decreased after modification with silica.

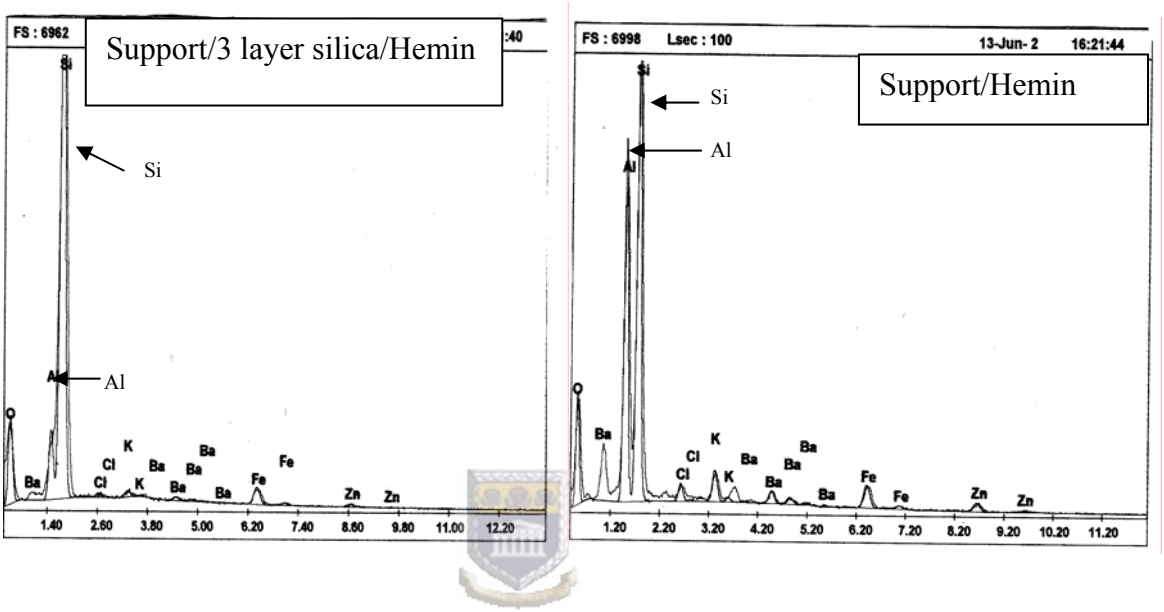

Figure 4.13: Elemental analysis graphs for Hemin-based catalysts obtained from EDX studies

Elemental analysis results using ICP-MS presented in Table 4.9 shows that the amount of Fe increased with the number of silica layers on the support although the iron adsorption was small with catalysts 5, 6 and 8 showing 13.6 ppm, 13.5 ppm and 14.0 ppm Fe respectively. This might be due to the fact that hemin is a bulk metal complex compound of a tetra-azamacrocyclic ligand with the Fe^{3+}ion[115] at the centre of the compound and hence Fe covers a small part on surface of the support.

Table 4.9: Elemental analysis (ICP-MS) for hemin-based catalysts

Sample description	Fe concentration (ppb)
Support/Hemin	13565
Support/1 layer silica/Hemin	13491
Support/3 layer silica/Hemin	14000

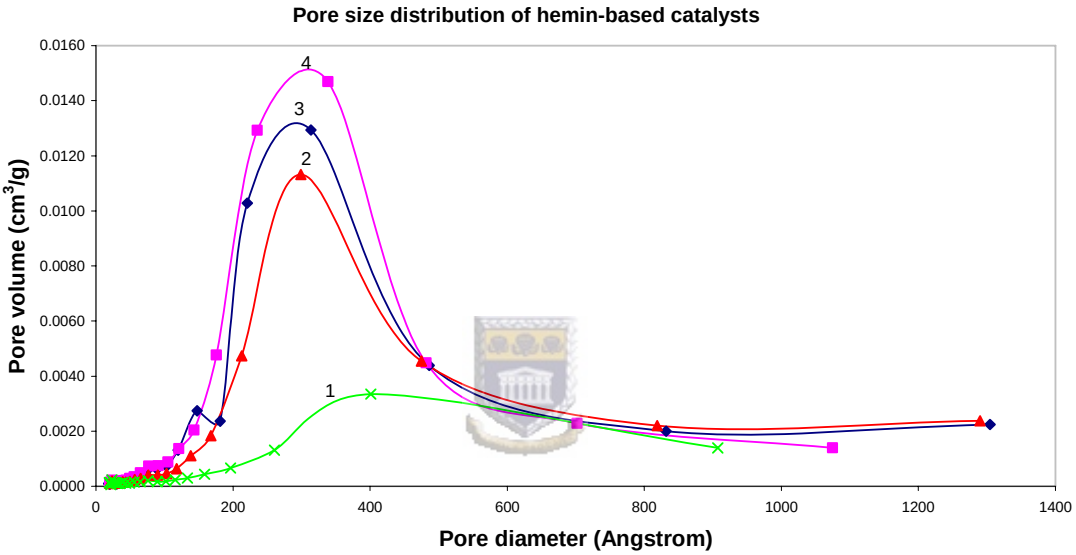

Figure 4.14: Pore size distributions of hemin-based catalysts, based on the pore volume (fv(rp)) 1: Support/hemin, 2: Support/1 layer silica/hemin, 3: Support/2 layer silica/hemin, 4: Support/3 layer silica/hemin

Figure 4.14 and Table 4.10 represent the pore size distribution of hemin-based catalysts. Hemin coated on the unmodified support showed a broad mesoporous region with a small pore volume, whilst a narrow mesopore distribution was observed

Table 4.10: Summary of the pore size distribution results for hemin-based catalysts

Sample description	0-200 (Å)	200-500 (Å)
Support/Hemin	No micropores	Broad mesopore peak, volume increase
Support/1 layer silica/Hemin	No micropores	Increase in mesopore volume
Support/2 layer silica/Hemin	Small micropores appear	Increase in mesopore volume
Support/3 layer silica/Hemin	No micropores	Large mesopore volume

with hemin deposited on silica modified support. Pore volume of the mesopore distribution increases with the number of silica layers coated on the support material increasing from 0.003 cm^3/g unmodified support to 0.015 cm^3/g in silica modified support. Figure 4.15 represents the XRD scans of hemin-based catalysts.

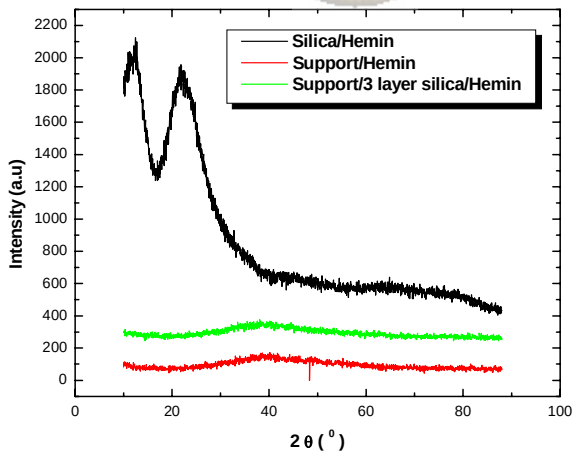

Figure 4.15: XRD scans for hemin-based catalysts

Hemin deposited on powder silica, unmodified support and 3 layer silica modified support showed the amorphous structure of fumed silica and support material indicating that hemin was in a highly dispersed state as shown by SEM results.

C. Deposition of Silicomolybdic acid hydrate [$H_4SiO_4.12MoO_3.xH_2O$] on the support material

Mass increase was observed on the unmodified and silica modified support after the impregnation of $H_4SiO_4.12MoO_3$ (SiMo) as presented in Table 4.11. The mass of SiMo increased with the number of silica layers deposited on the support material with a small increase between the successive silica layers. Silica introduces the acidity on the support and is more favoured for heteropoly acid deposition than basic supports since basic supports decompose the heteropoly acid.[118]

Table 4.11: Mass increase and surface area of SiMo-based catalysts

Catalyst no.	Sample description	SiMo on un/modified support (%)	Catalyst colour	Surface area -BET- (m^2/g)
16	Support/SiMo	1.86	Green/yellow	1.91
17	Support/1 layer silica/SiMo	1.55	Light yellow	7.08
18	Support/2 layer silica/SiMo	1.60	Light yellow	7.96
19	Support/3 layer silica/SiMo	1.95	Light yellow	16.48

The surface area of the SiMo-based catalysts increased with the number of silica layers used to modify the support as illustrated in Figure 4.16. A small difference in the BET value was observed between SiMo deposited on 1 layer silica and 2 layer silica. This might be due to the small difference in mass percentage of these catalysts at 1.55% and 1.60% respectively. The surface area increased from 1.91 m^2/g to 16.48 m^2/g due to the introduction of ≡Si-O-Si≡ bonds after modifying the support with silica. At low loading, SiMo forms finely dispersed species on the silica surface, and

the "interacting" species such as $(\equiv SiOH_2)^+(H_3SiMo_{12}O_{40})^-$ may form as illustrated in equation 3 below.[49]

$$\equiv Si\text{-}OH + H_4SiMo_{12}O_{40} \leftrightarrow \equiv Si\text{-}OH_2^+ \; H_3SiMo_{12}O_{40}^- \qquad (3)$$

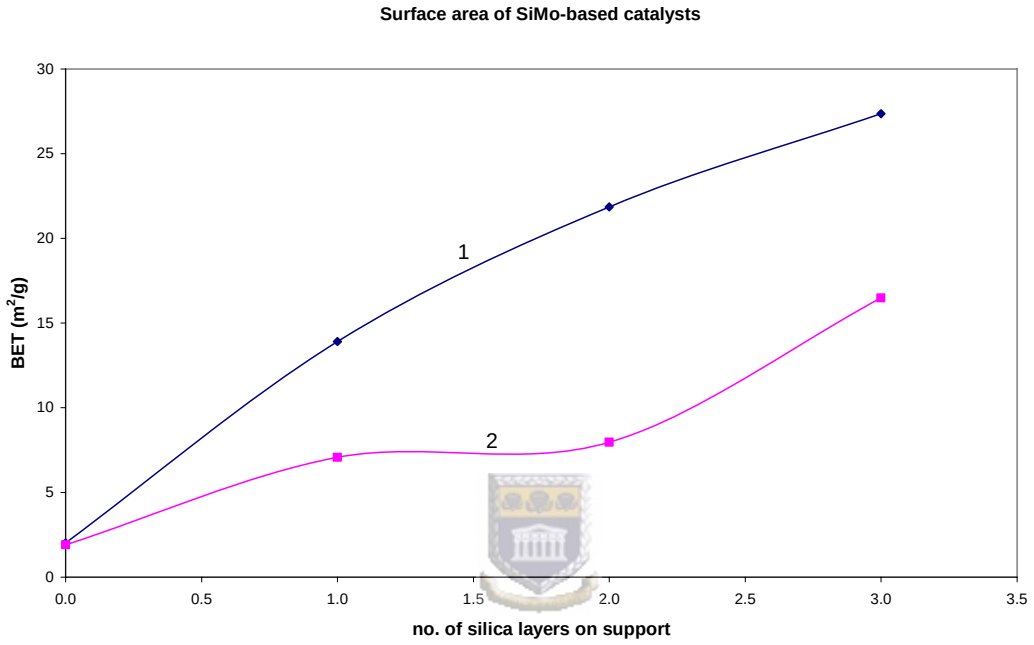

Figure 4.16: Surface area (BET) of SiMo-based catalysts 1: Silica on support, 2: SiMo on silica modified support

The surface area of silica modified support decreased after the deposition of SiMo. The reduction in surface area provides a proof that SiMo was adsorbed on the surface of silica.

Figure 4.17 shows SEM micrographs after depositing SiMo on the unmodified and silica modified support.

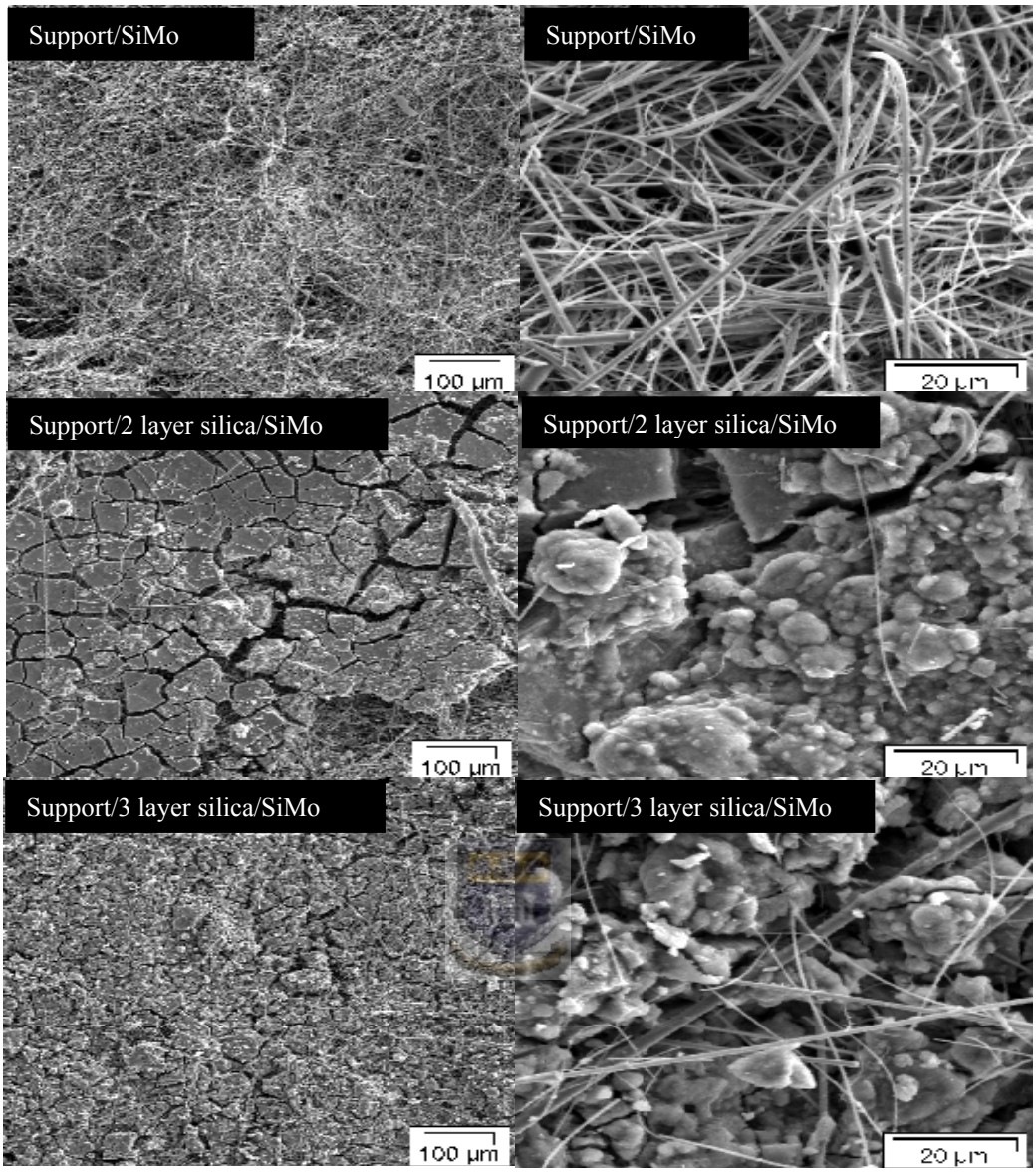

Figure 4.17: Micrographs of SiMo-based catalysts at 10kV

SiMo covered the fibres of the support on the surface for the unmodified support. It was difficult to observe SiMo particles on the silica modified support but only a layer of silica was visible on the catalyst modified with 2 layers of silica. Silica crakes were covered by SiMo particles for the catalyst modified with 3 layers of silica. Figure 4.18 shows the elemental analysis graphs for SiMo-based catalysts obtained from EDX studies. These results are summarised in Table 4.12.

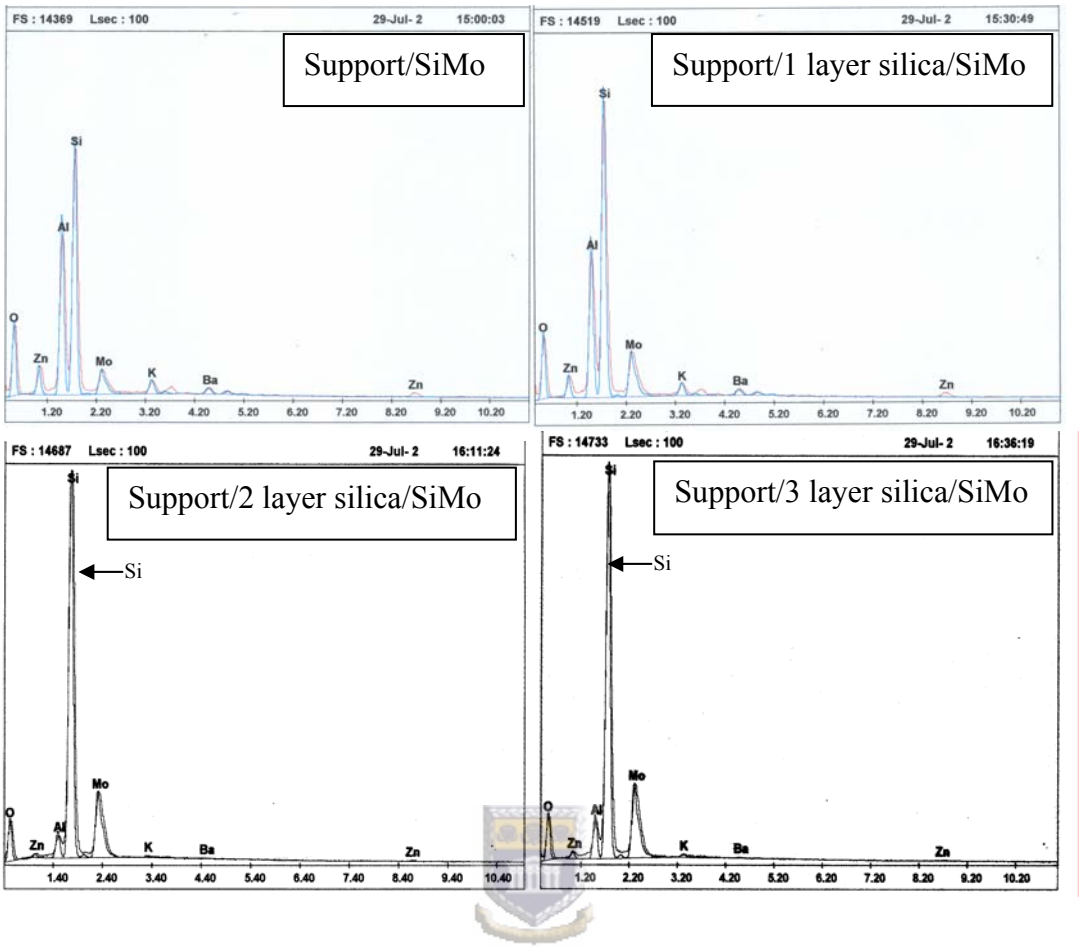

Figure 4.18: Elemental analysis graphs for SiMo-based catalysts obtained from EDX studies

According to Table 4.12 the ratio of Si to Mo for the catalyst that was modified with 3 layers of silica is closer to 1:1. This suggests that the more silica there is on the support the higher the surface area for Mo adsorption. At 200 μm the beam of electrons is focused on a larger area.

Table 4.12: Si:Mo ratio on the surface of SiMo-based catalysts obtained from EDX in weight%

Catalyst no.	Sample description	Si:Mo at 200 μm
16	Support/SiMo	3.6:1
17	Support/1 layer silica/SiMo	2.2:1
18	Support/2 layer silica/SiMo	1.6:1
19	Support/3 layer silica/SiMo	1.5:1

If the ratio of Si: Mo recorded at 200 μm at different positions on the catalyst surface is the same then Mo is homogeneously dispersed on the surface of silica. There was a good dispersion with catalysts 18 and 19. The EDX results confirmed the increase in the BET values as discussed above. The catalysts showed a decrease in the amount of impurities as shown in Figure 4.18 such as K, Zn and Ba metals. The decrease was observed where the support was modified with multiple layers of silica, that is, on the support modified with 3 layers of silica, Ba disappeared and the K weight% was close to zero as discussed above with Pt- and hemin-based catalysts.

Table 4.13: Elemental analysis (ICP-MS) for SiMo-based catalysts

Sample description	Mo concentration (ppb)
Support/SiMo	59086
Support/1 layer silica/SiMo	39985
Support/2 layer silica/SiMo	47338
Support/3 layer silica/SiMo	63015

The concentration of Mo at 59.1 ppm in SiMo-based catalyst was higher on the unmodified support than on 1 layer and 2 layers of silica. There was a huge increase in Mo concentration between 1 layer and 3 layers of silica. Mo concentration increased with the number of silica layers used to modify the support material.

Figure 4.19 and Table 4.14 represent the pore size distribution of SiMo-based catalysts.

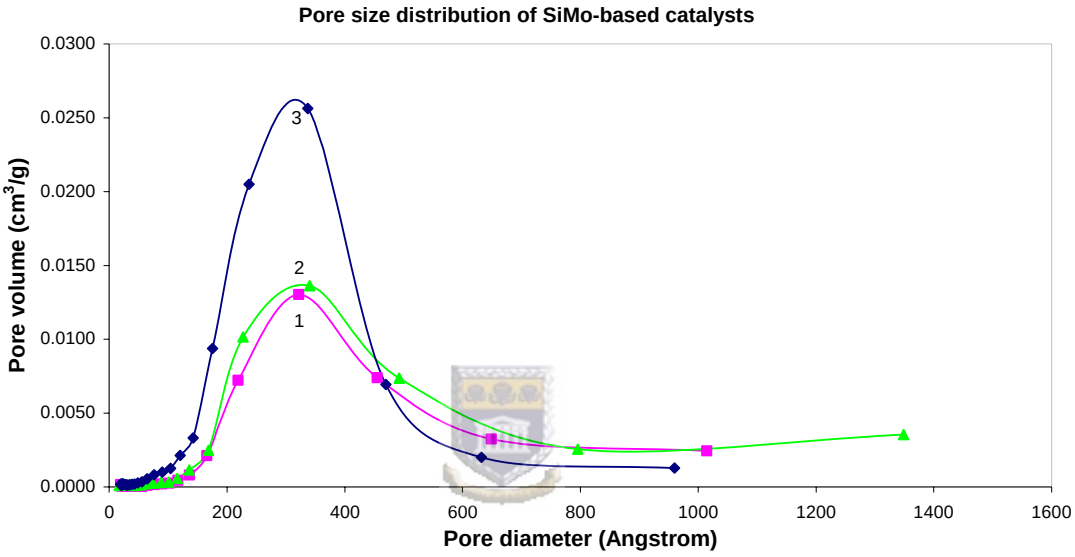

Figure 4.19: Pore size distributions of SiMo-based catalysts, based on the pore volume (fv(rp)) 1: Support/1 layer silica/SiMo, 2: Support/2 layer silica/SiMo, 3: Support/3 layer silica/SiMo

The shape of the pore size distribution curve for SiMo on unmodified support is similar to that of the support material and to the Pt- and hemin-base catalysts deposited on unmodified support as illustrated in Figure A1 in the appendix on page 167. A broad and a mesopore distribution were observed at a smaller volume of 0.0007 cm^3/g. There are two regions at 0-200 Å and 200-500 Å for SiMo deposited on

silica modified support. A narrow and large mesopore volume of 0.025 cm^3/g was observed in the catalyst where the support was modified with 3 layers of silica.

Table 4.14: Summary of the pore size distribution results for SiMo based catalysts

Sample description	0-200 (Å)	200-500 (Å)
Support/SiMo*	Small micropore volume	Broad area, small mesopore volume
Support/SiO_2 (1 layer) /SiMo	Small micropore volume	Increase in mesopore volume, broad area
Support/SiO_2 (2 layer) /SiMo	Small micropore volume	Broad mesopore area
Support/SiO_2 (3 layer) /SiMo	Increase in micropore volume	Mesopore volume increase, narrow area

*The pore size distribution of SiMo unmodified support is presented in Figure A1 in the appendix

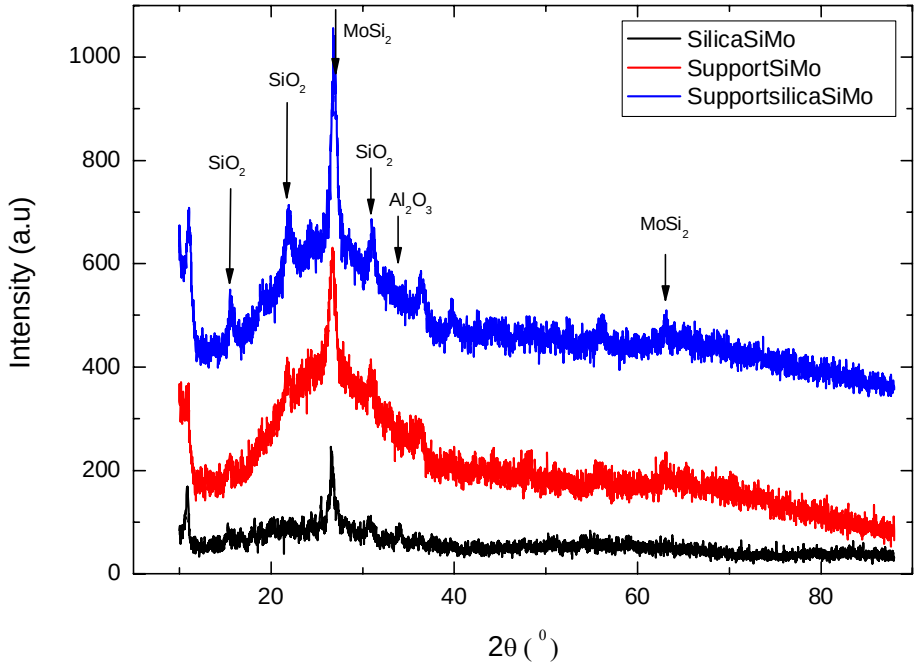

Figure 4.20: XRD scans of SiMo-based catalysts

Silica/SiMo showed the amorphous structure because of the high concentration of silica as presented in Figure 5.18 above. The SiO_2 peaks observed at 2θ = 22, 31 and 36.7° corresponded to the diffractogram of cristobalite obtained at low temperature and most of the SiO_2 peaks were from dodecasil 1H. Molybdenum silicide ($MoSi_2$) peaks were observed in all SiMo based-catalysts at 2θ = 26.7° and at 63° for Support/Silica/SiMo with d-spacing 3.34 and 1.48Å respectively.[98] Support/Silica/SiMo showed an extra small 2θ reflection at 40° representing metallic molybdenum particles at planes (110).[98] Refer to appendix A4 in page 168 for the diffractogram of cristobalite and dodecasil 1H.

D. Deposition of Phosphomolybdic acid [$H_3Mo_{12}O_{40}P.xH_2O$] on the support material

Table 4.15 illustrates the mass increase and the colour changes observed after the impregnation of [$H_3Mo_{12}O_{40}P.xH_2O$] (PMo) on the unmodified and silica modified support. The mass of PMo on the surface increased with the number of silica layers deposited on the support. The catalysts with 1 layer silica gave the lowest percentage of PMo. The highest mass increase was 60% for the catalyst with 3 layers of silica on support.

Table 4.15: Mass increase and surface area of PMo-based catalysts

Catalyst no.	Sample description	PMo on un/modified support (%)	Catalyst colour	Surface area –BET- (m^2/g)
13	Support/PMo	53.0	Yellow	5.26
14	Support/1 layer silica/PMo	43.1	Lime	6.14
15	Support/3 layer silica/PMo	60.0	Lime	7.55

The PMo was adsorbed very quickly due to the fast reaction between PMo and silica and the yellow or lime colour was spread evenly on the surface. Lime crystals of $H_3Mo_{12}O_{40}P$ were observed on the surface of silica at 60% loading. PMo covered the silica surface completely as illustrated by SEM micrographs in Figure 4.21. Fibres of the support material were not observed on the surface and there were less silica cracks on the surface after depositing PMo on support modified with 3 layer silica. Table 4.16 summarises the EDX results for the PMo-based catalysts in weight percentage. The results showed no impurities on the surface from the support material.

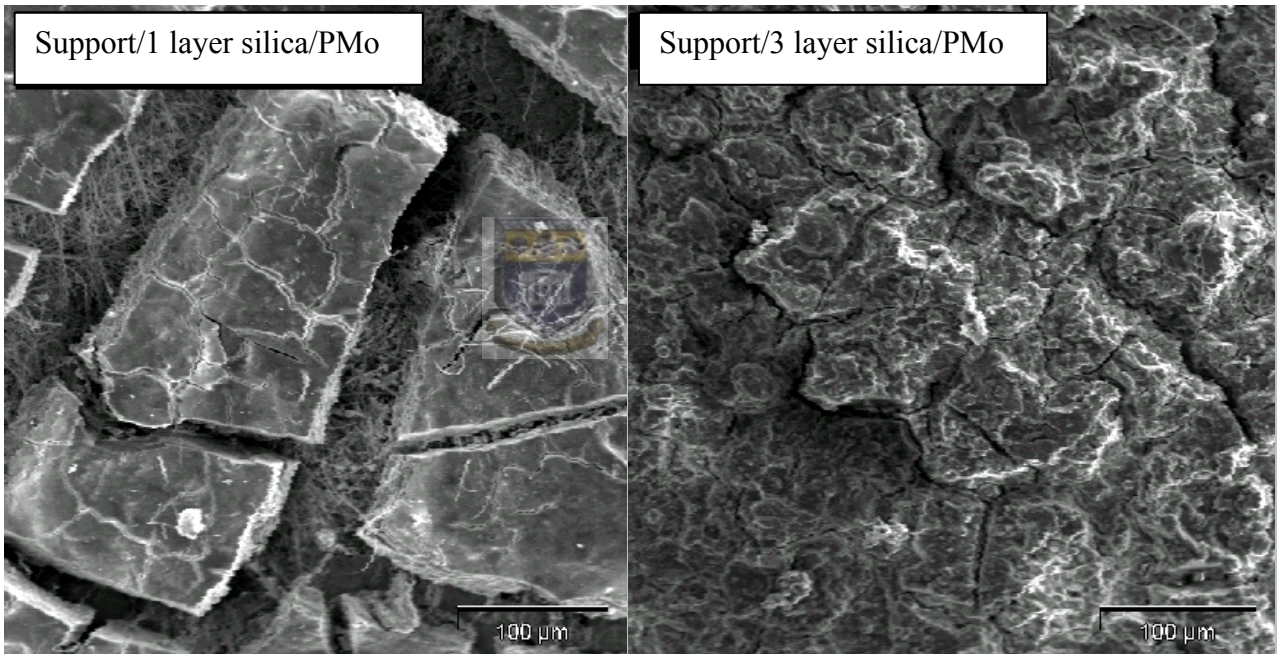

Figure 4.21: SEM Micrographs of PMo-based catalysts at 15 kV for 1 layer silica and 10 kV for 3 layer silica.

Mo weight percent was higher than Si on the surface for all the PMo-based catalysts. PMo on unmodified support gave the highest Mo weight percent implying that PMo was adsorbed on most of the available sites of the support material. Equal Si:Mo

ratios were obtained at 200 μm at different positions on the surface, suggesting that a homogeneous dispersion of PMo on the surface for all PMo-based catalysts was obtained.

Table 4.16: Si:Mo ratio on the surface of PMo-based catalysts obtained from EDX in weight%

Catalyst no.	Sample description	Si:Mo at 200 μm
13	Support/PMo	1:15.8
14	Support/1 layer silica/PMo	1:2.2
15	Support/3 layer silica/PMo	1:2.1

Elemental analysis results in Table 4.17 showed a high concentration of Mo in the case of catalyst with no silica modification at 1579.7 ppm of Mo. PMo on 1 layer silica gave the lowest concentration of 649.2 ppm Mo. The ICP results supported the EDX studies and the mass increase values for the unmodified and 1 layer silica modified catalysts.

Table 4.17: Elemental analysis (ICP-MS) for PMo-based catalysts

Sample description	Mo concentration (ppb)
Support/PMo	1579656
Support/1 layer silica/PMo	649207
Support/3 layer silica/PMo	657721

PMo-based catalysts contained higher concentrations of Mo than SiMo-based catalysts. As shown below in Figure 4.22, Mo concentration in PMo on unmodified support is greater than SiMo on unmodified support by a factor of 10^2.

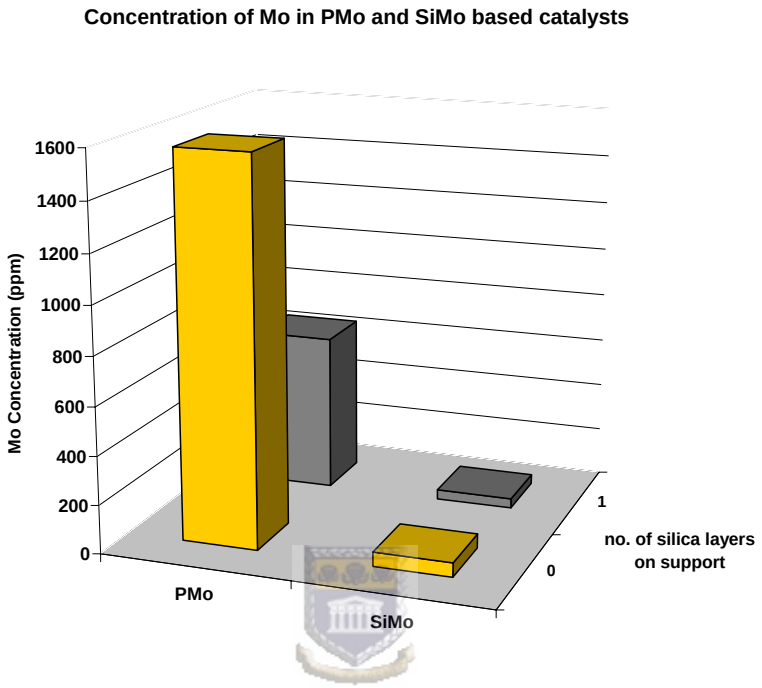

Figure 4.22: Mo concentration in PMo- and SiMo-based catalysts, based on ICP results

The BET surface area of PMo-based catalysts increased with the number of silica layers coated on the support material as illustrated in Figure 4.23, although a small increase in the surface area between successive layers of silica was observed. 7.55 m^2/g for PMo deposited on 3 layer silica modified support in Table 4.15, was the lowest surface area when compared to the other catalysts discussed above (Pt-, Hemin- and SiMo-based catalysts). It might be due to the layer of PMo covering the support surface and the void volume created after modification of the support with silica surface completely. Hence the void volume does not contribute to the surface

area of Support/3 layer silica/PMo catalyst. The average pore size of the catalysts was around 15.2 Å, which is in the micropore region. Support/3 layer silica/PMo had a large pore volume at this region as summarised in Table 4.18 below.

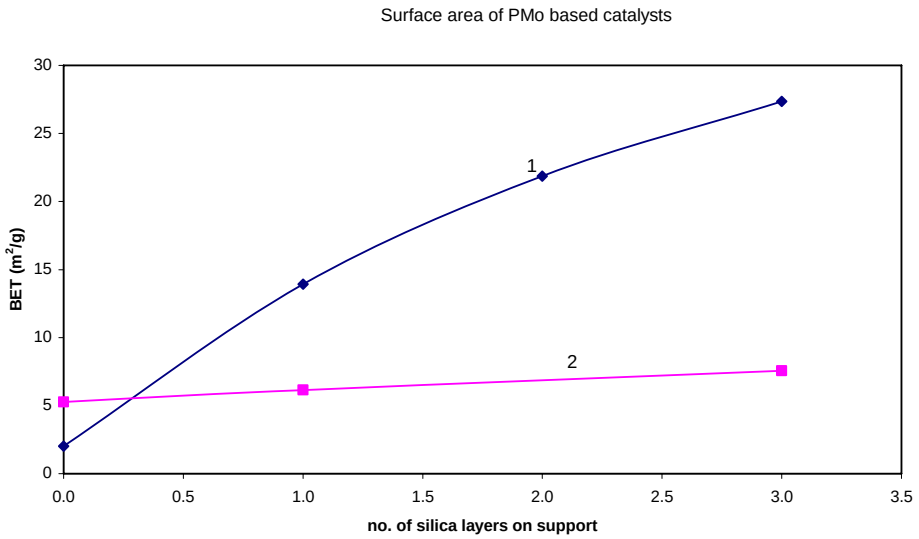

Figure 4.23: Surface area (BET) of PMo-based catalysts 1: Silica on support, 2: PMo on silica modified support.

Table 4.18: Summary of the surface area, pore volume and average pore volume results for PMo-based catalysts

Sample description	Surface area - BET- (m^2/g)	Pore volume (cm^3/g)	Average pore size (Å)
Support/3 layer silica/ PMo	7.55	0.002861	15.1565
Support/PMo	5.26	0.002003	15.2230

The high dispersion of PMo may be connected with low acidity (Bronsted acidity). The low acidity could arise from a strong interaction of silica and phosphomolybdic acid by means of the OH surface groups and the acidic protons, respectively, to form

OH_2^+ groups. This interaction resembles the solvation of H^+ by H_2O in solid heteropolyacids as discussed by Tatibouet et al in the case of $H_4SiMo_{12}O_{40}$.[52]

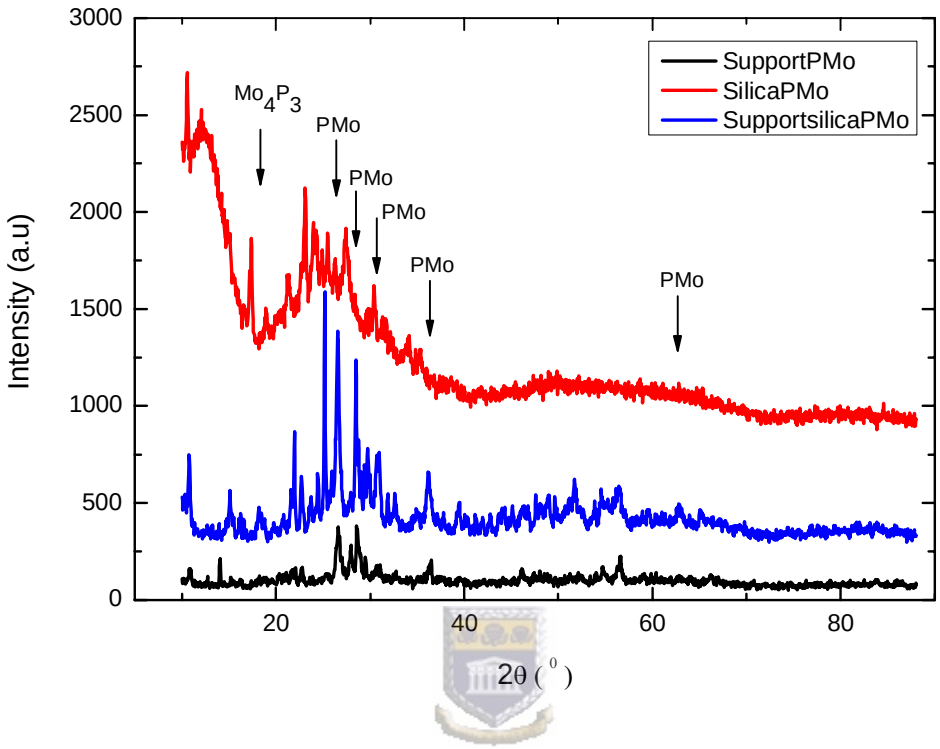

Figure 4.24: XRD scan of PMo-based catalysts

The XRD peaks observed when PMo was deposited on powder silica, corresponded to the $H_3Mo_{12}O_{40}P.6H_2O$ peaks from the XRD database as displayed in Figure 4.24. Silicon oxide peaks were also observed and amorphous silica was obtained at $2\theta > 40°$. At $2\theta = 17.5°$ molybdenum phosphide (Mo_4P_3) was identified at lower intensity/counts for all PMo-based catalysts. Support/Silica/PMo showed an extra small 2θ reflection at 40° representing metallic molybdenum particles at planes (110).[98]

4.3.3 Temperature programmed reactions

Active gases were calibrated to enable quantitation of the TCD signal. However, the calibration was found to be subject to error due to problems of automation of the gas flow in the instrument as well as the fact that the difference in thermal conductivity between hydrogen and the diluent used during calibration, namely helium, is low. Helium was used as diluent to enable automated control of the two consecutive experiments, as the oxidation stage was performed using oxygen in helium. The relative thermal conductivity of H_2 is 7.07, He is 5.84 and O_2 is 1.02. Therefore during the calibration of the H_2 the thermal conductivity recorded is dominated by the He signal below certain concentrations, creating non-linearity in the calibration curve. The results of active gas uptake represented by the peak area in tables and figures below can be compared qualitatively since each sample was treated with the same gas under identical testing conditions for each of the TPR, TPO and TPD experiments respectively. However, since calibration of the gas streams proved problematic, the relative ratios of volumes adsorbed/desorbed for each sample are not an accurate reflection of the proportion of uptake of the active gas for each sample, and thus are not reported.

Pt on silica powder showed a broad reduction peak reaching a maximum at 55°C as illustrated in Figure 4.25 and summarised in Table 4.19. Pt on silica modified and unmodified support was reduced to Pt metal, which was confirmed by the black colour after TPR. Pt reduction reached a maximum below 50°C for the supported catalysts- Pt on unmodified and silica modified support. A broad reduction peak of silica/Pt might be due to the larger amount of Pt on silica powder than on supported Pt

catalysts which was accessible for reduction with hydrogen. The presence of Pt reduced species will provide sites for adsorption of oxygen thus increasing reactivity in methane oxidation.[67]

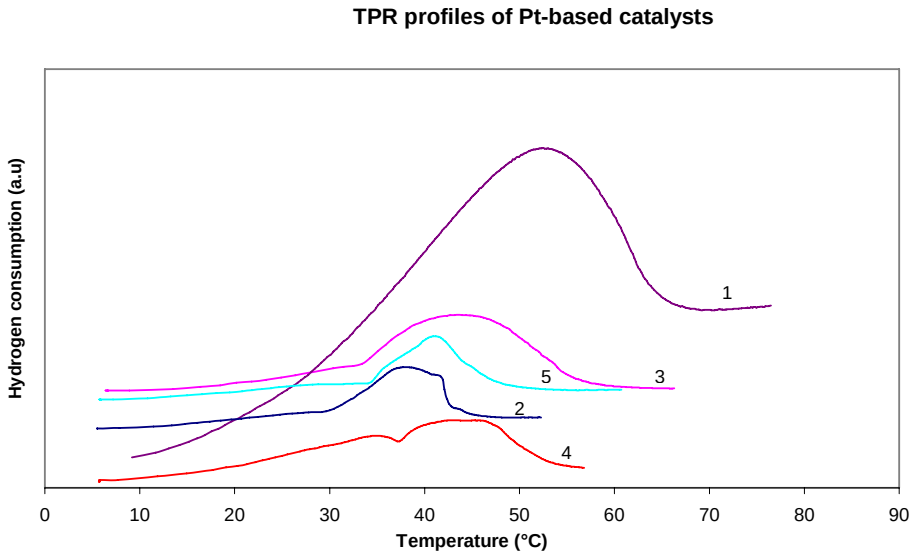

Figure 4.25: TPR profiles for Pt-based catalysts 1: Silica/Pt, 2: Support/Pt, 3: Support/1 layer silica/Pt, 4: Support/2 layer silica/Pt, 5: Support/3 layer silica/Pt

Table 4.19: Summary of temperature of active gas uptake of volume adsorbed during TPR for Pt-based catalysts

Sample description	Mass used (g)	TPR peak area	TPR temperature (°C)	Colour change
Support/Pt	0.2641	0.7200	5.6	Turned grey after TPR
		0.8187	37.5	
Support/1 layer SiO_2/Pt	0.2179	0.4624	6.5	Turned black after TPR
		0.9587	45.0	
Support/2 layer SiO_2/Pt	0.2430	0.6378	5.8	Turned black after TPR
		1.3556	40.6	
Support/3 layer SiO_2/Pt	0.2324	0.5186	5.8	Turned black after TPR
		0.7035	41.2	

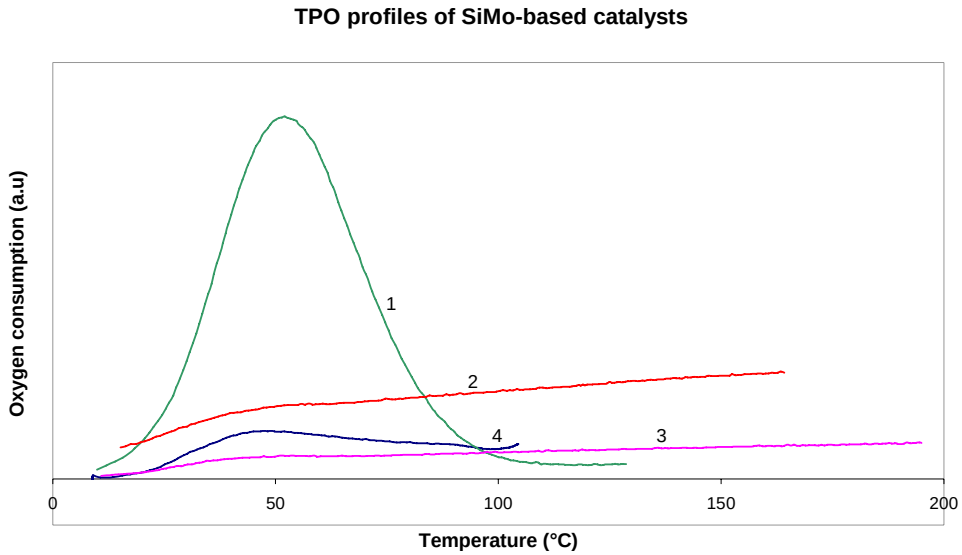

Figure 4.26: TPO profiles of SiMo-based catalysts 1: Silica/SiMo, 2: Support/SiMo, 3: Support/2 layer silica/SiMo, 4: Support/3 layer silica/SiMo

SiMo impregnated on amorphous silica consumed oxygen more than SiMo deposited on silica modified support as shown in Figure 4.26 above. A single oxidation peak with maximum at around 50°C was observed and no oxygen consumption at higher temperatures 750°C was observed for all SiMo-based catalysts. No TPR profile is presented for these catalysts since no hydrogen consumption was observed up to 350°C. TPR peaks were not expected at these temperatures since Mo can be reduced at temperatures above 500°C. SiMo-acid is not stable at temperatures higher than 300°C.[6, 28] It decomposes into silica and MoO_3 crystallites and thus TPR was performed at < 350°C. Very low oxygen consumption was obtained for SiMo-based catalysts when compared to PMo-based catalysts, as presented below in Figure 4.27, due to the low loading of Mo in SiMo as confirmed by ICP analysis. Therefore, there are no enough adsorption sites for oxygen on these catalysts and hence low activity is expected during the oxidation of methane.

The hemin deposited on the unmodified support showed two TPR peaks at 5°C and 219°C but no oxygen consumption was observed as summarised in Table 4.20. Hemin on support modified with 1 layer silica gave one peak at 5°C and 225°C for TPR and TPO respectively. Hemin on support modified with 2 layer silica gave two TPR peaks at lower temperatures around 5°C and 21°C. A TPO peak was observed at 249°C. Support/2 layer silica/hemin consumed more oxygen than support/1 layer silica/hemin and the peak shifted to 249°C suggesting a stronger interaction of oxygen with the surface than in Support/1 layer silica/hemin. Generally, hemin-based catalysts showed small TPR peak at 230°C and TPO peaks due to the small concentration of Fe on hemin catalysts. The hemin TPR/O profiles are presented in Figure A3 in the appendix on page 167.

Table 4.20: Summary of temperature of active gas uptake of volume adsorbed during TPR and TPO for hemin-based catalysts

Sample description	Mass used (g)	TPR peak area	TPR temperature (°C)	TPO peak area	TPO temperature (°C)	Colour change
Support material	0.2546	-	-	-	-	No colour change
Support/hemin	0.3017	0.6893 0.1401	5.4 219.2	-	-	No colour change
Support/1 layer silica/hemin	0.2873	0.9210	5.2	0.1404	225.4	Turned light brown after TPO
Support/2 layer silica/hemin	0.2980	0.5607 0.0696	5.5 21.3	0.3812	249.0	Turned light brown after TPO

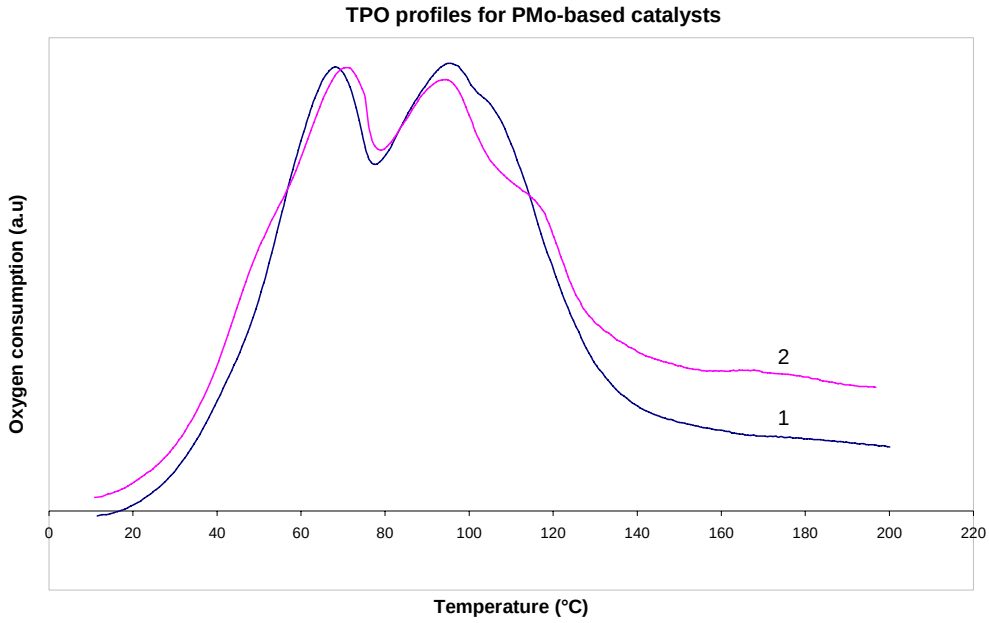

Figure 4.27: TPO profiles for PMo-based catalysts 1: Support/PMo, 2: Support/3 layer silica/PMo

PMo coated on unmodified support showed two oxidation maxima at about 69°C and 96°C respectively as shown in Figure 4.27 above, while a shift in oxidation maxima was observed at 71°C and 94°C for support/3 layer silica/PMo and a hump at 118°C. The same active species were present for both catalysts for these two oxidation maxima. This implies that the catalysts may contain more than one phase of oxides. The shift in oxygen consumption peaks might be due to the introduction of silica layers on the support material. PMo-based catalysts have adsorption sites for oxygen. The interaction of oxygen with the catalyst activates oxygen making it more reactive thus will promote methane activation. Zuzaniuk et al.[121] observed TPR peaks using supported HCP with maxima at 447°C and 817°C and hence provide sites for oxygen adsorption.[100]

TPD of carbon dioxide was used to determine the distribution of the basic species present on the surface of the catalysts. The basic strength distribution is evaluated from the capacity of the catalyst to retain the acid probe CO_2 during desorption at increasing temperature. The support material modified with silica showed a small CO_2 desorption peak between 25°C to 100°C as illustrated in Figure 4.28 below. This is attributed to the interaction of CO_2 with sites having weak basic strength. Silica coated on alumina enhances the surface acidity of the support material hence few basic sites were expected on the support.[98]

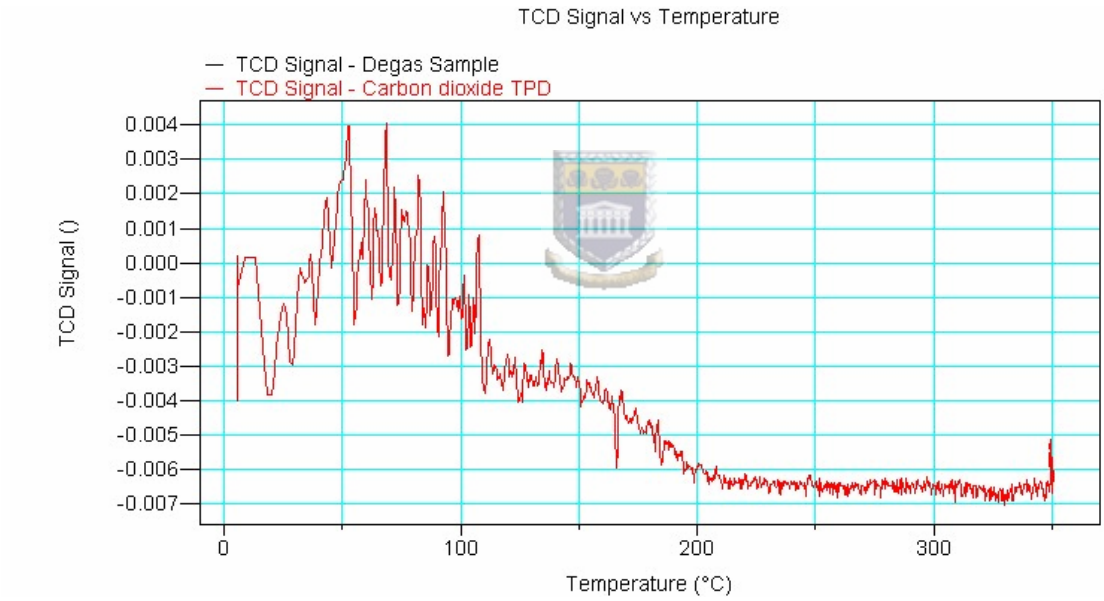

Figure 4.28: TPD of CO2 profile of silica modified support (support/silica).

Platinum-based catalysts adsorbed CO_2 but no desorption peaks were observed at temperatures lower than 350°C. CO_2 might be bonded strongly on the surface of the catalysts and therefore a higher temperature is required to desorb CO_2 species.

Figure 4.29 shows TPD of CO_2 for PMo-based catalysts. PMo coated on unmodified support showed 2 carbon dioxide desorption peaks-the first peak started at 25°C to 100°C attributed to the interaction of CO_2 with sites having weak basic strength. Few weak basic sites were obtained.

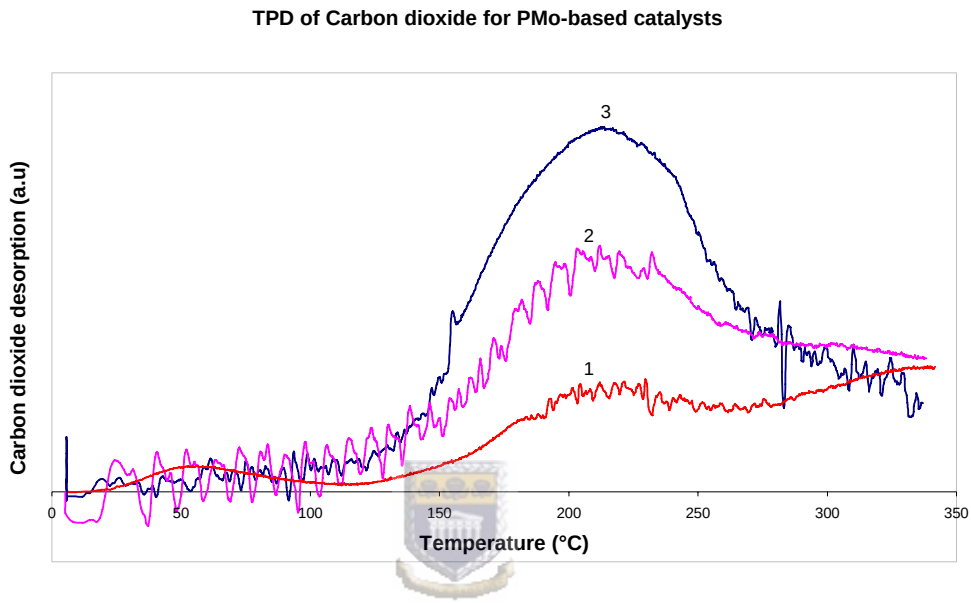

Figure 4.29: TPD of CO2 profiles for PMo-based catalysts 1: Support/1 layer silica/PMo, 2: Support/2 layer silica/PMo, 3: Support/3 layer silica/PMo

The second peak having a broad desorption area 130 to 300°C attributed to CO_2 desorbed from sites with medium-strong basic strength. In the second peak carbon dioxide was strongly bonded to these sites therefore a high temperature of 250°C was required to break the bond.[100] There were no basic sites present at temperatures lower than 130°C for PMo coated on silica modified support. A broad peak was obtained ranging from 140°C to 300°C for both the support/1 layer silica/PMo and support/3 layer silica/PMo due to the medium-strong basic sites on these catalysts. The maximum peak height was at 210°C and this temperature was required to break the

the bond between CO_2 and the catalysts. There were more basic sites on support/3 layer silica/PMo than on other catalysts at this region- 140 to 300°C- as observed from the peak height.

However, as SiMo-based catalysts did not desorb carbon dioxide between 10°C and 350°C there were no basic sites at this temperature range. Si molecules surround Mo thus enhancing the surface acidity of the support material. PMo had more basic sites compared to SiMo due to the different environment around Mo. The difference in electronegativity between silicon and phosphorus might have an effect on surface basicity.

The TPD of methane was studied in order to determine the behaviour of PMo-based catalysts towards methane. Banares et al.[67] found that the oxygen incorporated into the methane molecule came from the lattice oxygen and therefore a catalyst is needed to activate methane.[122]

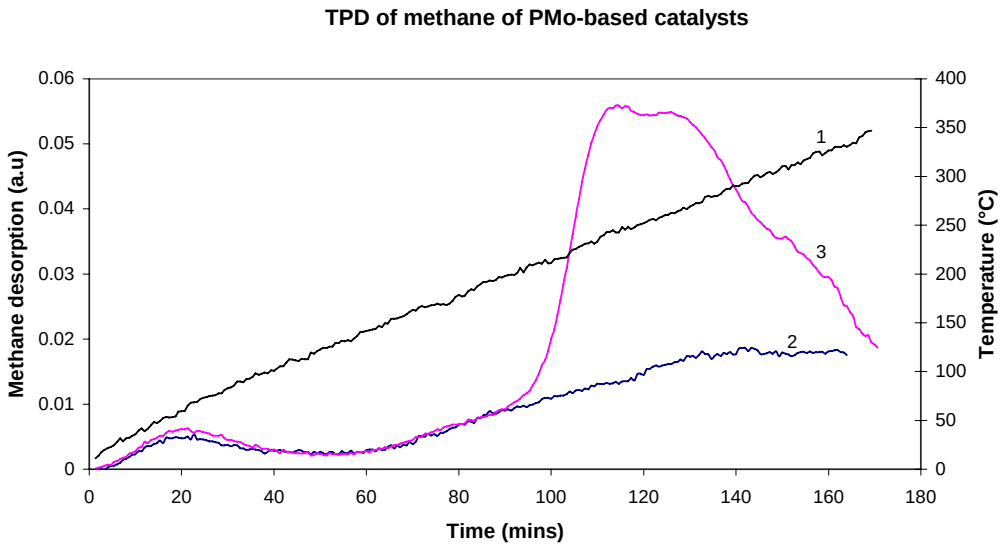

Figure 4.30: TPD of methane profiles for PMo-based catalysts 1: Temperature, 2: Support/PMo, 3: Support/3 layer silica/PMo

According to Figure 4.30, two desorption stages were obtained at 60°C and 260°C for support/PMo implying the presence of two different species on this catalyst. Support/3 layer silica/PMo showed three desorption stages at 60°C, 240°C and 260°C. The peak started at 180°C reaching maximum height at 260°C. A hump was also observed at 310°C forming a broad peak for this catalyst. The same active species were present for both catalysts at 60°C and 260°C and might be due to methane molecules adsorbed on PMo. Modification of the support material with silica layers introduced new active species on the catalyst hence extra peaks at 240°C and 310°C were observed and a higher TCD signal was obtained. Very low methane desorption was obtained at 60°C for both catalysts. Methane was strongly adsorbed by these catalysts hence high temperatures, around 240°C to 260°C, were required to break the bond between methane and the catalysts. Therefore methane activation is expected around these temperatures 60°C, 240°C and 260°C.

4.4 Conclusions

Given that amorphous silica is highly porous and hence introduces a large surface area inside the silica particles,[108] the ceramic membrane support was modified with amorphous silica to maintain and increase the surface area of the membrane support. The BET surface area of the support material increased with the number of silica layers, with 3 layers of silica showing 27.86 m^2/g. The pore volume and narrow mesoporous region (BDDT type IV isotherm) increased with the number of silica layers deposited on the support material. Pt, hemin, SiMo and PMo were deposited on the surface of the silica modified ceramic support based on the following general equilibrium equation:

$\equiv Si\text{-}OH^+ + C^+ \leftrightarrow \equiv Si\text{-}OC^+ + H^+$

The amount in weight% of Pt and PMo on the support increased with the number of silica layers while hemin and SiMo amounts were around that of the unmodified support. PMo showed the highest mass increase after deposition compared to Pt-, hemin- and SiMo-based catalysts, with 60% for the catalyst with 3 layer of silica on support. According to Figure 4.31 the decrease in the BET surface area after the deposition process confirmed that Pt, hemin, PMo and SiMo were successfully adsorbed on the surface of silica-modified support. PMo covered the support surface completely and hence the low surface area.

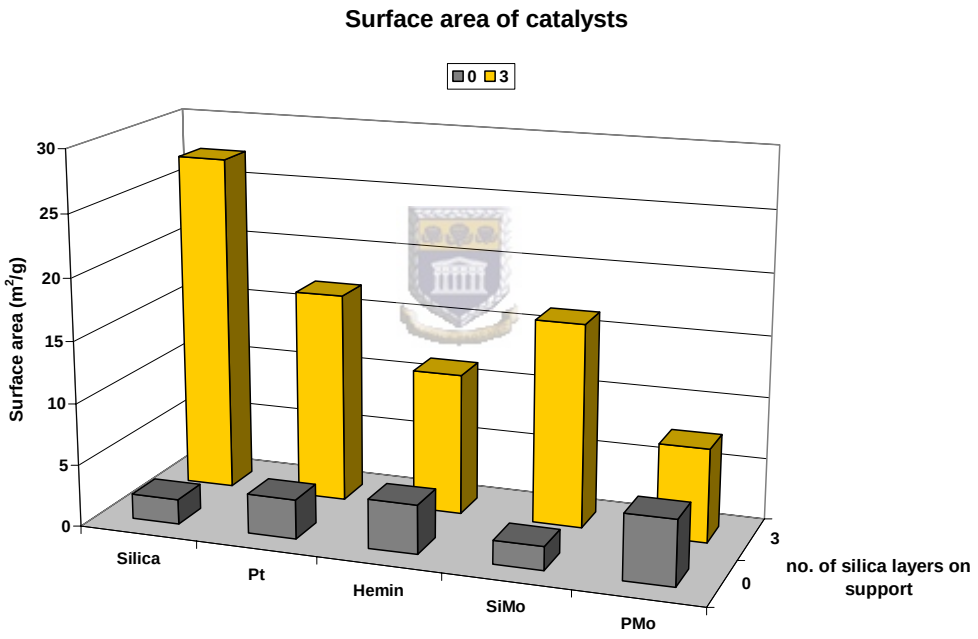

Figure 4.31: Surface area (BET) of prepared catalysts

Homogeneous distribution of Pt, PMo and hemin was observed on the surface of the support. PMo was highly dispersed on the modified support due to low acidity (Bronsted acidity) that could arise from a strong interaction of silica and

phosphomolybdic acid by means of the OH surface groups and the acidic protons, respectively, to form OH_2^+ groups.

TPD of carbon dioxide from 10°C to 350°C was used to determine the distribution of the basic sites present on the surface of the catalysts. Pt, SiMo and hemin based catalysts did not desorb carbon dioxide at temperatures between 10°C and 350°C. This suggested the absence of basic sites on these catalysts under these conditions.[100] PMo-based catalysts showed the presence of medium-strong basic sites present ranging from 140°C to 300°C. Hemin-based catalysts showed a small TPR peak at 230°C and TPO peaks due to the small concentration of Fe on hemin catalysts. Pt-based catalysts were reduced to Pt metal at temperatures lower than 60°C. The presence of Pt reduced species will provide sites for adsorption of oxygen. SiMo impregnated on amorphous silica consumed oxygen more than SiMo deposited on silica modified support. Very low oxygen consumption was obtained for SiMo-based catalysts when compared to PMo-based catalysts due to the low loading of Mo in SiMo as confirmed by ICP analysis. Therefore, there are few oxygen adsorption sites on these catalysts and hence low activity is expected during the oxidation of methane. PMo-based catalysts showed more than one oxidation peak suggesting that the catalysts may contain more than one phase of oxides and thus has adsorption sites for oxygen.

Since the catalyst is essential for methane activation, TPD of methane was studied on PMo-based catalysts in order to determine their behaviour towards methane. The TPD of methane has shown that PMo deposited on silica modified membrane support can easily activate the C-H bond of methane at low temperatures.

CHAPTER 5: Testing of catalyst activity

5.1 Introduction

In this research work, a non-separative catalytic inorganic membrane reactor was used, in which membrane permselectivity is not regarded as a significant property. The catalytic inorganic membrane reactor is generally a catalytically active diffusion barrier which does not contribute any relevant enhancement to the conversion of equilibrium limited reactions but influences the reaction selectivity of a supported catalyst.[75, 69] The catalysts prepared in Chapter 2 were evaluated for the partial oxidation of methane to methanol and formaldehyde using oxygen as oxidant under mild conditions.

5.2 Experimental procedure

All experimental details involving catalyst preparation, characterization and activity testing are given in Chapter 2.

5.3: Results and discussion

The results and discussion in this report are based on Pt and PMo catalysts, and some SiMo results for comparison with PMo catalysts. Hemin catalysts are not discussed due to the reasons mentioned in the conclusions section of Chapter 4. The effect of reactor wall composition on the oxidation reaction was studied at different temperatures and flow rates but no oxidation products were observed since low flow

rates and low temperatures (maximum=150°C) were used. A series of experiments were performed on a ceramic membrane material (support material) and silica modified support material without catalyst to determine the effect of the catalyst in methane oxidation. Methane conversion was very low at 0.001% and therefore negligible.

5.3.1 Pt-based catalysts results

The results summarised in Table 5.1 shows that supported platinum catalysts were active in the oxidation of methane. The reaction products were methanol, formaldehyde and water. Carbon dioxide was not detected under these conditions.

Table 5.1: Results of the catalytic activity testing of Platinum based catalysts (CH_4:O_2 15:1, time of experiment 2 h, Gas hourly space velocity GHSV = 666 h^{-1})

Catalyst	[Pt] (mg/cm^2)	Temperature (°C)	Conversion (%)		Selectivity (%)			
			CH_4	O_2	CH_3OH	CH_2O	H_2O	CO_2
Support/Pt	0.244	30	0.38	8.8	10.0	43.8	43.4	0.0
		60	0.32	6.1	30.5	34.3	34.8	0.0
		90	0.29	6.8	19.5	39.8	40.1	0.0
Support/3 layer silica/Pt	0.326	30	0.85	16.8	19.0	40.0	39.8	0.0
		60	0.71	14.6	18.1	41.0	40.7	0.0
		90	0.49	12.1	16.5	42.0	41.5	0.0

The influence of the amount of platinum on catalytic performance of supported platinum catalysts at different temperatures is shown in Figure 5.1 and Table 5.1.

Methane conversion at 0.326 mg/cm^2 Pt loading is higher than 0.244 mg/cm^2 Pt at all temperatures tested.

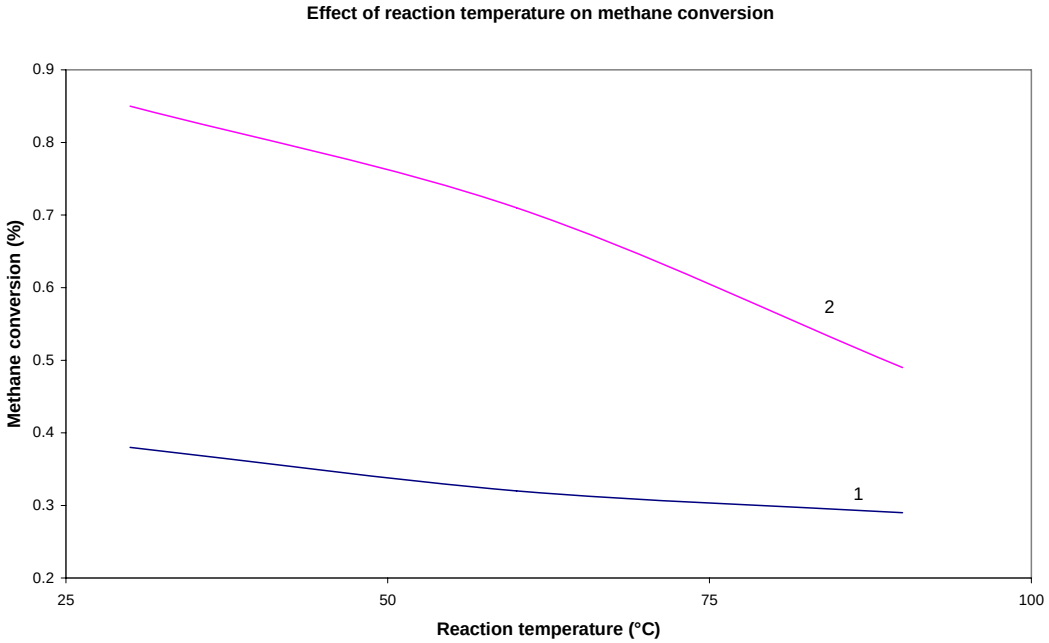

Figure 5.1: The effect of amount of platinum and reaction temperature on methane conversion 1: Support/Pt 2: Support/3 layer silica/Pt

The increase of methane conversion in support/3 layer silica/Pt can be attributed to an increase in the number of accessible surface Pt sites after modification of the support material with silica. Silica increased the surface area for the interaction of surface hydroxyls with platinum and thus platinum was available on the surface of silica where reaction takes place. The BET surface area for support/3 layer silica/Pt and support/Pt were 17.10 and 3.19 m^2/g respectively. SEM/EDX results (see Chapter 4.3.2 Figure 4.8) also confirmed the presence of Pt on the surface of silica modified support. The Pt in support/Pt was buried in the channels of the fibres of the support material as discussed in Chapter 4. More oxygen was used in the catalysts containing 0.326 mg/cm^2 Pt than 0.244 mg/cm^2 Pt with 16.8% and 8.8% respectively at 30°C.

Figure 5.1 shows the effect of reaction temperature on the conversion of methane on supported platinum catalysts. It can be seen that methane conversion decreases with an increase in temperature for both catalysts. The high methane conversion of 0.85% and 0.38% was observed at 30°C for support/3 layer silica/Pt and support/Pt catalysts respectively. A TPR profile showed that platinum, in this case Pt^{2+} was reduced to Pt at low temperature between 30°C and 50°C for support/3 layer silica/Pt and support/Pt catalysts suggesting the presence of active species for oxygen adsorption at these temperatures and thus confirms the high methane conversion at 30°C (see Chapter 4 Figure 4.25).

The effect of reaction temperature on the selectivity to methanol, formaldehyde and water for support/Pt and support/3 layer silica/Pt is shown in Figure 5.2 and Figure 5.3 respectively.

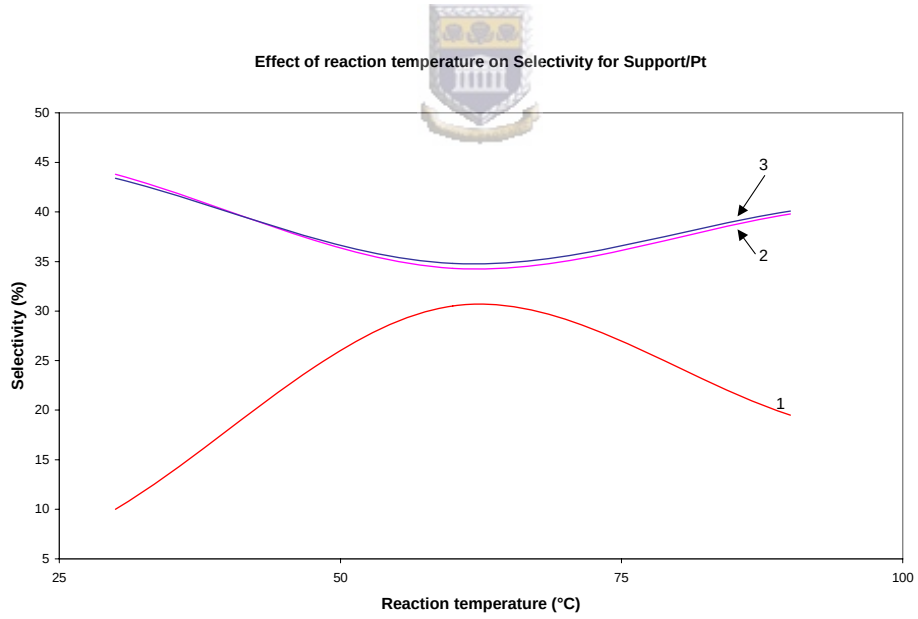

Figure 5.2: The effect of reaction temperature on selectivity to oxidation products for support/Pt 1: methanol, 2: formaldehyde, 3: water

From Figure 5.2 above, the selectivity to methanol, formaldehyde and water depends on temperature. Support/Pt at 90°C performed better than at 30°C producing high methanol selectivity of 19.5% at the lowest methane conversion of 0.29%. Selectivity to methanol reached a maximum at 60°C (30.5%) and decreasing to 19.5% at 90°C with 30°C giving the lowest selectivity of 10%. 60°C is the optimum temperature since production of methanol is a maximum while formaldehyde and water is at a minimum. At 30°C methanol production is a minimum while formaldehyde and water are a maximum and thus temperature control is a governing entity.

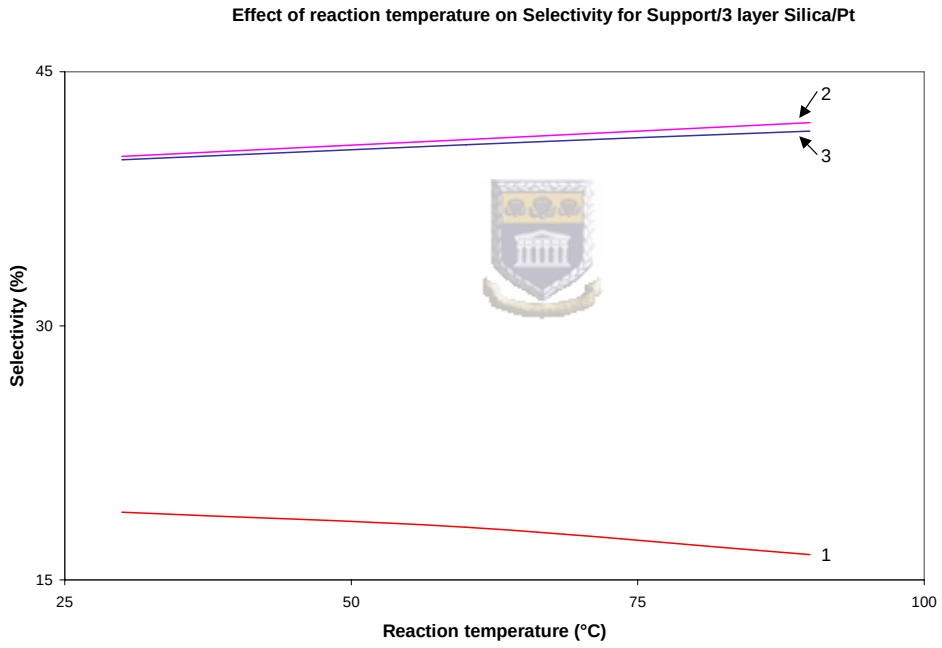

Figure 5.3: The effect of reaction temperature on selectivity to oxidation products for support/3 layer silica/Pt 1: methanol, 2: formaldehyde, 3: water

In Figure 5.3 a small decrease in methanol selectivity was observed from 30°C to 90°C while a small increase in selectivity towards formaldehyde and water was observed with a decrease in methane conversion. High selectivity to methanol (19%)

was obtained at 30°C. Support/3 layer silica/Pt behaved differently from support/Pt towards methane oxidation under the same conditions, with higher methane conversions favouring high selectivity to formaldehyde and water. Thus methanol was further oxidised to formaldehyde. It can be clearly seen from Figure 5.4 that high Pt loading on the support (0.326 mg/cm^2) gave low selectivity towards methanol with increase in temperature. This agrees with results in the literature at high metal loading (in this case Pt) where complete oxidation products are favoured.[32] This can be attributed to changes in the structure of the surface platinum species with platinum loading.[27] This catalyst would be the preferred one for the conversion of methane into formaldehyde at an optimum temperature of 90°C.

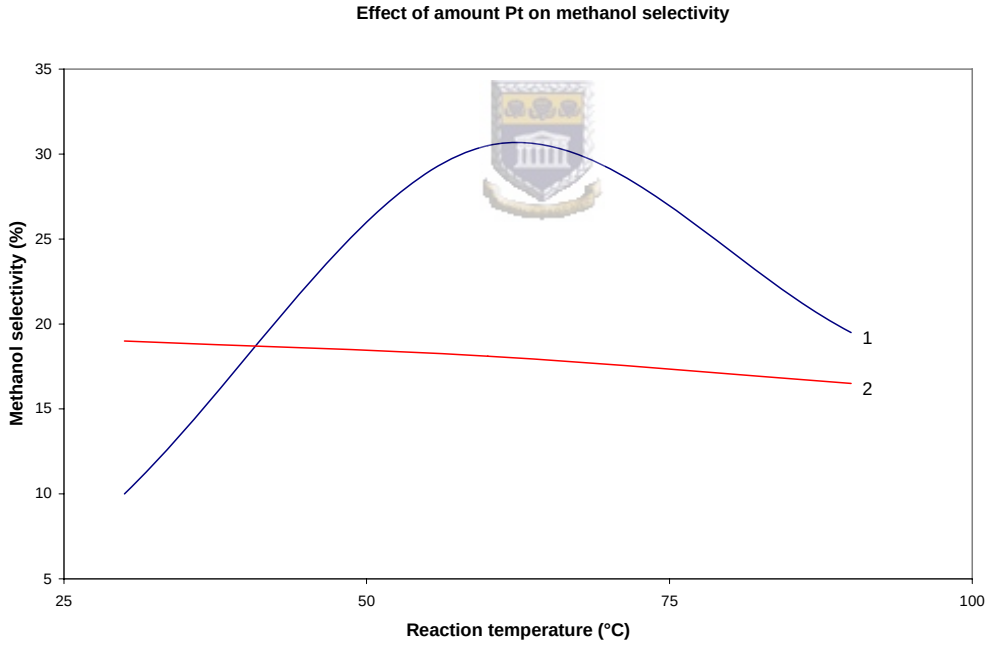

Figure 5.4: The effect of amount of platinum deposited on support on methanol selectivity 1: [Pt] = 0.244 mg/cm^2, 2: [Pt] = 0.326 mg/cm^2

The effect of contact time on the catalytic process was investigated by changing the flow rate of the gaseous mixture at constant CH_4:O_2 ratio. The results are shown in

Table 5.2. The contact time between the gaseous (feed) mixture and the catalyst was calculated as shown below

Contact time (s) = volume of catalyst (ml)/ flow rate (ml/s)

Table 5.2: Results of the catalytic activity testing of Support/3 layer silica/Pt

CH_4:O_2 5:1

CH_4:O_2	Contact time (s)	Temperature (°C)	CH_4 Conversion (%)	Selectivity (%)		
				CH_3OH	CH_2O	CO_2
5:1	2.7	60	0.43	12.1	31.8	0.0
		90	0.58	20.3	24.3	0.0
		120	0.68	15.2	28.8	0.0
	5.4	60	0.61	16.7	27.4	0.0
		90	0.70	23.8	20.6	0.0
		120	1.1	5.6	38.0	0.0
	7.2	120	1.39	1.35	40.8	1.2
	14.4	120	1.84	0.91	38.9	3.7

Increasing contact time increased methane conversion. High methane conversion of 1.84% was observed at 14.4 s and 120°C. Figure 5.5 compares the extent of methane oxidation at 2.7 and 5.4 s. Methane conversion is higher at 5.4 s over all temperatures examined than at 2.7 s. The longer contact time (14.4 s) between the reaction mixture and the catalyst enhances the production of carbon dioxide and high selectivity to formaldehyde 38.9%. Selectivity to methanol decreases with increase in contact time. The changes in product selectivities as function of time in Figure 5.6 shows that when the contact time approaches zero, the selectivity of methanol approaches higher

selectivity values than formaldehyde and that of carbon dioxide approaches zero. These results suggest that methanol is the primary product and then undergoes further oxidation to formaldehyde, and at longer contact times, the formaldehyde is oxidised to carbon dioxide and water.[123, 27]

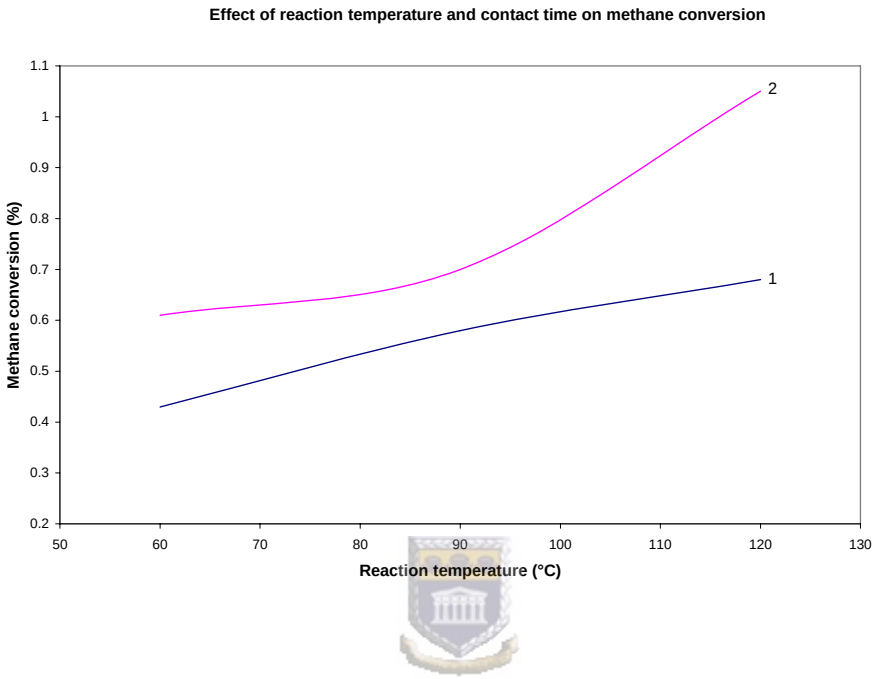

Figure 5.5: The effect of reaction temperature and contact time on methane conversion for support/3 layer silica/Pt. 1: 2.7 s, 2: 5.4 s

The effect of chemical composition n of the gaseous mixture on the catalytic process was investigated at constant contact time of 5.4 s, varying the CH_4:O_2 ratio from 20:1 to 3:1 on support/3 layer silica/Pt. Table 5.3 summarises the results at 15:1 and 5:1 CH_4:O_2 ratios. Increasing the oxygen content in the mixture from 15:1 to 5:1, increased the extent of methane oxidation with high methanol selectivity, 23.8%, at 90°C.

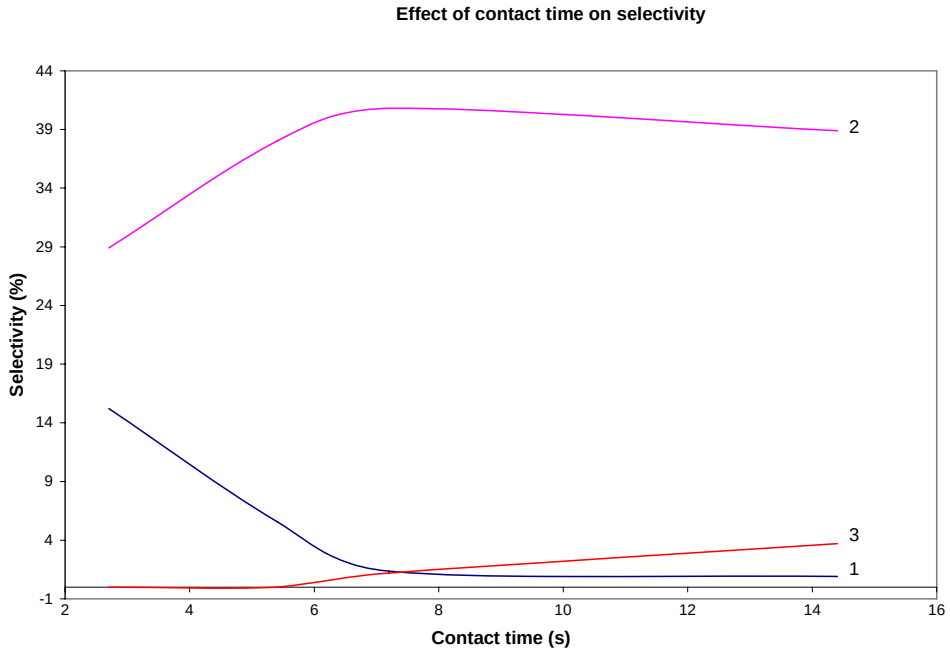

Figure 5.6: The effect of contact time on product selectivity for support/3 layer silica/Pt 1: methanol, 2: formaldehyde, 3: carbon dioxide

Table 5.3: Results of the catalytic activity testing of Support/3 layer silica/Pt at 40 ml/min

Flow rate (ml/min)	CH_4:O_2	Temperature (°C)	CH_4 Conversion (%)	Selectivity (%)		
				CH_3OH	CH_2O	H_2O
40	5:1	60	0.61	16.7	27.4	27.0
		90	0.70	23.8	20.6	20.0
	15:1	60	0.71	18.1	41.0	40.7
		90	0.49	16.5	42.0	41.5

A decrease in the oxygen content in the reaction mixture resulted in enhanced formation of formaldehyde and water (selectivity to both formaldehyde and water around 41%) at 60°C and 90°C. Hargreaves et al.[44] showed that, by limiting the oxygen conversion to very low levels, the product selectivity would be dramatically switched to CH_2O.

5.3.2 PMo- and SiMo-based catalysts results

PMo- and SiMo-based catalysts showed activity in the oxidation of methane with oxygen as discussed below. Table 5.4 presents the activity results for the support/PMo catalyst. It can be seen that methane and oxygen conversion decreases slightly with increase in temperature. Selectivity to methanol (5.4% to 7.5%) was higher than the selectivity to formaldehyde, water and carbon dioxide (less than 1%) at all temperatures examined, as shown in Figure 5.7. CO might be the major product since methane cracking is not expected at temperatures < 100°C.

Table 5.4: Results of the catalytic activity testing of Support/PMo at 40 ml/min GHSV= 666 h^{-1}

Reaction temp. (°C)	CH_4:O_2	Time on stream (h)	Conversion (%)		Selectivity (%)			
			CH_4	O_2	CH_3OH	CH_2O	H_2O	CO_2
40	5:1	1	12.25	12.39	6.75	0.18	0.25	0.44
		2	12.02	12.30	5.39	0.22	0.26	0.45
	10:1	1	12.48	8.76	7.98	0.15	0.29	0.46
		2	12.51	8.90	7.05	0.18	0.27	0.47
100	5:1	1	12.14	12.02	6.97	0.13	0.44	0.44
		2	12.05	12.40	5.77	0.18	0.30	0.45
	10:1	1	12.37	8.51	6.87	0.21	0.31	0.47
		2	12.24	8.62	4.84	0.24	0.27	0.47
	15:1	1	12.63	9.13	7.57	0.16	0.39	0.48
		2	12.65	13.50	7.58	0.18	0.33	0.47

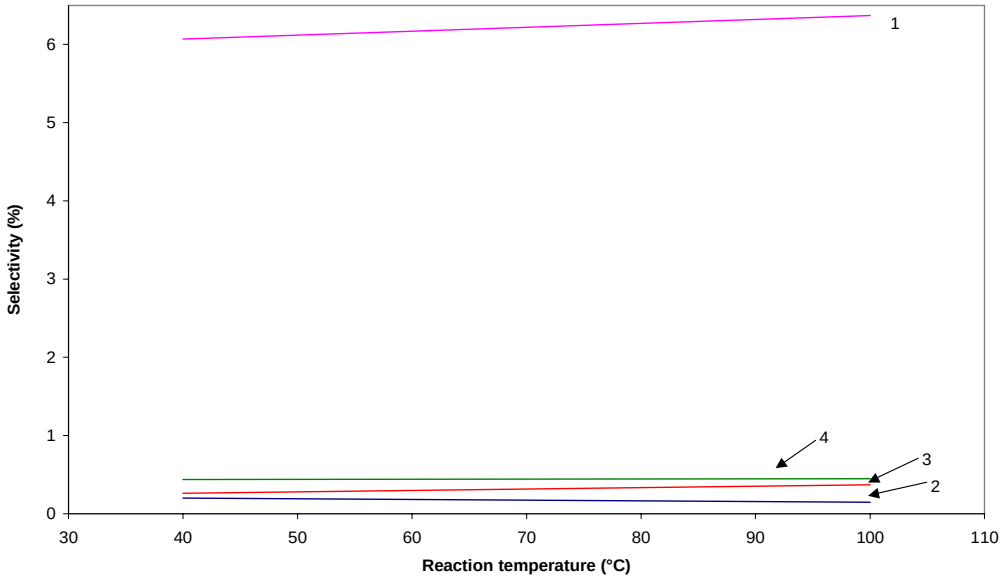

Figure 5.7: The effect of reaction temperature on product selectivity for support/PMo 1: methanol, 2: formaldehyde, 3: water, 4: carbon dioxide

Table 5.5: Results of catalytic activity testing of Support/3 layer silica/PMo and Support/3 layer silica/SiMo (GHSV= 666 h^{-1}, methane: oxygen ratio 15:1, time of experiment 2 h)

Catalyst	Reaction temp. (°C)	Conversion (%)		Selectivity (%)			
		CH_4	O_2	CH_3OH	CH_2O	H_2O	CO_2
Support/3 layer silica/PMo	40	0.19	1.68	58.3	21.8	21.5	0.0
	60	0.26	2.60	35.0	32.6	32.2	0.0
	90	0.23	2.10	47.5	26.5	25.8	0.0
Support/3 layer silica/SiMo	40	0.11	1.61	29.6	28.6	38.3	0.5
	60	0.17	2.46	22.6	21.2	40.5	4.8
	90	0.291	3.78	31.7	16.3	43.4	5.2

Table 5.5 compares the PMo and SiMo catalysts in the oxidation of methane at 40 ml/min and ratio of methane to oxygen of 15:1. Methane conversion increases with temperature up to 90°C for both SiMo (0.29%) and PMo (0.23%) based catalysts. Methane conversion for SiMo was lower than PMo at all temperatures except at 90°C. Oxygen conversion also increased with increase in temperature as presented in Figure 5.8. High oxygen conversion (3.78%) at 90°C for SiMo increased the selectivity to water and CO_2 compared to PMo. At this conversion, methanol was oxidised to formaldehyde which was oxidised further to water and carbon dioxide. This agrees with the findings of Hargreaves et al[44] that limiting the oxygen conversion to very low levels will increase formaldehyde selectivity.

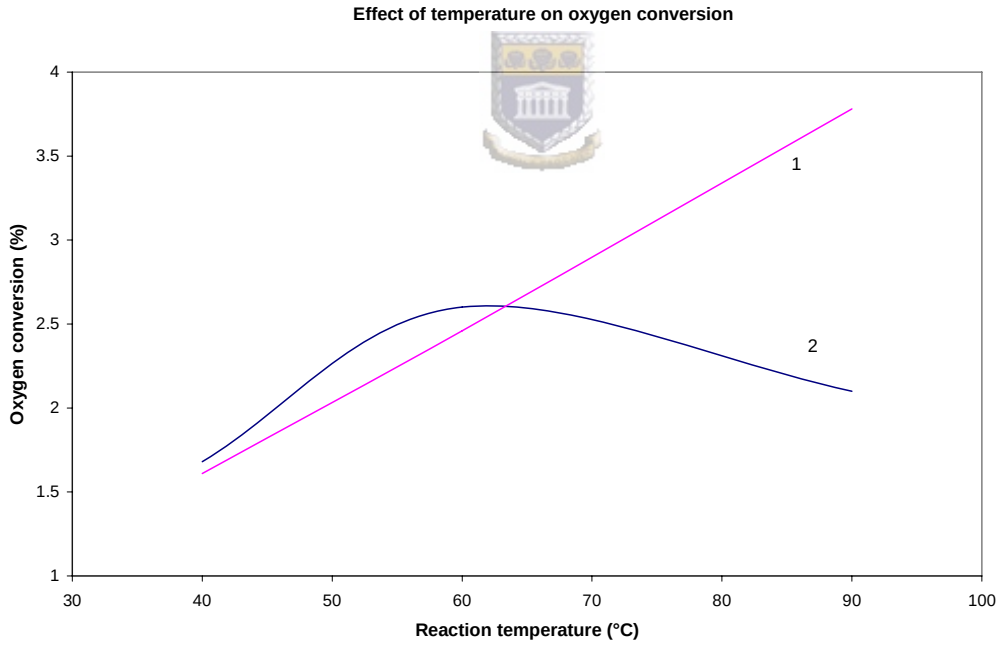

Figure 5.8: Effect of reaction temperature on oxygen conversion (GHSV 666 h^{-1} methane to oxygen ratio 15:1) 1: Support/3 layer silica/SiMo 2: Support/3 layer silica/PMo

From Table 5.5 the selectivity to methanol decreases with increase in temperature for a while and then increases at 90°C. PMo showed the highest methanol selectivity of 58.3% at low temperature (30°C) while SiMo methanol selectivity was 31.7% at 90°C as shown in Figure 5.9 and Figure 5.10 respectively. Carbon dioxide was not detected at the temperatures investigated for PMo catalyst whereas SiMo produced CO_2 which increased with increase in temperature and oxygen conversion as discussed above.

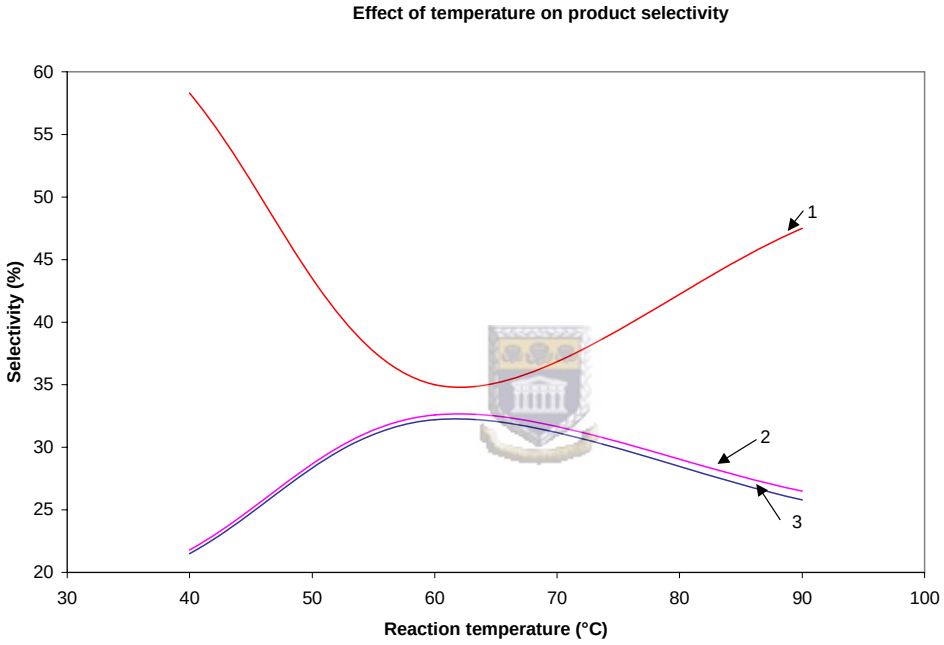

Figure 5.9: Effect of reaction temperature on product selectivity for Support/3 layer silica/PMo (GHSV 666 h^{-1} methane to oxygen ratio 15:1) 1: methanol 2: formaldehyde 3: water

Support/3 layer silica/PMo performed better than support/3 layer silica/SiMo giving high methanol selectivity (58.3%) at 0.19% methane conversion at 40°C. High formaldehyde selectivity (32.6%) was obtained at methane conversion of 0.26% at 60°C. This can be attributed to the different chemical environment around Mo in both

PMo and SiMo. The addition of phosphorus which is surrounded by four oxygen atoms arranged tetrahedrally[124] in HPA increased the activity of HPA in methane oxidation to methanol and formaldehyde. Mo provides a site for chemisorption of a reactive oxygen species. The reactive oxygen species is then responsible for activation of methane as discussed by McCormick and Alptekin.[29] The site is isolated by these phosphate groups inhibiting further oxidation to carbon dioxide. The surface phosphate group may also be necessary for the formation of methanol.

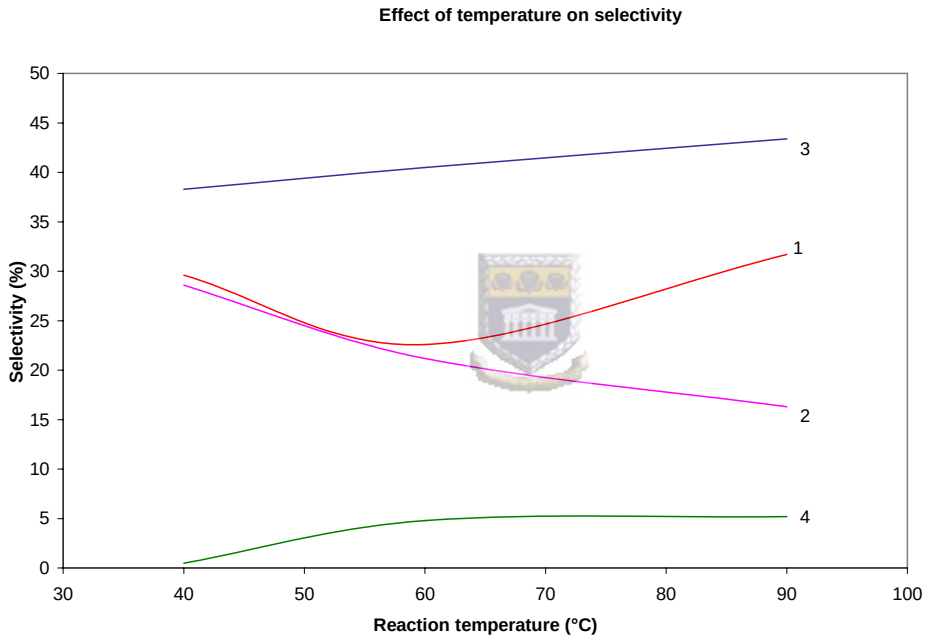

Figure 5.10: Effect of reaction temperature on product selectivity for Support/3 layer silica/SiMo (GHSV 666 h^{-1} methane to oxygen ratio 15:1) 1: methanol 2: formaldehyde 3: water 4: carbon dioxide

The properties of SiMo and PMo were discussed in Chapter 4. In Chapter 4.3.2 Figure 4.21 it was seen that PMo was highly dispersed on the modified support than SiMo (see Figure 4.17) and has more basic sites than SiMo (see TPD of CO_2 profile in

Figure 4.29 in Chapter 4.3.3) which favoured high methanol and formaldehyde production. It was also shown in Chapter 4.3.3 that support/3 layer silica/PMo can activate methane (TPD of methane in Figure 4.30) and oxygen (TPO in Figure 4.26 and Figure 4.27) more than support/3 layer silica/SiMo. Thus methane bonded to PMo.

Table 5.6: Results of the catalytic activity testing of Support/3 layer silica/PMo at 100°C with varying GHSV from 166 h^{-1} and 250 h^{-1}

GHSV (h^{-1})	CH_4:O_2	Time on stream (h)	Conversion (%)		Selectivity (%)			
			CH_4	O_2	CH_3OH	CH_2O	H_2O	CO_2 x10^{-3}
166	5:1	1	32.94	49.16	23.46	25.85	28.52	0.46
		2	22.02	47.40	3.80	24.14	15.80	0.47
250	5:1	1	23.58	51.86	5.85	28.14	19.08	0.71
		2	21.13	47.25	3.67	22.83	14.30	0.31
	10:1	1	19.78	57.47	2.41	15.70	12.45	0.34
		2	20.70	56.79	2.40	18.90	10.40	0.44

The data in Table 5.6 was used to plot the graph in Figure 5.11 in order to investigate the effect of contact time between the feed mixture and the catalyst surface on selectivity for Support/3 layer silica/PMo.

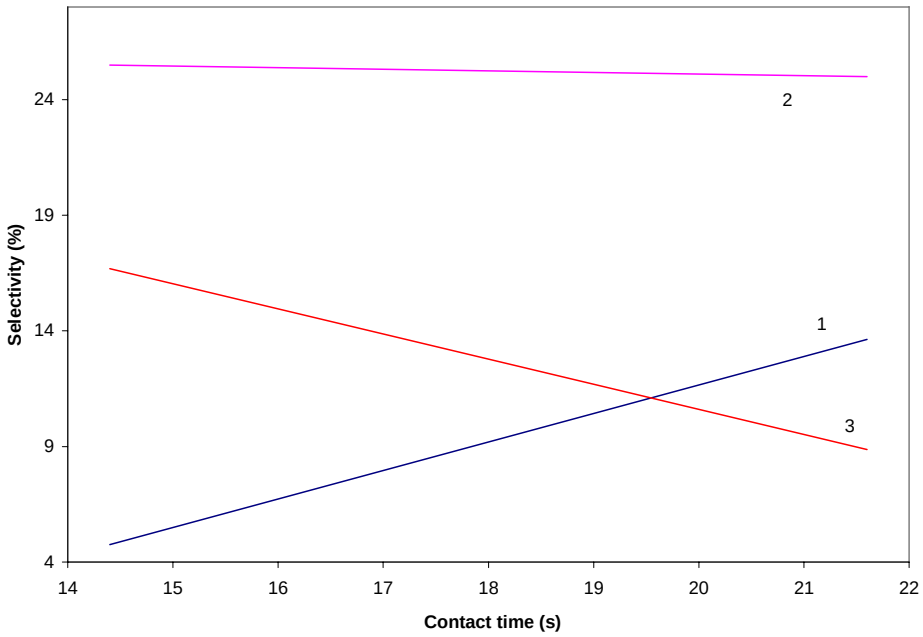

Figure 5.11: Effect of contact time on product selectivity for Support/3 layer silica/PMo methane to oxygen ratio 5:1 at 100°C. 1: methanol 2: formaldehyde 3: water

From Figure 5.11 it can be seen that formaldehyde selectivity remains high for both contact times at around 25% whereas selectivity to water decreases with increase in contact time. Methanol selectivity is high at 21.6 s (13.6%) than at 14 s (4.7%). Methane conversion and methanol selectivity decreased with increased time on stream at a CH_4:O_2 ratio of 5:1 that is, after 1 h the conversion and selectivity of methanol decreased. This suggests that to obtain high methanol selectivity a small residence time is needed to avoid further oxidation of methanol and formaldehyde to carbon oxides and water. This is the reason why in many previous studies the unstable product is removed from the reaction cycle after short residence time.[9, 69] In this research work the reactor was designed to offer the possibility of pre-mixing methane

with oxygen before entering the reactor, thus avoiding prolonged reaction times on the thin catalyst (layer) bed.

5.4 Conclusions

The prepared supported catalysts (Pt-, PMo- and SiMo- based catalysts) converted methane to methanol and formaldehyde under mild conditions. With an increase in the reaction temperature, hydrogen atoms in the methane molecule were progressively replaced by oxygen atoms and thus the nature of the oxidation products reflects this process. As a result, methanol selectivity decreased. A decrease in the reaction mixture flow rate through the reactor also reduced methanol selectivity. Pt- based catalysts showed the highest methane conversion than PMo- and SiMo based catalyst under all conditions examined. Table 5.7 presents the relative per pass CH_3OH and HCHO yields for Pt, PMo and SiMo catalysts calculated as follows:

Relative per pass CH_3OH yield = CH_4 conversion x CH_3OH selectivity

Relative per pass CH_2O yield = CH_4 conversion x CH_2O selectivity

It can be seen for Table 5.7 that methane conversion was low for SiMo catalyst (0.11%) with relative pass per yield of methanol and formaldehyde 0f 3.260 and 3.15 respectively. SiMo results are lower than those of Pt and PMo catalysts due to the low content of the active species –Mo- on the support as shown from ICP-MS results in Table 4.13 and thus few Mo sites were available for the oxidation of methane.

Table 5.7: Relative per pass CH_3OH and CH_2O yields for Pt, PMo and SiMo catalysts at 30°C, GHSV= 666 h^{-1} and CH_4:O_2= 15:1.

Catalyst	CH_4 conversion (%)	CH_3OH selectivity (%)	CH_2O selectivity (%)	Relative per pass CH_3OH yield	Relative per pass CH_2O yield
Support/3 layer silica/Pt	0.85	19.0	40.0	16.15	34
Support/3 layer silica/PMo	0.19	58.3	21.8	11.08	41.14
Support/3 layer silica/SiMo	0.11	29.6	28.6	3.26	3.15

Methanol selectivity was higher for PMo catalyst (58.3%) and the lower for Pt catalyst (19%). Pt and PMo enhanced methanol and formaldehyde yields with both catalysts favouring the production of formaldehyde more than methanol. 30°C, GHSV= 666 h^{-1} and CH_4:O_2= 15:1 are the optimum conditions for the catalytic oxidation of methane to methanol and formaldehyde for Pt, PMo and SiMo deposited on the support material modified with 3 layers of silica.

CHAPTER 6: Natural gas as feedstock

6.1 Introduction

The role of natural gas as the dominant energy source in the near future is increasing rapidly. Natural gas consists primarily of methane with varying proportions of ethane, propane, butane, nitrogen and impurities such as hydrogen sulphide, carbon dioxide or trace metals.[72, 125] The methane in the natural gas varies from 40 to 95 volume %. Natural gas with high methane content (85-95 volume %) may be used as pure gaseous fuel for various energy-intensive industries such as steel and cement manufacturing and electricity production.[44] Transportation of natural gas is technically difficult and requires highly sophisticated and expensive pipeline networks. Liquefied natural gas has low density of 0.4 g/ml and low boiling point temperature (-162°C). These properties make the transportation of the liquid form an energy inefficient process.[126, 72] Chapter 1 of this report discusses the need for converting natural gas to value-added products.

From the literature survey and results outlined in Chapter 5, it is found that platinum is the most active catalyst for the oxidation process. However, since the price of platinum is very expensive, heteropoly acids (HPA) loaded on silica modified support, in this case $H_3PMo_{12}O_{40}$, will reduce the cost. Hence PMo-based catalysts were chosen to study the oxidation of natural gas. In this section, the catalytic activity of PMo-based catalysts is described based on exposing the catalysts to a mixture of

natural gas and air. The conversion and selectivity results are also compared with those of using methane and oxygen as feed.

6.2 Experimental procedure

All experimental details involving catalyst preparation, characterization and activity testing are given in Chapter 2. The activity testing for natural gas oxidation was done at The Institute of General and Inorganic Chemistry, Kiev, Ukraine

6.3 Results and discussion

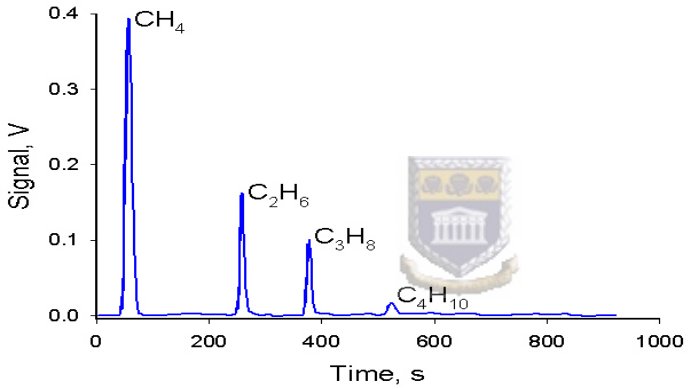

Figure 6.1: Gas components before detector (feed)

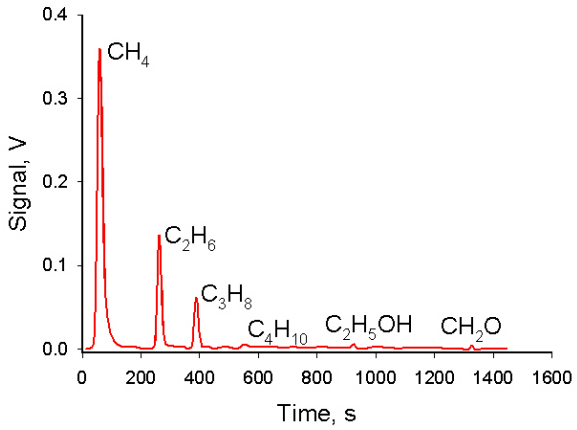

Figure 6.2: Components after detector (reaction products)

Table 6.1: Results of catalytic activity testing of Support/3 layer silica/PMo (GHSV = 952 h^{-1})

Conditions	Conversion of initial components (%)				Selectivity of finite components (%)		
	CH_4	C_2H_6	C_3H_8	C_4H_{10}	CH_3OH	CH_2O	C_2H_5OH
T=90^{0}C ratio Natural gas:Air – 3:1 Flow rate 40 ml/min	15.00	68.20	81.20	86.10	0.54	1.77	3.42
T=120^{0}C ratio Natural gas:Air – 3:1 Flow rate 40 ml/min	1.20	5.40	0.00	17.20	0.67	0.00	25.9
T=150^{0}C ratio Natural gas:Air – 3:1 Flow rate 40 ml/min	0.00	7.30	3.00	14.10	0.00	0.00	0.00
T=90^{0}C ratio Natural gas:Air – 1:1 Flow rate 40 ml/min	18.90	28.70	3.30	57.70	2.64	4.60	0.00
T=120^{0}C ratio Natural gas:Air – 1:1 Flow rate 40 ml/min	7.50	53.30	0.00	75.00	0.00	17.97	90.00
T=150^{0}C ratio Natural gas:Air – 1:1 Flow rate 40 ml/min	0.00	3.30	2.50	0.00	0.00	0.00	35.34
T=90^{0}C ratio Natural gas:Air – 1:3 Flow rate 40 ml/min	0.00	0.00	0.00	0.00	0.00	0.00	0.00
T=120^{0}C ratio Natural gas:Air – 1:3 Flow rate 40 ml/min	60.00	53.00	41.00	0.00	6.00	39.00	5.00
T=150^{0}C ratio Natural gas:Air – 1:3 Flow rate 40 ml/min	10.50	20.20	10.80	19.10	0.21	0.00	13.60

Figure 6.1 and Figure 6.2 the gas components in the feed (natural gas) and in the reaction products respectively. Table 6.1 shows the activity results of PMo supported on 3 layer silica modified support at GHSV = 952 h^{-1}. Supported PMo has catalytic activity in oxidizing saturated hydrocarbons (lower alkanes). Products of reaction for methane are carbon monoxide, methanol, and formaldehyde. Carbon dioxide was not detected in the products of reaction. For other hydrocarbons, only ethanol selectivity could be estimated for the oxidation of ethane. Propane and butane might have converted to carbon monoxide or the oxygenated products were too low to be detected. High natural gas conversion for methane, ethane, propane and butane were 15.0%, 68.2%, 81.2% and 86.1% respectively at 90°C, 40 ml/min and natural gas to air ratio of 3:1. When the temperature was raised to 150°C at 40 ml/min and natural gas to air ratio of 3:1, no methanol, formaldehyde and ethanol were detected.

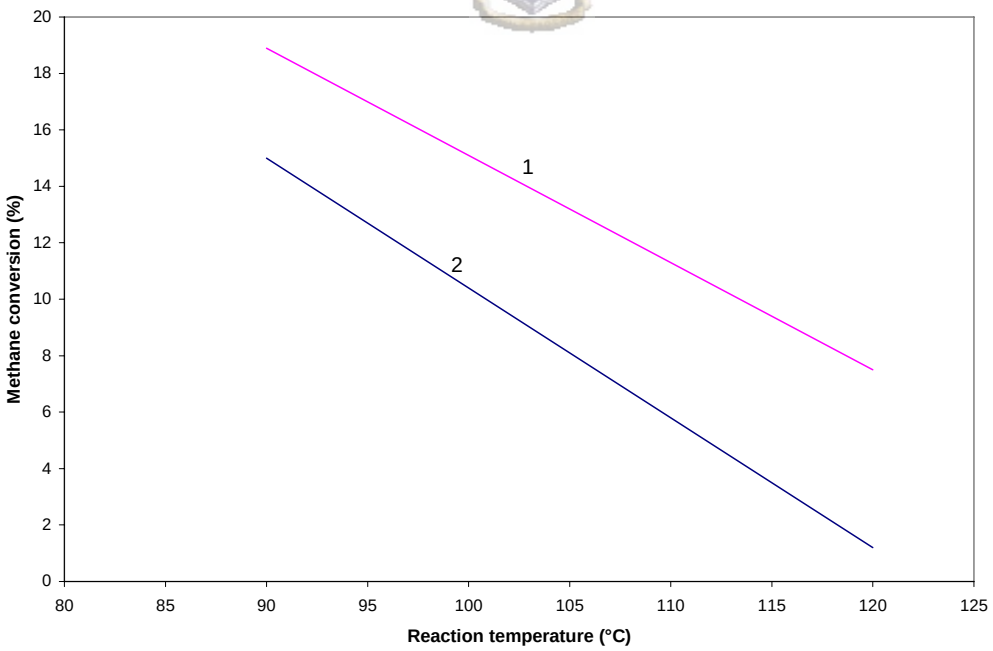

Figure 6.3: Effect of reaction temperature on methane conversion for Support/3 layer silica/PMo. 1: natural gas to air ratio of 1:1, and 2: natural gas to air ratio of 3:1

At 1:1 natural gas to air ratio, 40 ml/min and 90°C methane conversion of 18.9% was obtained with selectivity to methanol and formaldehyde of 2.64% and 4.6% respectively. Methane conversion decreased with increase in reaction temperature as shown in Figure 6.3. PMo catalyst didn't show catalytic activity (no natural gas conversion) at 40 ml/min, 90°C and 1:3 natural gas to air ratio. An increase in temperature at the same flow rate and gas ratio increased the catalytic activity, with the highest methane conversion (60%) and selectivity to methanol and formaldehyde at 6% and 39% respectively, being obtained at 120°C. Formaldehyde was a major product.

For most of the reaction conditions investigated selectivity towards formaldehyde was higher than methanol selectivity as shown in Table 6.1 above, which implies that methanol was probably produced first and then oxidised further to formaldehyde. Methanol was a primary product while formaldehyde a major product.

Methanol selectivity of 0.67% and 0.21% were obtained at 40 ml/min, 120°C, natural gas to air ratio of 3:1 and 40 ml/min, 150°C, natural gas to air ratio of 1:3 respectively. Formaldehyde was not produced under these conditions. Based on the experimental results, it can be assumed that the methane oxidation proceeded as shown below[127, 6]:

$$CH_4 \rightarrow CH_3OH \rightarrow HCHO + H_2O \rightarrow CO \rightarrow CO_2 + H_2O$$

Methane was converted (7.5%) directly to formaldehyde (selectivity 17.97%) at 40 ml/min, 120°C and 1:1 ratio of natural gas to air. Methanol was not detected. Since the 1:3 natural gas to air ratio showed the highest methane conversion (60%) and selectivity to methanol and formaldehyde at 6% and 39% respectively at 120°C for

Support/3 layer silica/PMo, these conditions were used to test the catalytic activity of PMo deposited on unmodified support. The results are shown in Table 6.2. PMo deposited on unmodified support showed catalytic activity for oxidation of saturated hydrocarbons under these conditions.

Table 6.2: Results of the catalytic activity testing of Support/PMo (GHSV = 952 h^{-1})

Conditions	Conversion of initial components (%)				Selectivity (%)		
	CH_4	C_2H_6	C_3H_8	C_4H_{10}	CH_3OH	CH_2O	C_2H_5OH
T=90^0C ratio Natural gas:Air – 1:3 Flow rate 40 ml/min	7.00	18.00	45.00	52.00	9.00	2.00	7.00

Table 6.2 shows that methane conversion (7%) and selectivity to methanol and formaldehyde at 9% and 2% respectively were obtained. Methanol is the major product for this catalyst while for Support/3 layer silica/PMo, formaldehyde was the major product. The introduction of silica to modify the support material improved the properties of the PMo catalyst in this case support/3layer silica/PMo has a higher surface area than support/PMo, as discussed in Chapters 4 and 5 and in the literature.[107, 119] The results are summarised in Table 6.3 below.

Table 6.3: Properties and activity results of PMo-based catalysts

Catalyst	Surface area - BET- (m^2/g)	Pore volume (cm^3/g)	GHSV (h^{-1})	Conditions	CH_4 in natural gas Conversion (%)	Selectivity (%)	
						CH_3OH	CH_2O
Support/PMo	5.26	0.002003	952	T=90 ^{0}C ratio Natural gas:Air – 1:3 Flow rate 40 ml/min	7.0	9.0	2.0
Support/3 layer Silica / PMo	7.55	0.002861	952	T=90 ^{0}C ratio Natural gas:Air – 1:3 Flow rate 40 ml/min	0.0	0.0	0.0
Support/3 layer Silica / PMo	7.55	0.002861	952	T=120 ^{0}C ratio Natural gas:Air – 1:3 Flow rate 40 ml/min	60.0	6.0	39.0

TPD of methane in Chapter 4.3.3 Figure 4.30 showed that support/3layer Silica/PMo activated methane better than support/PMo when the temperature was increased from 180°C to 310°C. Moreover support/3 layer silica/PMo has more basic sites (as shown in Figure 4.29) than support/PMo which contributed to the high methane conversion of 60% and 39% selectivity to formaldehyde. Furthermore the TPO profiles in Figures 4.26 and 4.27 of both catalysts are same with an extra hump at 118°C for support/3 layer silica/PMo. This implies that the catalysts may contain more than one phase of oxides which improves the oxidation of methane.

Figures 6.4 and 6.5 illustrate the dependence of natural gas conversion on molecular weight (methane, ethane, propane and butane). Methane conversion was lower than all the hydrocarbons present in natural gas at the temperatures examined. Methane conversion decreased with increase in temperature and no conversion was observed at 150°C.

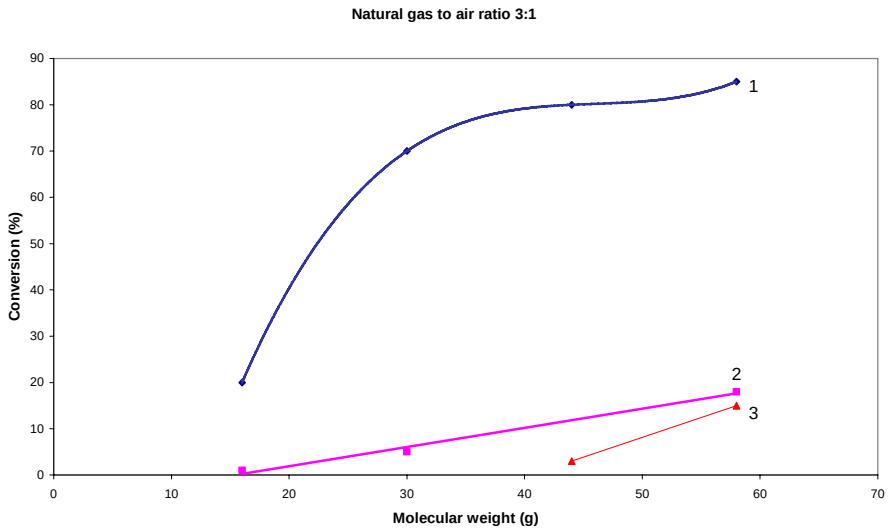

Figure 6.4: Dependence of conversion on molecular weight for a Natural gas: Air ratio of 3:1. 1: 90°C, 2: 120°C, 3: 150°C

Methane conversion was high at 90°C for both natural gas to air ratios of 3:1 and 1:1. Butane showed the highest conversion. Natural gas conversion increased with an increase in molecular weight.

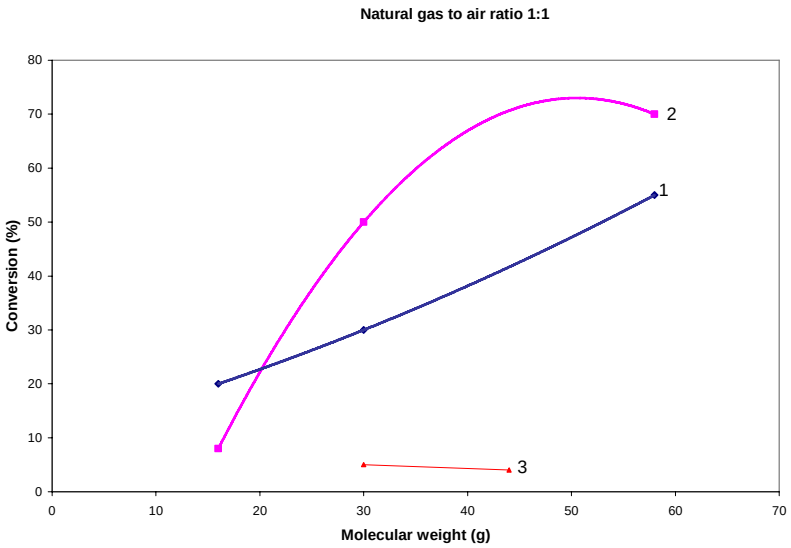

Figure 6.5: Dependence of conversion on molecular weight for Natural gas: Air ratio of 1:1. 1: 90°C, 2: 120°C, 3: 150°C

6.4 Conclusions

Supported PMo catalysts can activate methane in natural gas at low temperatures (less than 250°C) and at atmospheric pressure. Support/3 layer silica/PMo proved to be a better catalyst than PMo deposited on unmodified support for natural gas oxidation. It showed the highest methane conversion of 60% and selectivity to methanol and formaldehyde at 6% and 39% respectively, at 120°C and a 1:3 natural gas to air ratio. The properties of this catalyst were improved after modifying the support material with silica. Therefore the importance of silica is emphasized. Natural gas conversion depends on the composition of a reaction mixture and reaction temperature, and increases with an increase in molecular weight.

CHAPTER 7: Overall conclusions and recommendations

The data obtained using a low temperature and low pressure, inorganic ceramic membrane-based oxidation technology verify the improvements in converting methane to methanol and formaldehyde by suppressing further-oxidation. This chapter discusses the conclusions that were made based on the results that were obtained when using Pt, hemin, SiMo and PMo supported on the inorganic membrane paper as catalysts for the oxidation of methane to methanol and formaldehyde under mild conditions.

7.1 Oxidation of methane to methanol and formaldehyde under mild conditions

The active species -Pt, hemin, SiMo and PMo- were successfully deposited on the surface of the silica modified and unmodified support material.

7.1.1 Hemin-based catalysts

- Though hemin catalysts were successfully loaded on the support the concentration of Fe was low and therefore showed small TPR and TPO peaks suggesting few adsorption sites for oxygen. Thus the activity of hemin-based catalysts was not tested

Recommendation: In order to increase the concentration of Fe on the support the use of a linker compound such as aminopropyltriethoxysilane (APTS) to chemically

modify the silica prior to deposition of hemin as discussed by Kolotusha, Belyakova and Tertykh.[74]

7.1.2 Pt-based catalysts

- The prepared Pt-based catalysts were characterised using various techniques. Characterisation with XRD was difficult and only Pt deposited on silica powder showed crystalline Pt with crystal plane at 111, 200 and 220.
- The presence of Pt reducible species after TPR experiments will provide sites for adsorption of oxygen in the oxidation of methane
- Supported Pt catalysts were active in the oxidation of methane to methanol and formaldehyde at GHSV = 666 h^{-1}, atmospheric pressure and low temperature.
- Methane conversion increased with an increase in the amount of Pt on the support. Methane conversion of 0.85% at 30°C was obtained for 0.326 mg/cm^2 Pt and 0.38% for 0.244 mg/cm^2 Pt. High Pt loading on the support (0.326 mg/cm^2) gave low selectivity towards methanol (16.5%) with increase in temperature.
- Methane conversion decreases with an increase in temperature for both catalysts. Selectivity to methanol and formaldehyde depend on temperature with methanol selectivity reaching a maximum at 60°C (30.5%).
- Increasing contact time increased methane conversion. High methane conversion of 1.84% was observed at 14.4 s and 120°C. The longer contact time (14.4 s) between the reaction mixture and the catalyst enhanced the production of carbon dioxide and high selectivity to formaldehyde 38.9%. Selectivity to methanol decreased with increase in contact time (0.19%).

- Increasing the oxygen content in the mixture from 15:1 to 5:1, increased the extent of methane oxidation with high methanol selectivity, 23.8% at 90°C.

7.1.3 SiMo- based catalysts

- SiMo-based catalysts consumed less oxygen during TPO experiments due to the low loading of Mo in SiMo as confirmed by ICP analysis. Therefore, there are few oxygen adsorption sites on these catalysts and hence low activity was obtained during the oxidation of methane.
- Activity tests of SiMo-based catalysts were done for comparison with PMo-based catalysts

7.1.4 PMo-based catalysts

- PMo-based catalysts were successfully loaded on silica modified and unmodified support with the highest loading of 60%. PMo was highly dispersed on the modified support and covered the surface of the support resulting in low surface area (BET).
- TPO results showed that PMo-based catalysts have adsorption sites for oxygen. The interaction of oxygen with the catalyst activates oxygen making it more reactive for the activation of methane.
- Results of TPD of CO_2 showed presence of medium-strong basic sites on PMo-based catalysts in the temperature range 140°C – 300°C. Very low methane desorption was obtained at 60°C in TPD of methane. Methane was strongly adsorbed by PMo-based catalyst hence high temperatures, around 240°C to 260°C, were required to break the bond between methane and the catalysts.

- Supported SiMo and PMo catalysts were active in the oxidation of methane to methanol and formaldehyde at GHSV = 666 h^{-1}, atmospheric pressure and low temperature.
- Methane conversion increases with temperature up to 90°C for both SiMo (0.29%) and PMo (0.23%) based catalysts. Methane conversion for SiMo was lower than PMo at all temperatures except at 90°C.
- High oxygen conversion (3.78%) at 90°C for SiMo increased the selectivity to water and CO_2 compared to PMo. At this conversion, methanol was oxidised to formaldehyde which was oxidised further to water and carbon dioxide.
- PMo showed the highest methanol selectivity of 58.3% at low temperature (30°C) while SiMo methanol selectivity was 31.7% at 90°C.
- Supported PMo catalyst performed better than supported SiMo catalyst with high methanol selectivity (58.3%) at 0.19% methane conversion at 40°C. High formaldehyde selectivity (32.6%) was obtained at methane conversion of 0.26% at 60°C.
- Formaldehyde selectivity remained high at 25% for 21.6 s and 14 s. Methanol selectivity was high at 21.6 s (13.6%) than at 14 s (4.7%).

30°C, GHSV= 666 h^{-1} and CH_4:O_2= 15:1 were found to be the optimum conditions for the catalytic oxidation of methane to methanol and formaldehyde for Pt, PMo and SiMo deposited on the support modified with 3 layers of silica. Methanol selectivity was higher for PMo catalyst (58.3%) followed by SiMo at 29.6% and lower for Pt catalyst (19%). Formaldehyde selectivity was 40%, 21.8% and 28.6% for Pt, PMo and SiMo respectively.

7.2 Oxidation of natural gas to methanol and formaldehyde

Platinum is the most active catalyst for the oxidation process. However, since the price of platinum is very expensive, heteropoly acids loaded on silica modified support, in this case $H_3PMo_{12}O_{40}$, will reduce the cost. Hence PMo-based catalysts were chosen to study the oxidation of natural gas under mild conditions. Supported PMo catalyst showed catalytic activity in oxidation of natural gas (lower alkanes) under mild conditions at GHSV = 952 h^{-1}.

- Natural gas conversion for methane, ethane, propane and butane were 15.0%, 68.2%, 81.2% and 86.1% respectively at 90°C, 40 ml/min and natural gas to air ratio of 3:1 for support/3 layer silica/PMo.
- High methane conversion (60%) and selectivity to methanol and formaldehyde at 6% and 39% respectively were obtained at 120°C, 40 ml/min and 1:3 natural gas to air ratio on support/3 layer silica/PMo. Formaldehyde was a major product.
- Methane conversion (7%) and selectivity to methanol and formaldehyde at 9% and 2% respectively were obtained at 90°C, 40 ml/min and 1:3 natural gas to air ratio on support/PMo.

The idea of this technology is to convert natural gas from small deposits to liquid products such as methanol without building expensive gas to liquid (GTL) plants or long pipelines. Methanol can be applied as a fuel through direct methanol fuel cell (DMFC) or via reforming via hydrogen. Formaldehyde can be oxidized into formic acid which can also be applied in direct fuel cell.

REFERENCES

1. V. Fornés, C. López, H.H. López, and A. Martınez, Applied Catalysis A: General 249 (2003) 345–354

2. A. M. Diskin, R. H. Cunningham, and R. M. Ormerod, Catalysis Today 46 (1998) 147-154

3. J H. Lunsford, Catalysis Today 63 (2000) 165-174

4. A. G. Steghuis, J. G. van Ommen, and J. A. Lercher, Catalysis Today 46 (1998) 91-97

5. R. H. Crabtree, Natural gas conversion II, @Elsevier Science B.V. 83-85 (1994)

6. R. G. Herman, Q. Sun, C. Shi, K. Klier, C. Bao, H. Hu, I. E. Wachs, and M. M. Bhasin, Catalysis Today 37 (1997) 1-14

7. J.M. Fox and D.J. Slocum, Proceedings 1989 World Methanol Conference, Houston TX, December 1989

8. Malcom Pirnie, Inc, Technical Memorandum Oakland, California, 1-49 (January 1999) 3522-002

9. V.D. Sokolovskii, N.J. Coville, A. Parmaliana, I. Eskendirov, and M. Makoa, Catalysis Today 42 (1998) 191-195

10. T. J. Hall, J. S. J, Hargreaves, G. J. Hutchings, R. W. J. and S. H. Taylor, Fuel Processing Technology 42 (1995) 151-178

11. Y. Wang, and K. Otsuka, Journal of Molecular Catalysis A: Chemical 111 (1996) 341-354

12. Y. Moro-oka, Catalysis Today 45 (1998) 3-12

13. K. Fujimuto, Natural gas conversion II, @Elsevier Science B.V. 73-82 (1994)

14. J. C. Vedrine, 3rd World Congress on Oxidation Catalysis, Elsevier Science B.V., 61-76 (1997)

15. G. Centi, F. Cavani, and F. Trifiro, Fundamental and Applied Catalysis, Kluwer Academic/ Plenum Publishers, New York (2001) 364-365

16. Y. Wang, K. Otsuka and K. Ebitani, Catalysis Letters 35 (1995) 259-263

17. Hunter N.R., Gesser H.D. et al., Applied Catalysis 57 (1990) 45-54

18. M.J Brown and N.D. Parkyns, Catalysis Today 8 (1991) 305-335

19. G. J. Hutchings and M. S. Scurrell, CATTECH 7 (3) (2003) 90- 103

20. S. H. Yaylor, J. S.J. Hargreaves, G. J. Hutchings, et.al, Catalysis Today 42 (1998) 217-224

21. G. J. Hutchings, S. H. Taylor, Catalysis Today 49 (1999) 105-113

22 E.R.S. Winter, Journal of Physical Chemistry A (1968) 2889

23. E.R.S. Winter, Journal of Chemical Society A (1969) 1832

24. R. D. Noble, American Chemical Society, Symposium on Natural Gas Upgrading II, 11-14, (April 5-10 1992)

25. F. Pinna, Catalysis Today 41 (1998) 129-137

26. F. Cavani and F Trifiro, Catalysis Today 51 (1999) 561-580

27. Y. Moro-oka, Applied Catalysis A: General 181 (1999) 323-329

28. K. Aoki, M. Ohmae, T. Nanba, K. Takeishi, N. Azuma, A. Ueno, H. Ohfune, H. Hayashi, Y. Udagawa, Catalysis Today 45 (1998) 29- 33

29. R.L. McCormick, G.O. and Alptekin, Catalysis Today, 55 (2000) 269-280

30. A. Parmaliana, V. Sokolovskii, D. Miceli, F. Arena, and N. Giordano, Journal of Catalysis 148 (1994) 514

31. N.D. Spencer, C.J. Pereira, and R.K. Grasselli, Journal of Catalysis 126 (1990) 546

32. Q. Liu, J. Rogut, B. Chen, J. L. Falconer and R. D. Noble, Fuel 15 (1996) 1748-1754

33. X. Zhang, De-hua He, Qi-jian Zhang, Q. Ye, Bo-qing Xu, and Qi-ming Zhu, Applied Catalysis A: General 249 (2003) 107–117

34. T. Takemoto, K. Tabata, Y. Teng, Lian-Xin Dai, and Eiji Suzuki, Catalysis Today 71 (2001) 47–53

35. T. Kawabe, K. Tabata, E. Suzuki, Y. Ichikawa, and Y. Nagasawa, Catalysis Today 71 (2001) 21–29

36. J.A. Barbero, M.A. Bañares, M.A. Peña, and J.L.G. Fierro, Catalysis Today 71 (2001) 11–19

37. Y. Wang and K. Otsuka, Journal of catalysis 155 (1995) 256-267

38. B. Michalkiewicz, K. Kalucki, and J. G. Sosnicki, Journal of Catalysis 215 (2003) 14–19

39. K. Otsuka and M. Hatano, Journal Catalysis 108 (1987) 252

40. T.R. Baldwin, R. Burch, G.D. Squire and S.C. Tsang, Applied Catalysis 74 (1991) 137-152

41. J. Min, and N. Mizuno, Catalysis Today 71 (2001) 89–96

42. Y. W. Chan, and R. B. Wilson, ACS Division Fuel Chemistry 33 (1988) 453

43. R. Raja, P. Ratnasamy, Applied Catalysis A: General 158 (1997) L7-L15

44. J. S.J. Hargreaves, G. J. Hutchings and R. W. Joyner, Nature 348 (29 November 1990) 428-429

45. C. Perego, and P. Villa, Catalysis Today 34 (1997) 281-305

46. K. V.R. Chary, K. R. Reddy, and C. P. Kumar, Catalysis Communications 2 (2001) 277-284

47. P. W. Jacobs, and G. A. Somorjai, Journal of Molecular Catalysis A: Chemical 131 (1998) 5–18

48. Y. Yazawa, H. Yoshida, and T. Hattori, Applied Catalysis A: General 237 (2002) 139–148

49. W. Kuang, A. Rives, M. Fournier, and R. Hubaut, Applied Catalysis A: General 250 (2003) 221–229

50. B.K. Min, A.K. Santra, and D.W. Goodman, Catalysis Today 85 (2003) 113–124

51. R. D. Adams, and F. A. Cotton, Catalysis by Di- and Polynuclear metal cluster complexes, Wiley-VCH (1998) 510

52. J. Tatibouet, M. Che, M. Amirouche, M. Fournier, and C. Rocchiccioli-Deltcheff, Journal of Chemical Society, Chemistry Communication (1988) 1260-1261

53. L. Cairati and F. Trifiro, Journal of Catalysis 80 (1983) 25-30

54. K. Muto, N. Katada, and M. Niwa, Catalysis Today 35 (1997) 145-151

55. Z. Qi-Ming, Y. Zhuo, Y. Xiang, and Z. Mei-Zhen, Journal of Gas Chemistry 4 (1993) 263-270

56. A. Parmaliana and F. Arena, Journal of Catalysis 167 (1997) 57-65

57. K.J. Zhen, M.M. Khan, C.H. Mak, K.B. Lewis, and G.A. Somorjai, Journal of Catalysis 94 (1985) 501

58. N.D. Spencer, and C.J. Pereira, Journal of Catalysis 116 (1989) 399

59. M.M. Koranne, J.G. Goodwin Jr., and G. Marcelin, Journal of Physical Chemistry 97 (1993) 673

60. Chuan-Bao Wang, R. G. Herman, C. Shi, Q. Sun, and J. E. Roberts, Applied Catalysis A: General 247 (2003) 321–333

61. G. O. Alptekin, A. M. Herring, D. L.Williamson, T. R. Ohno, and R. L McCormick, Journal of Catalysis 181 (1999) 104–112

62. X. Wang, Y. Wang, Q. Tang, Q. Guo, Q. Zhang, and H. Wan, Journal of Catalysis 217 (2003) 457–467

63. Y. Yamada, A. Ueda, H. Shioyama, and T. Kobayashi, Applied Catalysis A: General 254 (2003) 45–58

64. V. S. Arutyunov, V. Ya. Basevich, and V. I. Vedeneev, Industrial Engineering Chem. Res. 34 (1995) 4238-4243

65. E. H. Boomer, and V. Thomas, Can. J. Res., Sect. B; 15 (1937) 414-433

66. A. W. Sexton, E. Mac Giolla Coda, and B. K. Hodnett, Catalysis Today 46 (1998) 127-136

67. P M.A. Banares, L.J. Alemany, M Lopez Granados, M. Faraldos, and J.L.G. Fierro, Catalysis Today 33 (1997) 73-83

68. M. Mulder, Basic Principles of Membrane Technology, second edition, Kluwer Academic Publishers (1991) 59-61

69. J. S. Rafelt, J. H. Clark, Catalysis Today 57 (2000) 33-44

70. M. Lin and A. Sen, Journal of American Chemical Society, 114 (1992) 7307

71. G. Centi, F. Cavani, and F. Trifiro, Fundamental and Applied Catalysis, Kluwer Academic/ Plenum Publishers, New York (2001) 8-9

72. J. Zaman, Fuel Processing Technology 58 (1999) 61–81

73. Y. Saito, M. Kuwa, and O. Hashimoto, Fluidization Engineering: Fundamentals and Applications, AlChE Symposium Series 84 262, 102-113

74. R. W. Carr, Clean reaction technologies available at http://www.cpas.mtu.edu/cencitt/report1997/create.html

75. G. Saracco and V. Specchia, Catalysis Rev.-SCI. ENG., 36:2 (1994) 305-384

76. V. Ponec, Journal of Molecular Catalysis A: Chemical 133 (1998) 221-239

77. J. Coronas, and J. Santamaria, Catalysis Today 51 (1999) 377-389

78. M. Lyubovsky, H. Karim, P. Menacherry, S. Boorse, R. LaPierre, W. C. Pfefferle, and S. Roychoudhury, Catalysis Today 83 (2003) 183–197

79. G. Emig, and M.A. Liauw, Topics in Catalysis 21 (2002) 11-24

80. H. J.M. Bouwmeester, Catalysis Today 82 (2003) 141–150

81. P.Ciavarella, H. Moueddeb and J.A. Dalmon, Esf Network Catalytic Membrane Reactors 16-17 October (1997).

82. D. Farrusseng, A. Julbe, and C. Guizard, Separation and Purification Technology 25 (2001) 137–149

83. S. Miachon, V. Perez, G. Crehan, E. Torp, H. Raeder, R. Bredesen, and J.A. Dalmon, Catalysis Today 82 (2003) 75–81

84. J. N. Armor, Catalysis Today 25 (1995) 199-207

85. D. Uzio, S. Miachon, and Jean-Alain Dalmon, Catalysis Today 82 (2003) 67–74

86. J. R.H. Ross, E. Xue, Catalysis Today 25 (1995) 291-301

87. P. Ferreira-Aparicio, I. Rodriguez-Ramos, and A. Guerrero-Ruiz, Applied Catalysis A: General 237 (2002) 239–252

88. M. Reif, and R. Dittmeyer, Catalysis Today 82 (2003) 3–14

89. M.A. Gondal, A. Hameed, and A. Suwaiyan, Applied Catalysis A: General 243 (2003) 165–174

90. D. W. Larkin, L. L. Lobban, and R. G. Mallinson, Catalysis Today 71 (2001) 199–210

91. S.Azgui, F. Guillaume, B. Taouk, and E. Bordes, Catalysis Today 25 (1995) 391-396

92. E. Barrett, L. Joyner, and P. Halenda, Journal of the American Chemical Society 28 (1951) 373

93. J. M. Thomas, and W. J. Thomas, Principles and practice of heterogeneous catalysis, VCH, Weinheim (1997) 105

94. E.F. Vansant, P. Van Der Voort and K.C. Vrancken, Studies in Surface Science and Catalysis, 93 Elsevier (1995) 32-59

95. M. Radojevic and V. N. Bashkin, Practical Environmental Analysis, Royal Society of Chemistry (1999) 369

96. G. Vitulli, E. Pitzalis, P Salvadori, G. Capannelli, O. Monticelli, A. Servida, A. Julbe, Catalysis Today 25 (1995) 249-253

97. XRD database available at http://www.webmineral.com/X-Ray/shtml

98. D. L. Windt, Journal of Vacuum Science Technology A: 18:3 (2000) 980-991

99. J. L. Falconer and J. A. Schwarz, Catal. Rev.-Sci. Eng. 25(2), (1983) 141-227

100. M. Boaro, M. Vicario, C. de Leitenburg, G. Dolcetti, and A. Trovarell, Catalysis Today 77 (2003) 407–417

101. T.J. McCarthy, C.M.P. Marques, H. Trevino, and W.M.H. Sachtler, Catalysis Letters 43 (1997) 11

102. L. Guczi, Z. Konya, Z. Koppany, G. Stefler, and I. Kiricsi, Catalysis Letters 44 (1997) 7

103. M. Vaarkamp, J.T. Miller, F.S. Modica, and D.C. Koningsberger, Journal of Catalysis 163 (1996) 294

104. P.V. Menacherry, M. Fernandez-Garcia, and G.L. Haller, Journal of Catalysis 166 (1997) 75

105. R. Burch, and Z. Paal, Applied Catalysis 114 (1994) 9

106. Lytherm ceramic fiber paper, Lydall Filtration/Separation Group, USA, available at http://.www.lydall.com

107. A. Slagtern, H. M. Swaan, U. Olsbye, I. M. Dahl, and C. Mirodatos, Catalysis Today 46 (1998) 107-115

108. K. Muto, N. Katada and M. Niwa, Catalysis Today 35:1 (1997) 145 -151

109. E.F. Vansant, P. Van Der Voort and K.C. Vrancken, Studies in Surface Science and Catalysis, 93 Elsevier (1995) 32

110. C.Serre, F Garin, G. Belot and G. Maire, Journal of Catalysis 141 (1993) 1-8

111. J.J.Ehrhardt, L. Colin, A. Accorsi, M. Kazmierczak and I. Zdanevitch, Sensors and Actuators B: 7 (1992) 656-660

112. B. Samuneva, Y. Dimitriev, V. Dimitrov, E. Kashchieva and G. Encheva, Journal of Sol-Gel Science and Technology 13 (1998) 969-974

113. G. A. Somorjai, Introduction to surface chemistry and catalysis, John Wiley & sons Inc. New York (1994) 500-513

114. V. A. Hackley and M. A. Anderson, Journal of Membrane Science 70 (1992) 41-51

115. S. Betteridge, C. R. A. Catlow, D. H. Gay, R. W. Grimes, et al., Topics in Catalysis 1 (1994) 103-110

116. S.C. Street, G. Liu, and D.W. Goodman, Surface Science 385 (1997) L971-L977

117. S. A. Borshch, H. Duclusaud, and J. M. Millet, Applied Catalysis A: General 200 (2000) 103–108

118. B. Bachiller-Baeza and J. A. Anderson, Journal of Catalysis 212 (2002) 231–239

119. B. C. Gates, Catalytic Chemistry, John Wiley and Sons, Inc (1992) 320-420

120. V. Perez, S. Miachon, J. Dalmon, R. Bredesen, G. Pettersen, H. Raeder, and C. Simon, Separation and Purification Technology 25 (2001) 33–38

121. V. Zuzaniuk and R. Prins, Journal of Catalysis 219 (2003) 85–96

122. T. Ito, T. Tashiro, T. Watanabe, K. Toi, and I. Ikemoto, The Chemical Society of Japan, Chemistry Letters (1987) 1723-1726

123. A. Erdohelyi, R. Nemeth, A. Hancz, and A. Oszko, Applied Catalysis A: General 211 (2001) 109-121

124. S. Ahmed, S. Kasztelan and J. B. Moffat, Faraday Discussion Chemical Society 87 (1989) 23-32

125. S. H. Oh, P. J. Mitchell, and R. M. Siewert, Journal of Catalysis 132 (1991) 287-301

126. H. Sadamori, Catalysis Today 47 (1999) 325-338

127 A.W. Sexton, B. Kartheuser, C. Batiot, H. W. Zanthoff, and B.K. Hodnett, Catalysis Today 40 (1998) 245-250

128. T.P Kolotusha, L.A Belyakova and V.A. Tertykh, Reaction Kinetics Catalysis Letters 46:1 (1992) 225-231

APPENDICES

Table A1: Thermal analysis of ceramic paper Lydall Technical Paper 3000-LAH.

T °C	Initial mass g	Final mass g	Mass loss g	Colour and structure of sample	Mass loss mg/g	Mass loss %	Difference in mass loss mg/g
50	0.29065	0.29015	0.00050	White, weak	1.72	0.172	0.50
100	0.29370	0.29330	0.00040	White, weak	1.36	0.136	0.75
150	0.30780	0.30660	0.00120	White, weak	3.90	0.390	0.75
200	0.30350	0.30165	0.00185	Yellow, weak	6.09	0.609	2.75
250	0.30254	0.28700	0.01540	Brown, weak	50.90	5.090	17.0
300	0.31040	0.28675	0.02365	Dark brown, weak	76.20	7.620	17.0
350	0.30770	0.28115	0.02655	Light brown, weak	86.28	8.628	2.50
400	0.30015	0.27430	0.02585	White, loose	86.12	8.612	0.50
450	0.30485	0.27830	0.02655	White, loose	87.09	8.709	0.25
500	0.29155	0.27110	0.02045	White, loose	70.14	7.014	0
550	0.29305	0.27220	0.02085	White, loose	71.14	7.114	0
600	0.30285	0.27635	0.02650	White, loose	87.50	8.750	0
650	0.30205	0.27510	0.02695	White, loose	89.22	8.922	0
700	0.30565	0.27840	0.02725	White, loose	89.15	8.915	0
750	0.30490	0.27805	0.02685	White, loose	88.06	8.806	0
800	0.30265	0.27555	0.02710	White, loose	89.54	8.954	0

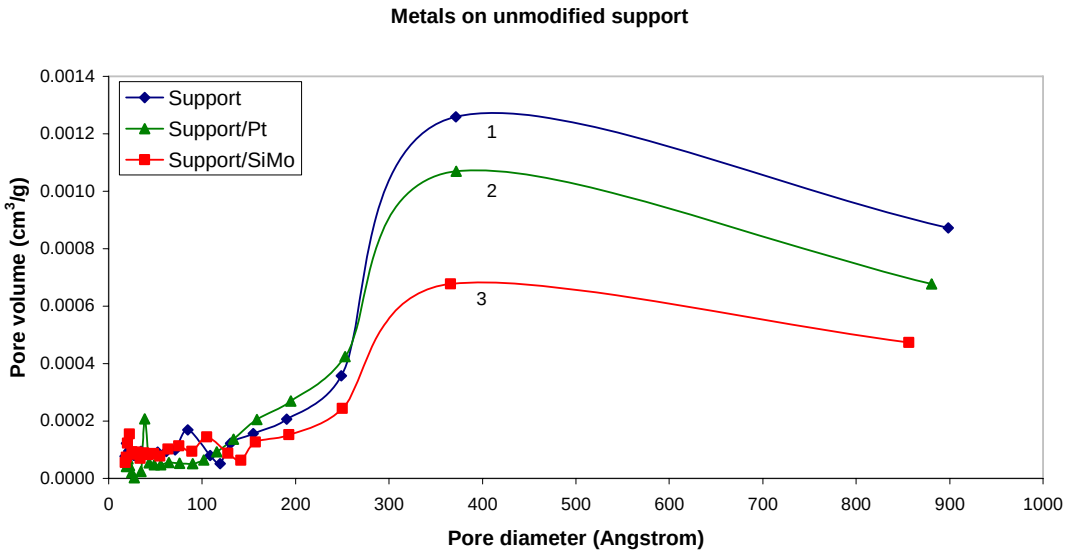

Figure A1: Pore size distributions of the metal centre on the unmodified support, based on the pore volume ($f_v(r_p)$) 1: support, 2: support/Pt and 3: support/SiMo

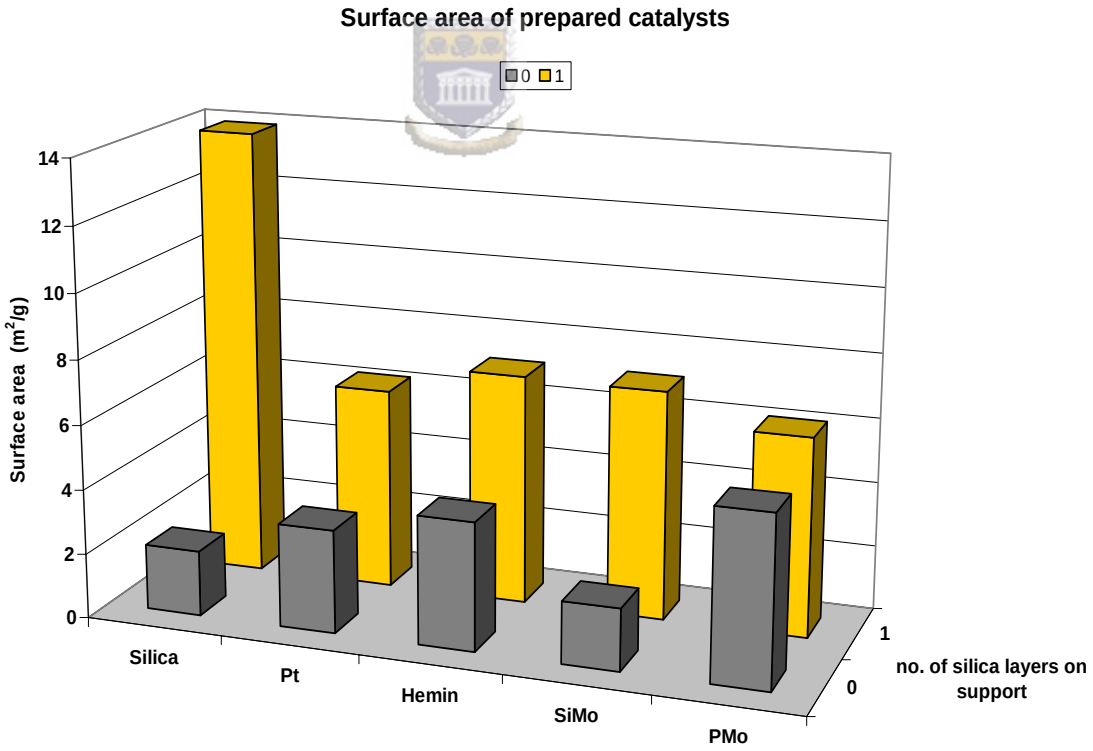

Figure A2: Surface area of prepared catalysts on unmodified support and on support modified with 1 layer silica

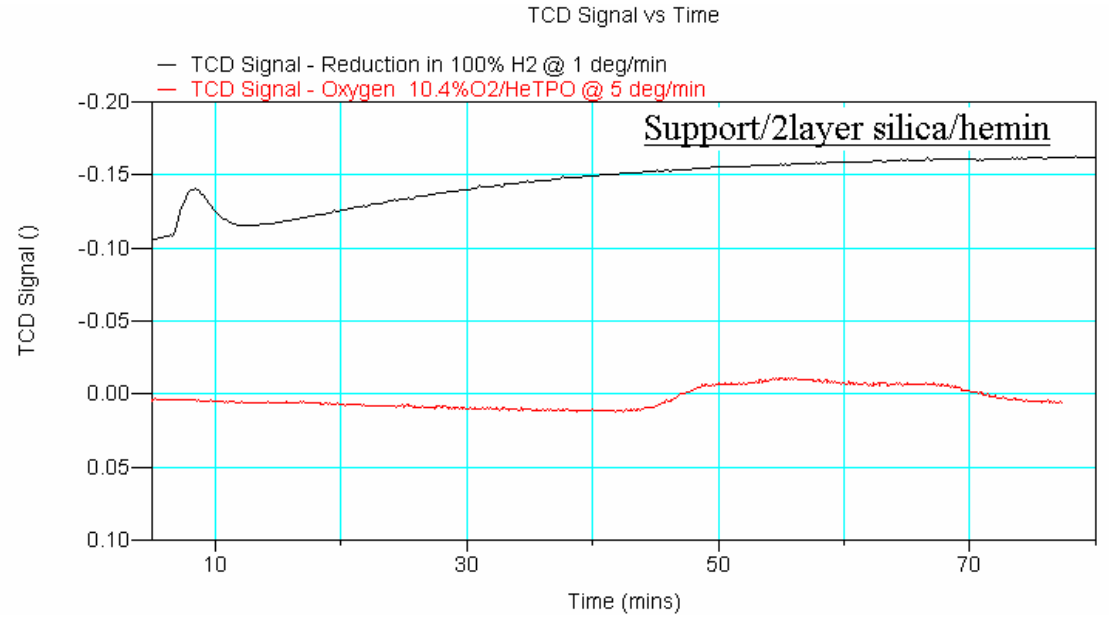

Figure A3: TPO/TPR profile for hemin on silica modified support

Figure A4: XRD diffractograms obtained from JCPDS database

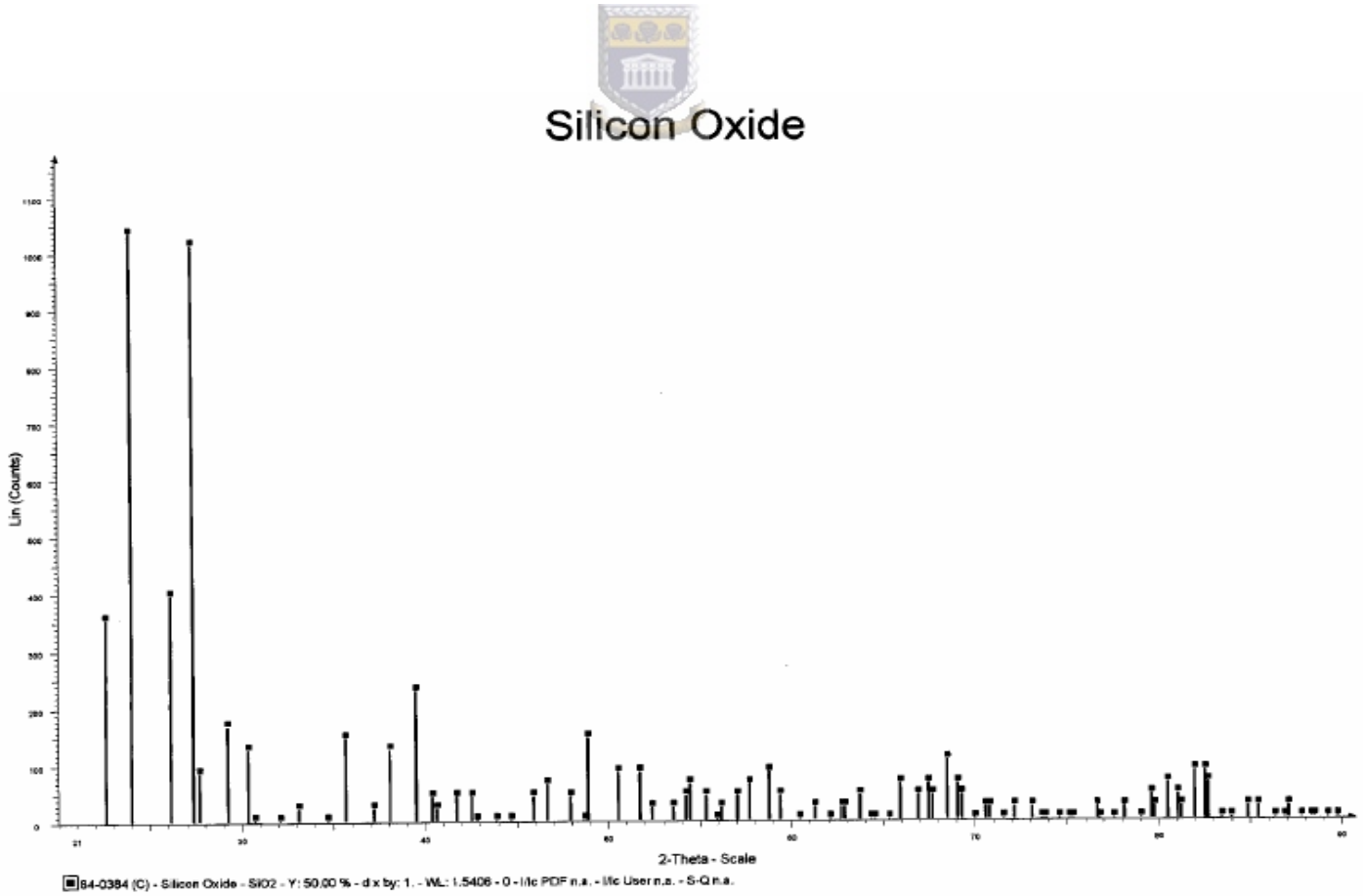

Figure A4

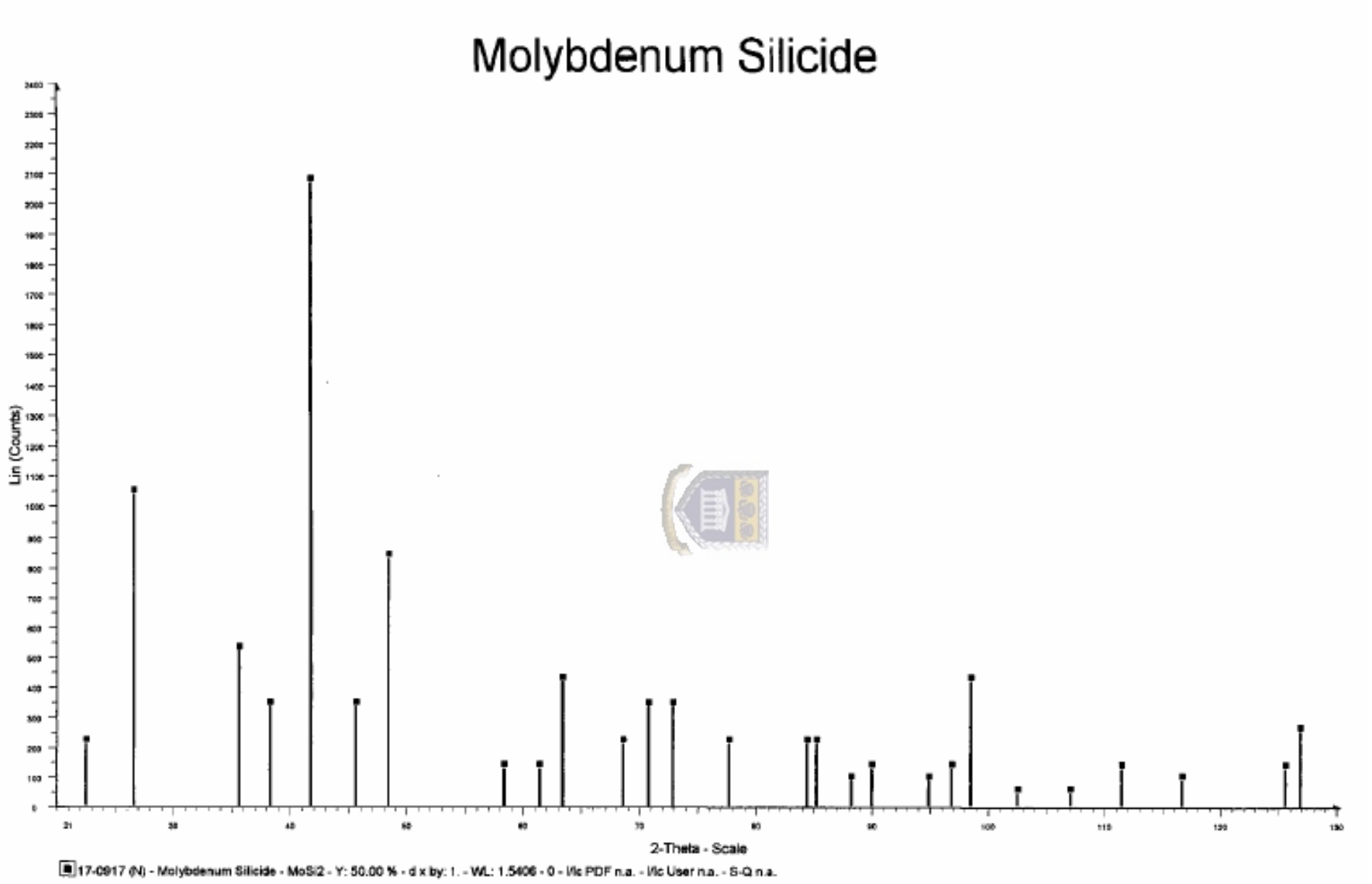
Molybdenum Silicide
Lin (Counts)
2-Theta - Scale
17-0917 (N) - Molybdenum Silicide - MoSi2 - Y: 50.00 % - d x by: 1. - WL: 1.5406 - 0 - I/Ic PDF n.a. - I/Ic User n.a. - S-Q n.a.

Figure A4
2

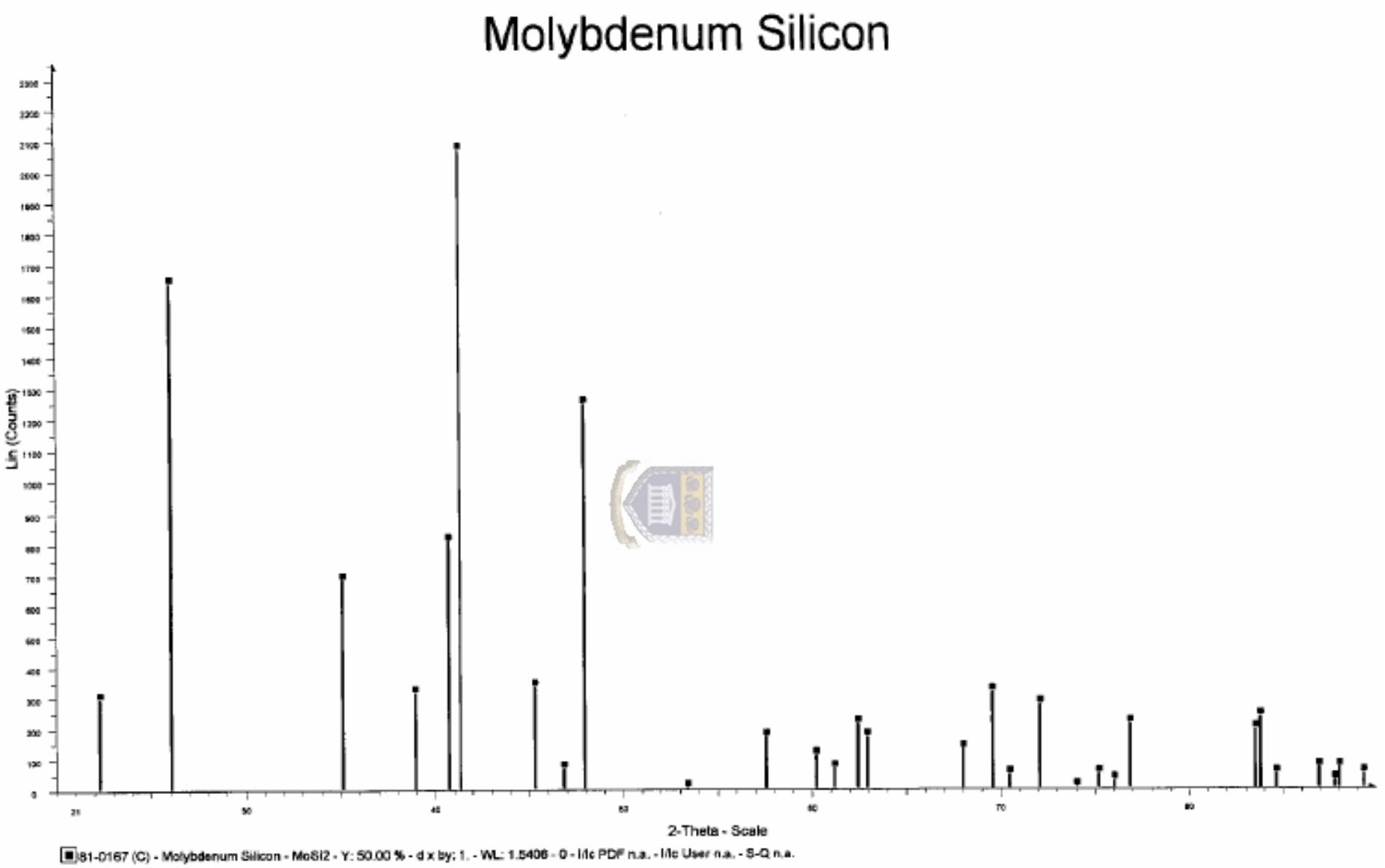
Molybdenum Silicon
Lin (Counts)
2-Theta - Scale
01-0167 (C) - Molybdenum Silicon - MoSi2 - Y: 50.00 % - d x by: 1. - WL: 1.5406 - 0 - I/Ic PDF n.a. - I/Ic User n.a. - S-Q n.a.

Figure A4
3

Hydrogen Molybdenum Phosphate Hydrate

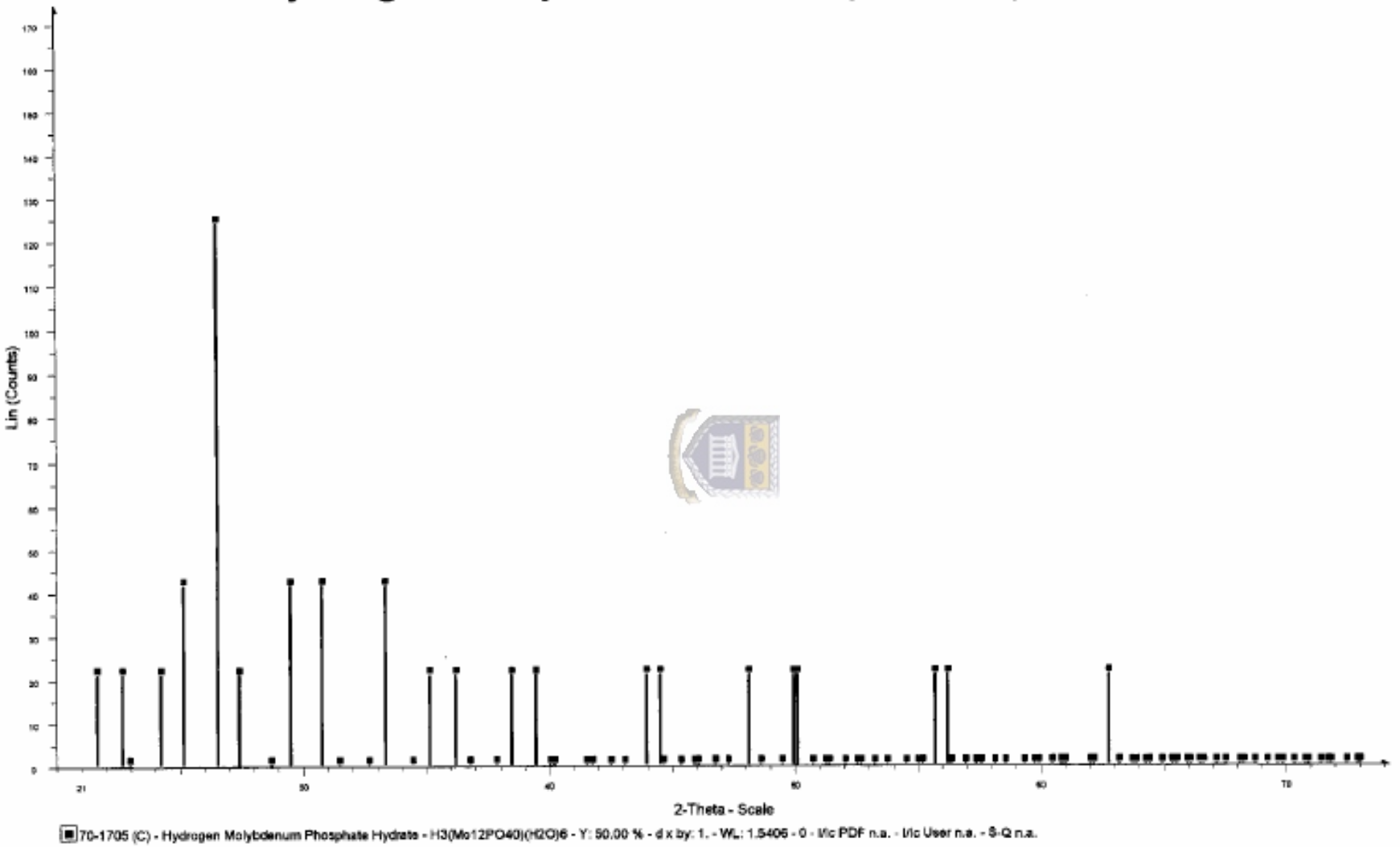

Figure A4

4

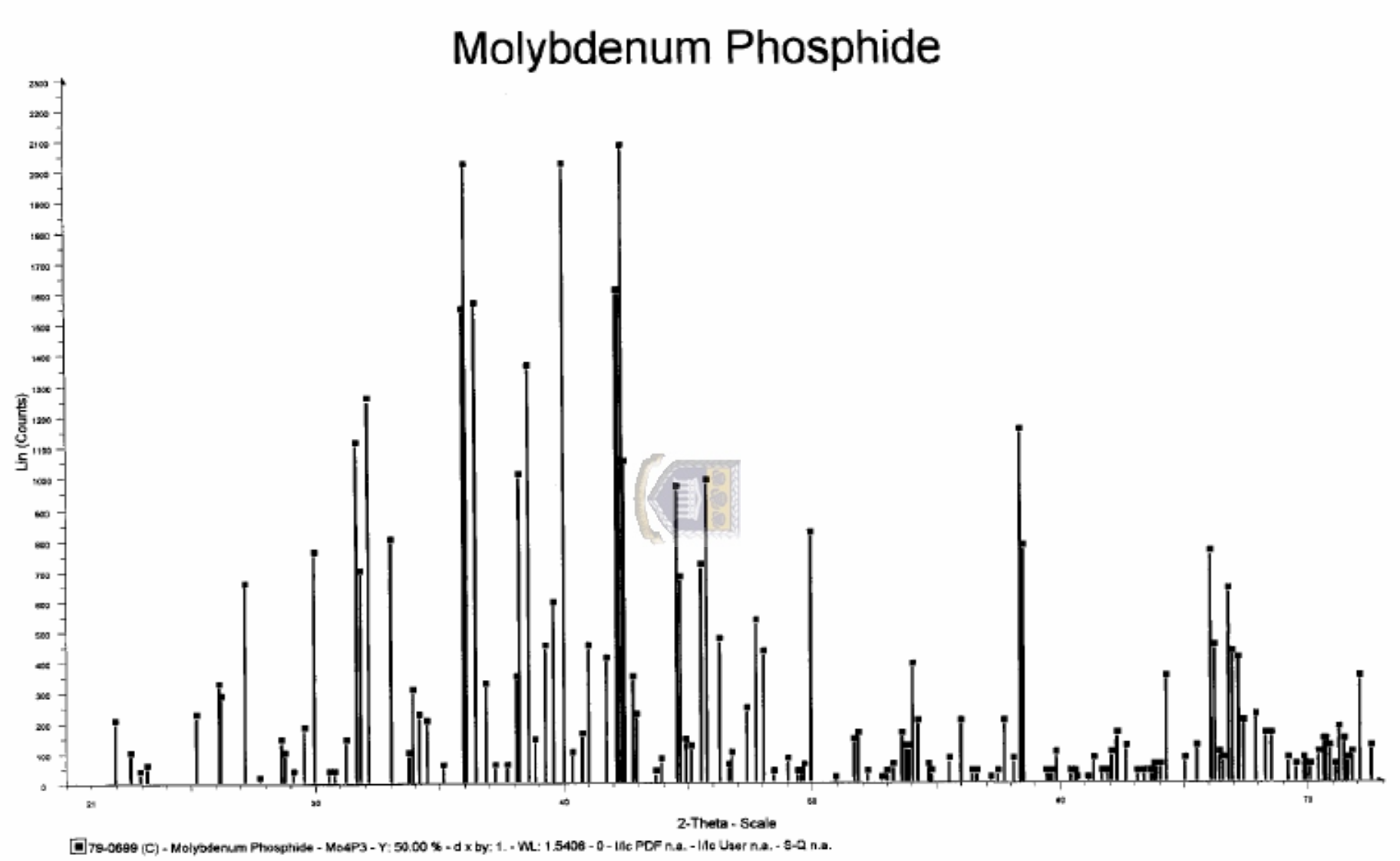
Molybdenum Phosphide
Lin (Counts)
2-Theta - Scale
79-0699 (C) - Molybdenum Phosphide - Mo4P3 - Y: 50.00 % - d x by: 1. - WL: 1.5406 - 0 - I/Ic PDF n.a. - I/Ic User n.a. - S-Q n.a.

Figure A4.5

Dodecasil 1H

Figure A4.6

Table A2: Initial methane and oxygen concentrations

Initial methane and oxygen concentrations Methane:Oxygen ratio	total flow rate	Vm (ml/min)	Vo (ml/min)	Vm + Vo	Cmethane (µmol/ml)	Coxygen (µmol/ml)
10:1	40	45	3.68	48.68	41.228	0.677
5:1	40	41	6.75	47.75	38.295	1.267
3:1	40	37	10.12	47.12	35.021	1.924
15:1	30	35	1.90	36.9	42.304	0.461
5:1	30	31	5.06	36.06	38.342	1.257
3:1	30	28	7.59	35.59	35.089	1.911
15:1	20	23	1.27	24.27	42.266	0.469
5:1	20	21	3.37	24.37	38.432	1.239
3:1	20	19	5.06	24.06	35.220	1.884
10:1	15	17	1.38	18.38	41.251	0.673
5:1	15	15	2.53	17.53	38.163	1.293
5:1	10	10	1.69	11.69	38.152	1.295
20:1	30	35	1.45	36.45	42.826	0.356
20:1	40	47	1.93	48.93	42.841	0.353

CALIBRATION CURVES

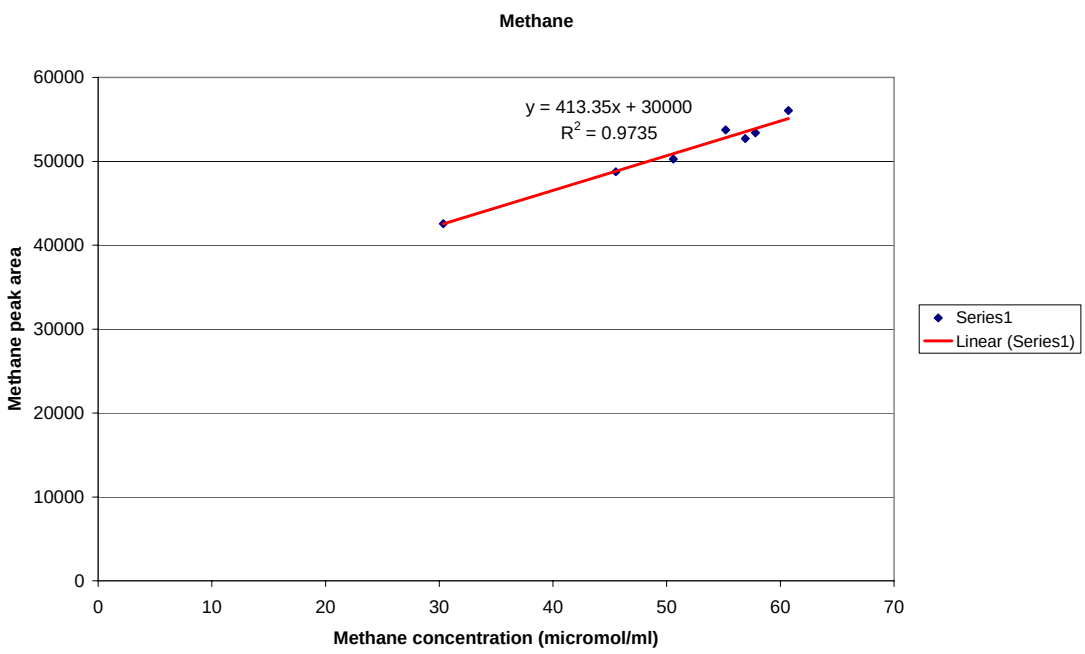

Figure A5: Methane calibration curve

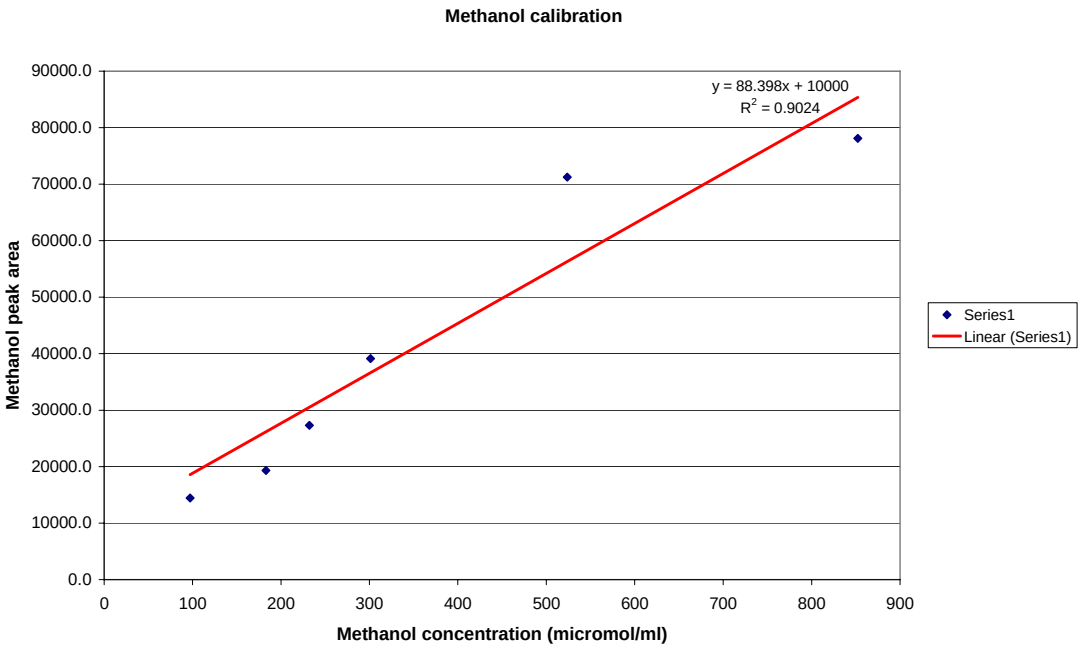

Figure A6: Methanol calibration

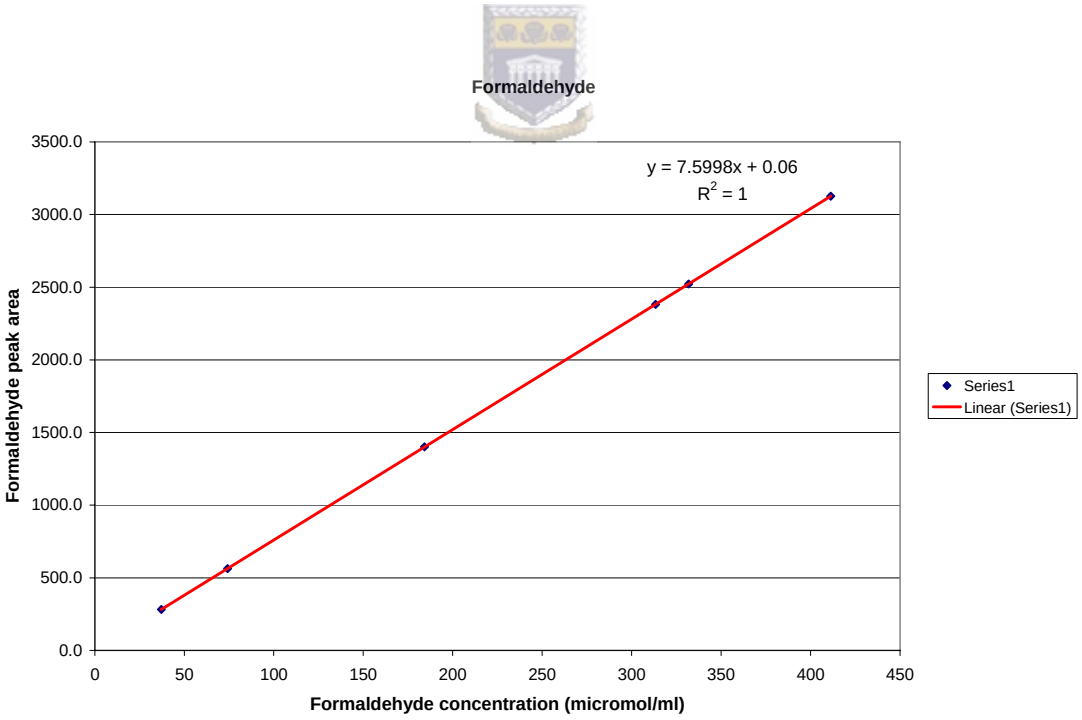

Figure A7: Formaldehyde calibration